

# An Analysis of Global Positioning System (GPS) Standard Positioning System (SPS) Performance for 2015

TR-SGL-17-04

March 2017

Space and Geophysics Laboratory  
Applied Research Laboratories  
The University of Texas at Austin  
P.O. Box 8029  
Austin, TX 78713-8029

Brent A. Renfro,  
Jessica Rosenquest,  
Audric Terry,  
Nicholas Boeker

Contract: NAVSEA Contract N00024-01-D-6200  
Task Order: 5101147

**Distribution A:** Approved for public release; Distribution is unlimited.

This Page Intentionally Left Blank

# Executive Summary

Applied Research Laboratories, The University of Texas at Austin (ARL:UT) examined the performance of the Global Positioning System (GPS) throughout 2015 for the Global Positioning Systems Directorate (SMC/GP). This report details the results of that performance analysis. This material is based upon work supported by the US Air Force Space & Missile Systems Center Global Positioning Systems Directorate through Naval Sea Systems Command Contract N00024-01-D-6200, task order 5101147, “FY15 GPS Signal and Performance Analysis”.

Performance is defined by the 2008 Standard Positioning Service (SPS) Performance Standard (SPS PS). The performance standards provide the U.S. government’s assertions regarding the expected performance of GPS. This report does not address each of the assertions in the performance standards. This report emphasizes those assertions which can be verified by anyone with knowledge of standard GPS data analysis practices, familiarity with the relevant signal specification, and access to a Global Navigation Satellite System (GNSS) data archive.

The assertions evaluated include those of accuracy, integrity, continuity, and availability of the GPS signal-in-space (SIS) and the position performance standards. Chapter 2 of the report includes a tabular summary of the assertions that were evaluated and a summary of the results. The remaining Chapters present details on the analysis associated with each assertion.

All the SPS PS metrics examined in the report were met in 2015.

# Contents

<b>1</b>	<b>Introduction</b>	<b>1</b>
<b>2</b>	<b>Summary of Results</b>	<b>4</b>
<b>3</b>	<b>Discussion of Performance Standard Metrics and Results</b>	<b>6</b>
3.1	SIS Accuracy . . . . .	6
3.1.1	URE Over All AOD . . . . .	8
3.1.1.1	An Alternate Approach . . . . .	12
3.1.2	URE at Any AOD . . . . .	12
3.1.3	URE at Zero AOD . . . . .	20
3.1.4	URE Bounding . . . . .	20
3.1.5	UTC Offset Error Accuracy . . . . .	21
3.2	SIS Integrity . . . . .	21
3.2.1	URE Integrity . . . . .	21
3.2.2	UTC OE Integrity . . . . .	23
3.3	SIS Continuity . . . . .	23
3.3.1	Unscheduled Failure Interruptions . . . . .	23
3.3.2	Status and Problem Reporting Standards . . . . .	27
3.3.2.1	Scheduled Events . . . . .	27
3.3.2.2	Unscheduled Outages . . . . .	29
3.3.2.3	Suspect NANUs . . . . .	30
3.4	SIS Availability . . . . .	31
3.4.1	Per-slot Availability . . . . .	31
3.4.2	Constellation Availability . . . . .	31
3.4.3	Operational Satellite Counts . . . . .	33

3.5	Position/Time Domain Standards . . . . .	35
3.5.1	PDOP Availability . . . . .	35
3.5.2	Additional DOP Analysis . . . . .	36
3.5.3	Position Service Availability . . . . .	44
3.5.4	Position Accuracy . . . . .	44
3.5.4.1	Results for Daily Average . . . . .	48
3.5.4.2	Results for Worst Site 95 <sup>th</sup> Percentile . . . . .	52
<b>4</b>	<b>Additional Results of Interest</b>	<b>56</b>
4.1	Frequency of Different SV Health States . . . . .	56
4.2	Age of Data . . . . .	56
4.3	User Range Accuracy Index Trends . . . . .	59
4.4	Extended Mode Operations . . . . .	60
<b>A</b>	<b>URE as a Function of AOD</b>	<b>64</b>
A.1	Notes . . . . .	65
A.2	Block IIA SVs . . . . .	66
A.3	Block IIR SVs . . . . .	67
A.4	Block IIR-M SVs . . . . .	70
A.5	Block IIF SVs . . . . .	72
<b>B</b>	<b>URE Analysis Implementation Details</b>	<b>75</b>
B.1	Introduction . . . . .	75
B.2	Clock and Position Values for Broadcast and Truth . . . . .	75
B.3	95 <sup>th</sup> Percentile Global Average As Per the SPS PS . . . . .	76
B.4	An Alternate Approach . . . . .	77
B.5	Limitations of URE Analysis . . . . .	79
<b>C</b>	<b>SVN to PRN Mapping for 2015</b>	<b>80</b>
<b>D</b>	<b>NANU Activity in 2015</b>	<b>82</b>
<b>E</b>	<b>SVN to Plane-Slot Mapping for 2015</b>	<b>84</b>
<b>F</b>	<b>Translation of URE Statistics Between Signals</b>	<b>88</b>

F.1	Group Delay Differential . . . . .	88
F.2	Intersignal Bias . . . . .	89
F.3	Adjusting PPS dual-frequency Results for SPS . . . . .	90
<b>G</b>	<b>Acronyms and Abbreviations</b>	<b>91</b>

# List of Figures

1.1	Maps of the Network of Stations Used as Part of this Report . . . . .	3
3.1	Range of the Monthly 95 <sup>th</sup> Percentile Values for All SVs . . . . .	11
3.2	Range of the Monthly 95 <sup>th</sup> Percentile Values for all SVs (via Alternate Method) . . . . .	14
3.3	Range of Differences in Monthly Values for all SVs . . . . .	14
3.4	Worst Performing Block IIA SV in Terms of Any AOD (SVN 40/PRN 10)	17
3.5	Worst Performing Block IIR/IIR-M SV in Terms of Any AOD (SVN 44/PRN 28) . . . . .	17
3.6	Worst Performing Block IIF SV in Terms of Any AOD (SVN 65/PRN 24)	18
3.7	Best Performing Block IIA SV in Terms of Any AOD (SVN 23/PRN 32)	18
3.8	Best Performing Block IIR/IIR-M SV in Terms of Any AOD (SVN 60/PRN 23) . . . . .	19
3.9	Best Performing Block IIF SV in Terms of Any AOD (SVN 63/PRN 01)	19
3.10	Daily Average Number of Occupied Slots . . . . .	33
3.11	Count of Operational SVs by Day . . . . .	34
3.12	Daily PDOP Metrics Using all SVs, 2015 . . . . .	39
3.13	Daily PDOP Metrics Using All SVs, 2013 . . . . .	40
3.14	Daily PDOP Metrics Using All SVs, 2014 . . . . .	40
3.15	GPS Visibility on Day 035 at 01:11 Relative to 63N, 36.44E . . . . .	43
3.16	Daily Averaged Position Residuals Computed Using a RAIM Solution . .	50
3.17	Daily Averaged Position Residuals Computed Using No Data Editing . .	50
3.18	Daily Averaged Position Residuals Computed Using a RAIM Solution (enlarged) . . . . .	51
3.19	Daily Averaged Autonomous Position Residuals Computed Using No Data Editing (enlarged) . . . . .	51

3.20	Worst Site 95 <sup>th</sup> Daily Averaged Position Residuals Computed Using a RAIM Solution . . . . .	54
3.21	Worst Site 95 <sup>th</sup> Daily Averaged Position Residuals Computed Using No Data Editing . . . . .	54
4.1	Constellation Age of Data for 2015 . . . . .	59
B.1	Global Average URE as defined in SPS PS . . . . .	76
B.2	Illustration of the 577 Point Grid . . . . .	78
C.1	PRN to SVN Mapping for 2015 . . . . .	81
D.1	Plot of NANU Activity for 2015 . . . . .	83
E.1	Time History of Satellite Plane-Slots for 2015 . . . . .	87



# List of Tables

2.1	Summary of SPS PS Metrics Examined for 2015 . . . . .	5
3.1	Characteristics of SIS URE Methods . . . . .	7
3.2	Monthly 95 <sup>th</sup> Percentile Values of SIS RMS URE for All SVs . . . . .	10
3.3	Monthly 95 <sup>th</sup> Percentile Values of SIS Instantaneous URE for all SVs (via Alternate Method) . . . . .	13
3.4	95 <sup>th</sup> Percentile Global Average UTCOE for 2015 . . . . .	22
3.5	Probability Over Any Hour of Not Losing Availability Due to Unscheduled Interruption . . . . .	26
3.6	Scheduled Events Covered in NANUs for 2015 . . . . .	28
3.7	Decommissioning Events Covered in NANUs for 2015 . . . . .	29
3.8	Unscheduled Events Covered in NANUs for 2015 . . . . .	30
3.9	Per-Slot Availability in 2015 for Baseline 24 Slots . . . . .	32
3.10	Summary of PDOP Availability . . . . .	36
3.11	Additional DOP Annually-Averaged Visibility Statistics for 2012 through 2015 . . . . .	38
3.12	Additional PDOP Statistics . . . . .	38
3.13	Satellite and NANUs Associated with Single-Day Large DOP Values . . . . .	41
3.14	DOP Results for 63N, 36.44E on Day 34/35 . . . . .	42
3.15	Organization of Positioning Results . . . . .	47
3.16	Mean of Daily Average Position Errors for 2015 . . . . .	49
3.17	Median of Daily Average Position Errors for 2015 . . . . .	49
3.18	Maximum of Daily Average Position Errors for 2015 . . . . .	49
3.19	Standard Deviation of Daily Average Position Errors for 2015 . . . . .	49
3.20	Mean of Daily Worst Site 95 <sup>th</sup> Percentile Position Errors for 2015 . . . . .	55
3.21	Median of Daily Worst Site 95 <sup>th</sup> Percentile Position Errors for 2015 . . . . .	55

3.22	Maximum of Daily Worst Site 95 <sup>th</sup> Percental Position Errors for 2015 . .	55
3.23	Standard Deviation of Daily Worst Site 95 <sup>th</sup> Percentile Position Errors for 2015 . . . . .	55
4.1	Frequency of Health Codes . . . . .	57
4.2	Age of Data of the Navigation Message by SV Type . . . . .	58
4.3	Distribution of URA Index Values . . . . .	61
4.4	Distribution of URA Index Values As a Percentage of All Collected . . .	62
4.5	Summary of Occurrences of Extended Mode Operations . . . . .	63
E.1	Summary of SV-Slot Relationships for 2015 . . . . .	86
G.1	List of Acronyms and Abbreviations . . . . .	91

# Chapter 1

## Introduction

Applied Research Laboratories, The University of Texas at Austin (ARL:UT)<sup>1</sup> examined the performance of the Global Positioning System (GPS) throughout 2015 for the Global Positioning Systems Directorate (SMC/GP). This report details the results of our performance analysis. This material is based upon work supported by the US Air Force Space & Missile Systems Center Global Positioning Systems Directorate through Naval Sea Systems Command Contract N00024-01-D-6200, task order 5101147, “FY15 GPS Signal and Performance Analysis”.

Performance is assessed relative to selected assertions in the 2008 Standard Positioning Service (SPS) Performance Standard (SPS PS) [1]. (Hereafter the term SPS PS, or SPSPS08, are used when referring to the 2008 SPS PS.) Chapter 2 contains a tabular summary of performance stated in terms of the metrics provided in the performance standard. Chapter 3 contains explanations and amplifications regarding the summary values. Chapter 4 details additional findings of the performance analysis.

The performance standards define the services delivered through the L1 C/A code signal. The metrics are limited to characterizing the signal in space (SIS) and do not address error sources such as atmospheric errors, receiver errors, or error due to the user environment (e.g. multipath errors, terrain masking, and foliage). This report addresses assertions in the SPS PS that can be verified by anyone with knowledge of standard GPS data analysis practices, familiarity with the relevant signal specification [2], and access to a data archive (such as that available via the International Global Navigation Satellite System (GNSS) Service (IGS)) [3]. The assertions examined include those related to user range error (URE), availability of service, and position domain standards (specifics can be found in Table 2.1).

The majority of the assertions related to URE values are evaluated through comparison of the space vehicle (SV) clock and position representations as computed from the broadcast Legacy Navigation (LNAV) message data against the SV truth clock and position data as provided by a precise orbit calculated after the time of interest. The broadcast clock and position data is denoted in this report by BCP and the truth clock

---

<sup>1</sup>A complete list of abbreviations found in this document is provided in Appendix G.

and position data by TCP. The process by which the URE values are calculated is described in Appendix B of this report.

Observation data from tracking stations are used to cross-check the URE values and to evaluate non-URE assertions. Examples of the latter application include the areas of Continuity (3.3), Availability (3.4), and Position/Time Availability (3.5). In these cases, data from two networks are used. The two networks considered are the National Geospatial-Intelligence Agency (NGA) Monitor Station Network (MSN) [4] and a subset of the tracking stations that contribute to the IGS. The distribution of these stations is shown in Figure 1.1. These sets of stations ensure continuous observation of all space vehicles by multiple stations.

Several metrics in the performance standards are stated in terms of the Base 24 constellation of six planes and four slots/plane or the Expandable 24 constellation in which three of the 24 slots may be occupied by two SVs. Currently, there are more than 32 GPS SVs on-orbit. Of these, at most 31 SVs may be operationally broadcasting at any time. Of the SVs on-orbit, 27 are located in the expandable 24 constellation. The SVs in excess of those located in defined slots are assigned to locations in various planes in accordance with operational considerations.

The majority of the metrics in this report are evaluated on either a per-SV basis or for the full constellation. The metrics associated with continuity and availability are defined with respect to the slot definitions.

The GPS SVs are referred to by pseudo-random noise ID and by space vehicle number (referred to hereafter as PRN and SVN, respectively). As the number of active PRNs has increased to nearly the total available number, PRNs are now being used by multiple SVs within a given year (but by no more than one SV at a time). Therefore, the SVN represents the permanent unique identifier for the vehicle under discussion. In general, we list the SVN first and the PRN second because the SVN is the unique identifier of the two. The SVN-to-PRN relationships were provided by the Master Control Station (MCS), however another useful summary of this information may be found on the U.S. Naval Observatory (USNO) website [5].

The authors acknowledge and appreciate the effort of several ARL:UT staff members who reviewed these results. For 2015 this included Shannon Kolensky, Scott Sellers, and Johnathan York.

Karl Kovach of Aerospace provided valuable assistance in interpreting the SPSPS08 metrics. John Lavrakas of Advanced Research Corporation and P.J. Mendicki of Aerospace Corporation have long been interested in GPS performance metrics and provided comments on the final draft. Their inputs were very valuable. However, the results presented in this report are derived by ARL:UT, and any errors are the responsibility of ARL:UT.

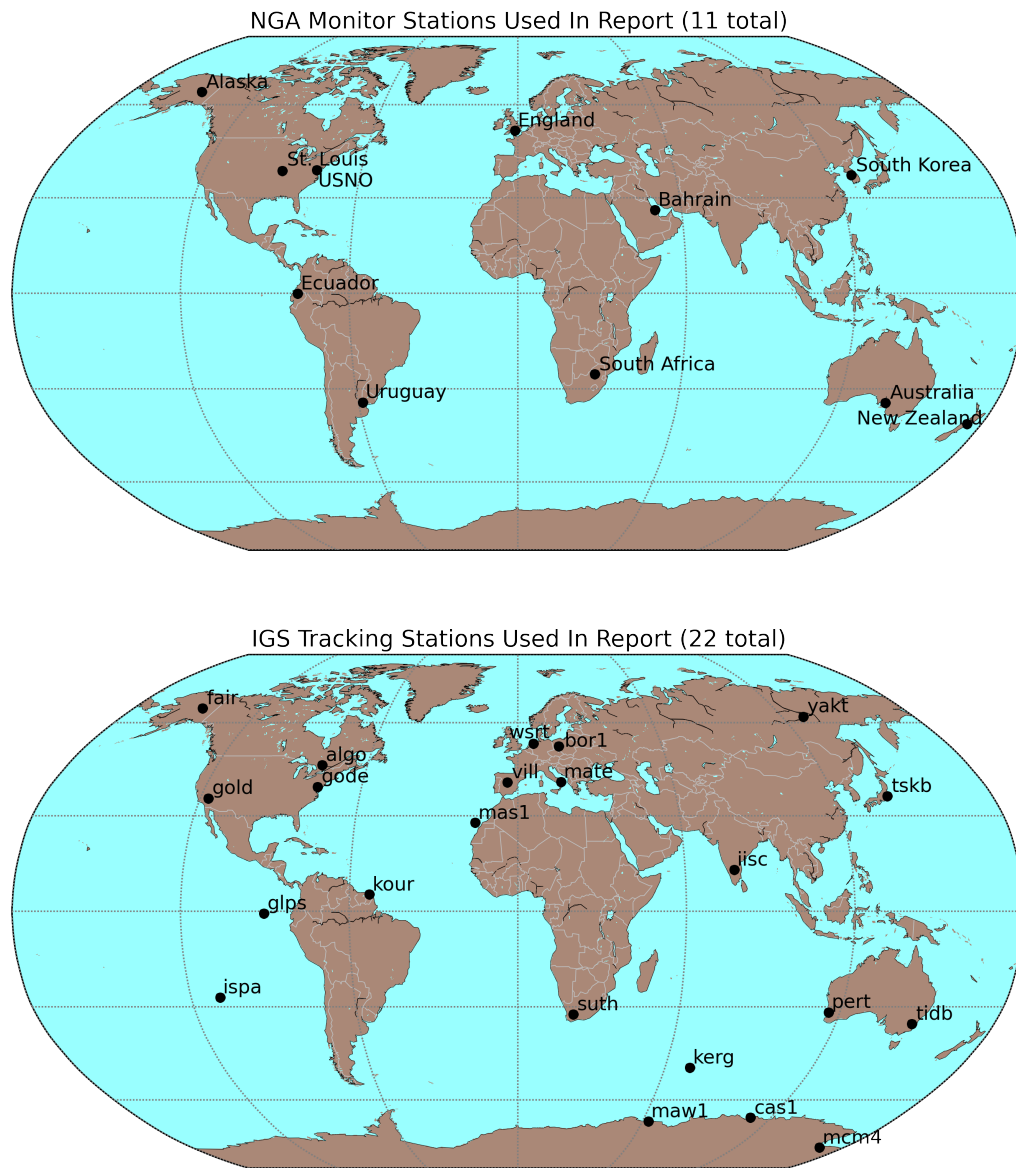


Figure 1.1: Maps of the Network of Stations Used as Part of this Report

# Chapter 2

## Summary of Results

Table 2.1 is a summary of the assertions defined in the performance standards. The table is annotated to show which assertions are evaluated in this report and the status of each assertion that was evaluated.

All the SPS PS metrics examined in the report were met in 2015.

Details regarding each result may be found in Chapter 3.

**Table 2.1:** Summary of SPS PS Metrics Examined for 2015

SPSPS08 Section	SPS PS Metric	2015 Status
3.4.1 SIS URE Accuracy	$\leq 7.8$ m 95% Global average URE during normal operations over all AODs	✓
	$\leq 6.0$ m 95% Global average URE during normal operations at zero AOD	✓
	$\leq 12.8$ m 95% Global average URE during normal operations at any AOD	✓
	$\leq 30$ m 99.94% Global average URE during normal operations	✓
	$\leq 30$ m 99.79% Worst case single point average URE during normal operations	✓
	$\leq 388$ m 95% Global average URE after 14 days without upload	not eval.
3.4.2 SIS URRE Accuracy	$\leq 0.006$ m/s 95% Global average at any AOD	not eval.
3.4.3 SIS URAE Accuracy	$\leq 0.002$ m/s <sup>2</sup> 95% Global average at any AOD	not eval.
3.4.4 SIS UTCOE Accuracy	$\leq 40$ nsec 95% Global average at any AOD	✓
3.5.1 SIS Instantaneous URE Integrity	$\leq 1 \times 10^{-5}$ Probability over any hour of exceeding the NTE tolerance without a timely alert	✓
3.5.4 SIS Instantaneous UTCOE Integrity	$\leq 1 \times 10^{-5}$ Probability over any hour of exceeding the NTE tolerance without a timely alert	✓
3.6.1 SIS Continuity - Unscheduled Failure Interruptions	$\geq 0.9998$ Probability over any hour of not losing the SPS SIS availability from the slot due to unscheduled interruption	✓
3.6.3 Status and Problem Reporting	Appropriate NANU issue at least 48 hours prior to a scheduled event	✓
3.7.1 SIS Per-Slot Availability	$\geq 0.957$ Probability that (a.) a slot in the baseline 24-slot will be occupied by a satellite broadcasting a healthy SPS SIS, or (b.) a slot in the expanded configuration will be occupied by a pair of satellites each broadcasting a healthy SIS	✓
3.7.2 SIS Constellation Availability	$\geq 0.98$ Probability that at least 21 slots out of the 24 slots will be occupied by a satellite (or pair of satellites for expanded slots) broadcasting a healthy SIS	✓
	$\geq 0.99999$ Probability that at least 20 slots out of the 24 slots will be occupied by a satellite (or pair of satellites for expanded slots) broadcasting a healthy SIS	✓
3.7.3 Operational Satellite Counts	$\geq 0.95$ Probability that the constellation will have at least 24 operational satellites regardless of whether those operational satellites are located in slots or not	✓
3.8.1 PDOP Availability	$\geq 98\%$ Global PDOP of 6 or less	✓
	$\geq 88\%$ Worst site PDOP of 6 or less	✓
3.8.2 Position Service Availability	$\geq 99\%$ Horizontal, average location	✓
	$\geq 99\%$ Vertical, average location	
	$\geq 90\%$ Horizontal, worst-case location	
	$\geq 90\%$ Vertical, worst-case location	
3.8.3 Position Accuracy	$\leq 9$ m 95% Horizontal, global average	✓
	$\leq 15$ m 95% Vertical, global average	
	$\leq 17$ m 95% Horizontal, worst site	
	$\leq 37$ m 95% Vertical, worst site	
	$\leq 40$ nsec time transfer error 95% of the time	

✓ - Met

# Chapter 3

## Discussion of Performance Standard Metrics and Results

While Chapter 2 notes the SPSPS08 specifications were met for 2015, the statistics and trends reported in this chapter provide both additional information and support for these conclusions.

### 3.1 SIS Accuracy

SIS URE accuracy is asserted in Section 3.4 of the SPSPS08. The following standards (from Table 3.4-1) are considered in this report:

- “ $\leq 7.8$  m 95% Global Average URE during Normal Operations over all AODs”
- “ $\leq 6.0$  m 95% Global Average URE during Normal Operations at Zero AOD”
- “ $\leq 12.8$  m 95% Global Average URE during Normal Operations at any AOD”
- “ $\leq 30$  m 99.94% Global Average URE during Normal Operations”
- “ $\leq 30$  m 99.79% Worst Case Single Point Average URE during Normal Operations”
- “ $\leq 40$  nsec 95% Global Average UTCOE during Normal Operations at Any AOD”

The remaining standard associated with operations after extended periods without an upload are not relevant in 2015 as periods of extended operations were very limited. (This is discussed in Section 4.4)

The URE statistics presented in this report are based on a comparison of the BCP against the TCP. (Refer to Appendix B for further details on the process by which the URE are computed.) This is a useful approach, but one that has specific limitations,



the most significant of which is that the TCP may not reflect the effect of individual discontinuities or large effects over a short time (such as a frequency step or clock runoff). Nonetheless, this approach is appropriate given the long period of averaging implemented in determining URE, namely 30 days. Briefly, this approach allows the computation of URE without direct reference to observations from any particular ground sites, though the TCP carries an implicit network dependency based on the set of ground stations used to derive the precise orbits from which the TCP is derived.

In the case of this report, the BCP and TCP are both referenced to the L1/L2 P(Y)-code signal. As a result the resulting URE values are best characterized as PPS dual-frequency URE values. The SPS results are derived from the PPS dual-frequency results by a process described in Appendix F.

Throughout this section and the next, there are references to several different SIS URE expressions. Each of these SIS URE expressions means something slightly different. It is important to pay careful attention to the particular SIS URE expression being used in each case to avoid misinterpreting the associated URE numbers. Appendix C of the PPSPS07 and SPSPS08 provides definitions for the two ways SIS URE are computed, *Instantaneous SIS URE*, which expresses URE on an instantaneous basis and *root mean square (RMS) SIS URE*, which expresses URE on a statistical basis. When the BCP and TCP are used to estimate the range residual along a specific satellite-to-receiver line-of-sight vector at a given instant in time, then that is an “Instantaneous SIS URE”. Some of the primary differences between Instantaneous basis SIS UREs and statistical basis SIS UREs are given below.

**Table 3.1:** Characteristics of SIS URE Methods

<b>Instantaneous Basis SIS URE</b>	<b>Statistical Basis SIS URE</b>
Always algebraically signed ( $\pm$ ) number	Never an algebraic sign
Never a statistical qualifier	Always a statistical qualifier (RMS, 95%, etc.)
Specific to a particular time and place	Statistic over span of times, or places, or both
Next section of this report (Section 3.2)	This section of this report (Section 3.1)

Throughout this section, there are references to the “Instantaneous RMS SIS URE.” This is a statistical basis SIS URE (note the “RMS” statistical qualifier), where the measurement quantity is the Instantaneous SIS URE, and the span of the statistic covers that one particular point (“instant”) in time across a large range of spatial points. This is effectively the evaluation of the Instantaneous SIS URE across every spatial point in the area of the service volume visible to the SV at that particular instant in time. Put another way; consider the signal from a given SV at a given point in time. That signal intersects the surface of the Earth over an area, and at each location there is a unique Instantaneous SIS URE value based on geometric relationship between the SV and the location of interest. In the name “Instantaneous RMS SIS URE,” the “Instantaneous” means that no time averaging occurs. The “RMS” refers to taking the RMS of all the individual Instantaneous SIS URE values across the area visible to the SV. This concept is explained in SPSPS08 Section A.4.11, and the relevant equation is presented in Appendix B of this report.

### 3.1.1 URE Over All AOD

The performance standard URE metric that most closely matches a user's observations is the calculation of the 95<sup>th</sup> percentile Global Average URE over all ages of data (AODs). This is associated with the SPSPS08 Section 3-4 metrics:

- “ $\leq 7.8$  m 95% Global Average URE during Normal Operations over all AODs”

These metrics can be decomposed into several pieces to better understand the process. For example, the first metric may be decomposed as follows:

- 7.8 m - This is the limit against which to test. The value is unique to the signal under evaluation.
- 95<sup>th</sup> Percentile - This is the statistical measure applied to the data to determine the actual URE. In this case, there are a sufficiently large number of samples to allow direct sorting of the results across time and selection of the 95<sup>th</sup> percentile.
- Global Average URE - This is another term for the Instantaneous RMS SIS URE, a statistical quantity representing the average URE across the area of the service volume visible to the SV at a given point in time. The expression used to compute this quantity is provided in Appendix B.
- Normal Operations - This is a constraint related to normal vs. extended mode operations. See IS-GPS-200 20.3.4.4 [2].
- over all AODs - This constraint means that the Global Average URE will be considered at each evaluation time regardless of the AOD at the evaluation time. A more detailed explanation of the AOD and how this quantity is computed can be found in Section 4.2.

In addition, there are three general statements in Section 3.4 that have a bearing on this calculation:

- These statistics include only data from periods when each SV was healthy.
- These statistics are “per SV” - that is, they apply to the signal from each satellite, not for averages across the constellation.
- “*The ergodic period contains the minimum number of samples such that the sample statistic is representative of the population statistic. Under a one-upload-per-day scenario, for example, the traditional approximation of the URE ergodic period is 30 days.*” (SPSPS08 Section 3.4, Note 1) Therefore the statistics will be computed over a monthly period and not daily. Because outages do occur, we have computed the statistic for each month, regardless of the number of days of availability, but identified these values when displayed.

Based on this set of assumptions and constraints, the monthly 95<sup>th</sup> percentile values of the RMS SIS URE were computed for each SV as provided in Table 3.2. Values computed for incomplete months are shown with shaded cells. For each SVN we show the worst of these values across the year in red. The gaps in URE indicate that the satellite was decommissioned (SVN 26, 34, 40), or not yet launched (SVN 71, 72, 73). Note that none of the values in this table exceed the threshold of 7.8 m. In all cases, no values exceed 7.8 m and so this requirement is met for 2015.

Figure 3.1 provides a summary of these results for the entire constellation. For each SVN, shown along the x-axis, the median value of the monthly 95<sup>th</sup> percentile SIS URE is computed and displayed as a point. The full range of the annual monthly 95<sup>th</sup> percentile SIS URE is shown by the vertical bars. Color distinguishes between the Block II/IIA, Block IIR, Block IIR-M, and Block IIF SVs. The red horizontal line at 7.8 m indicates the upper bound given by the SPSPS08 Section 3-4 performance metric.

A number of points are evident from Figure 3.1:

1. All SVs meet the performance specification of the SPSPS08, even when only the worst performing month is considered. Even the worst value for each SV (indicated by the upper extent of the range bars) is a factor of 2 or more smaller than the threshold.
2. As a general rule, the newer satellites outperform the older Block IIA satellites in terms of the 95<sup>th</sup> Percentile SIS URE metric. The average performance of the Block IIA SVs nearly a meter greater than that of the Block IIR, IIR-M, and IIF SVs if SVN 65/PRN 24 and SVN 72/PRN 08 are omitted (see Table 3.2 and point 6. below).
3. For most of the SVs, the value of the 95<sup>th</sup> Percentile SIS URE metric is relatively stable over the course of the year, as indicated by relatively small range bars.
4. For some SVs there are large range extents for the bars. This includes SVNs 45, 54, 69, and 71, each of which have spreads of URE values of greater than 1 m. For 45, 54, and 69, the maximum value was from a single month of out-of-family performance. For SVN 71, the large value was the first month of operation following launch.
5. The “best” SVs appear to be the Block IIR, Block IIR-M, and Block IIF which cluster near the 1.0 m level, and whose range variation is small. This includes SVNs 50, 51, 55, 56, 58, 59, 60, 61, 62, 63, 66, and 67.
6. The values for SVN 65 and SVN 72 are noticeably different than the other Block IIF SVs. These are the only Block IIF SVs operating on a Cesium frequency standard.
7. Three new SVs were launched in 2015: SVN 71, 72, and 73. The RMS SIS URE values for new SVs are sometimes slightly worse for the first few months of operation. See the April value for SVN 71 in Table 3.2 for an example.

**Table 3.2:** Monthly 95<sup>th</sup> Percentile Values of SIS RMS URE for All SVs in Meters

SVN	PRN	Block	Jan.	Feb.	Mar.	Apr.	May	Jun.	Jul.	Aug.	Sept.	Oct.	Nov.	Dec.	2015
23	32	IIA	1.69	1.25	1.42	1.69	1.25	1.30	1.48	1.30	1.80	1.53	1.40	1.39	1.47
26	26	IIA	1.17												1.17
34	4	IIA	1.80	2.13	2.06	1.67	1.96	1.86	1.77	1.98	1.62	1.53	1.83		1.85
40	10	IIA	2.48	2.31	2.46	2.72	2.81	2.77	2.74						2.64
41	14	IIR	1.02	1.03	1.24	1.01	1.18	1.04	1.16	1.07	1.11	1.09	1.06	1.00	1.08
43	13	IIR	1.19	1.12	1.10	1.28	1.15	1.16	1.26	1.56	1.23	1.19	1.08	1.06	1.20
44	28	IIR	2.42	2.30	2.45	2.44	2.22	2.55	2.48	2.59	2.46	2.40	2.50	2.52	2.45
45	21	IIR	1.85	1.32	1.26	1.34	1.05	1.14	1.09	1.19	1.10	1.05	0.98	1.02	1.17
46	11	IIR	1.24	1.33	1.60	1.29	1.37	1.53	1.30	1.47	1.37	1.81	1.80	1.84	1.50
47	22	IIR	1.95	2.02	2.05	1.74	1.80	1.71	1.87	1.76	2.07	1.91	1.91	1.72	1.88
48	7	IIR-M	1.18	1.11	1.18	1.12	1.20	1.09	1.12	1.04	1.20	1.30	1.23	1.18	1.16
50	5	IIR-M	0.93	0.92	1.04	0.97	0.95	0.96	1.01	1.03	0.95	0.96	0.95	0.94	0.97
51	20	IIR	0.93	0.94	0.98	1.12	0.94	1.02	0.99	1.03	0.96	0.96	0.95	0.98	0.98
52	31	IIR-M	1.21	1.29	1.15	1.43	1.27	1.21	1.31	1.18	1.39	1.33	1.27	1.40	1.29
53	17	IIR-M	1.69	1.59	2.02	1.44	1.60	1.62	1.53	1.33	1.59	1.26	1.79	1.65	1.60
54	18	IIR	0.94	0.95	0.95	0.95	0.99	0.94	0.91	1.26	1.93	1.26	1.43	1.57	1.16
55	15	IIR-M	0.97	0.92	0.92	0.93	0.91	0.99	0.95	0.93	0.93	0.96	0.96	0.98	0.95
56	16	IIR	0.98	0.93	0.95	0.99	0.91	0.91	0.92	0.93	0.92	0.94	0.97	0.93	0.94
57	29	IIR-M	1.11	1.36	1.62	1.36	1.43	1.36	1.26	1.49	1.55	1.27	1.39	1.36	1.37
58	12	IIR-M	1.06	1.14	0.91	0.94	0.92	1.00	0.99	1.01	0.96	1.01	0.97	0.95	0.99
59	19	IIR	0.97	1.06	1.07	1.01	0.96	0.98	0.97	1.03	0.95	0.98	0.96	0.95	0.98
60	23	IIR	0.93	0.97	0.96	0.94	0.94	0.97	0.94	0.93	0.92	0.90	0.93	0.96	0.94
61	2	IIR	1.00	1.07	0.97	0.95	1.02	1.08	1.04	1.00	0.96	0.97	0.96	0.97	1.00
62	25	IIF	0.92	0.92	0.98	1.05	0.97	0.97	0.99	1.03	1.10	0.95	0.97	0.96	0.99
63	1	IIF	0.95	0.99	0.95	0.90	0.88	0.92	0.94	0.98	0.96	0.94	0.91	0.92	0.94
64	30	IIF	1.18	1.01	0.93	1.28	0.99	1.04	1.09	1.20	0.97	0.97	0.97	1.07	1.04
65	24	IIF	2.43	2.44	2.32	2.36	2.61	2.25	2.39	2.35	2.08	2.25	2.36	2.55	2.39
66	27	IIF	0.97	0.94	0.89	0.90	0.93	0.97	0.99	0.95	0.94	0.94	0.97	0.96	0.95
67	6	IIF	0.97	1.00	0.93	0.89	0.88	0.91	0.97	1.04	0.94	0.95	0.89	0.93	0.95
68	9	IIF	0.98	0.92	0.94	0.99	1.06	1.01	0.94	0.92	1.21	0.97	0.99	0.94	0.99
69	3	IIF	1.06	1.29	1.67	1.34	1.04	0.87	0.93	0.99	1.01	1.07	1.06	0.95	1.13
71	26	IIF				1.98	1.48	1.09	1.07	1.06	1.11	1.01	0.98	0.97	1.13
72	8	IIF								1.97	2.00	1.99	1.92	2.24	2.03
73	10	IIF												1.17	1.17
Block IIA			2.01	2.04	2.07	2.20	2.37	2.20	1.94	1.66	1.71	1.53	1.48	1.39	2.00
Block IIR/IIR-M			1.30	1.27	1.34	1.30	1.27	1.26	1.26	1.25	1.36	1.30	1.31	1.33	1.30
Block IIF			1.24	1.30	1.33	1.47	1.33	1.18	1.16	1.43	1.34	1.39	1.44	1.50	1.35
All SVs			1.42	1.41	1.47	1.50	1.43	1.39	1.33	1.35	1.40	1.35	1.36	1.39	1.40

Notes: Values not present indicate that the satellite was unavailable during this period. Months during which an SV was available for less than 25 days are shown shaded. Months with the highest SIS RMS URE for a given SV are colored red. The column labeled "2015" is the 95<sup>th</sup> Percentile over the year. The four rows at the bottom are the monthly 95<sup>th</sup> Percentile values over various sets of SVs.

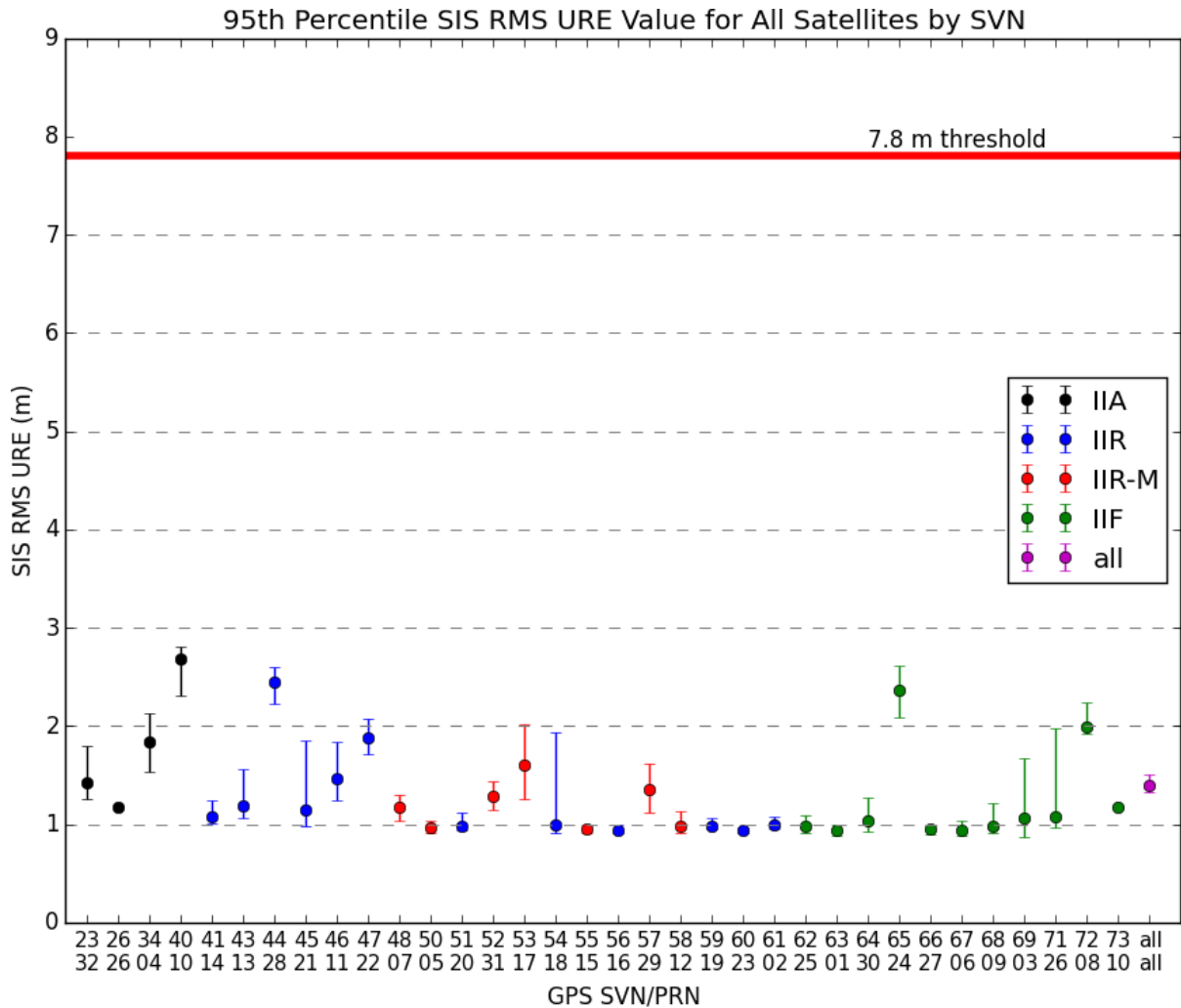


**Figure 3.1:** Range of the Monthly 95<sup>th</sup> Percentile Values for All SVs

Notes: Each SVN with valid data is shown sequentially along the x-axis. The median value of the monthly 95<sup>th</sup> Percentile SIS URE displayed as a point along the vertical axis. The full range of the monthly 95<sup>th</sup> Percentile SIS URE for 2015 is shown by the vertical bars. Color distinguishes between the Block II/IIA, Block IIR, Block IIR-M, and Block IIF SVs. The red horizontal line at 7.8 m indicates the upper bound given by the SPSPS08 Section 3-4 performance metric. The markers for “all” represent the monthly 95<sup>th</sup> Percentile values across all satellites.

### 3.1.1.1 An Alternate Approach

As described toward the end of Section 3.1, the 95<sup>th</sup> percentile Global Average URE values are formed by first deriving the Instantaneous RMS SIS URE at a succession of time points, then picking the 95<sup>th</sup> percentile value over that set of results. This has the computational advantage that the Instantaneous RMS SIS URE is derived from a single equation in radial, along-track, cross-track, and time errors at a given instant in time (as explained in Appendix B.3). However, it leads to a two-step implementation under which we first derive an RMS over a spatial area at a series of time points, then derive a 95<sup>th</sup> percentile statistic over time.

Given current computation and storage capability, it is practical to derive a set of 95<sup>th</sup> percentile URE values in which the Instantaneous SIS URE values are derived over a reasonably dense grid at a uniform cadence throughout the period of interest. The 95<sup>th</sup> percentile value is then selected from the entire set of Instantaneous SIS URE values. This was done in parallel to the process that produced the results shown in Section 3.1.1. A five-degree uniform grid was used along with a 5 minute cadence. Further details on the implementation are provided in Appendix B.4.

Table 3.3 presents a summary of the results obtained by this alternate method. This table is in the same format as Table 3.2. Figure 3.2 (which is in the same format as Figure 3.1) presents the values in Table 3.3 in a graphical manner. The values in Table 3.3 are larger than the values in Table 3.2 by an average of 0.02 m. The maximum difference (alternate - original) for a given SV-month is 0.14 m; the minimum difference is -0.12 m.

Figure 3.3 is an illustration of the differences between the Monthly 95<sup>th</sup> percentile SIS URE values calculated by the two different methods. Each pair of monthly values for a given SV found in Table 3.2 and Table 3.3 were taken and the difference computed as the quantity [alternate - original]. The median, maximum, and minimum differences were then selected from each set and plotted in Figure 3.3. (Note: The single monthly value for SVN 26/PRN 26 is based on five days of data prior to decommissioning.) Figure 3.3 illustrates that the two methods agree to within 20 cm and generally a good deal less with the alternate method typically being a few cm larger.

None of the values in Table 3.3 exceed the threshold of 7.8 m. Therefore, the threshold is met for 2015 even under this alternate interpretation of the metric.

### 3.1.2 URE at Any AOD

The next URE metric considered is the calculation of URE at any AOD. This is associated with the following SPSPS08 Section 3-4 metrics:

- “ $\leq 12.8$  m 95% Global Average URE during Normal Operations at Any AOD”

This metric may be decomposed in a manner similar to the previous metrics. The key difference is the term “at any AOD” and the change in the threshold values. The

**Table 3.3:** Monthly 95<sup>th</sup> Percentile Values of SIS Instantaneous URE for all SVs in Meters (via Alternate Method)

SVN	PRN	Block	Jan.	Feb.	Mar.	Apr.	May	Jun.	Jul.	Aug.	Sept.	Oct.	Nov.	Dec.	2015
23	32	IIA	1.67	1.28	1.45	1.71	1.30	1.30	1.49	1.32	1.85	1.59	1.43	1.40	1.50
26	26	IIA	1.05												1.05
34	4	IIA	1.88	2.20	2.11	1.71	1.94	1.86	1.81	2.04	1.67	1.53	1.82		1.88
40	10	IIA	2.45	2.32	2.50	2.74	2.83	2.77	2.76						2.65
41	14	IIR	1.05	1.08	1.30	1.03	1.21	1.05	1.17	1.13	1.13	1.13	1.10	1.01	1.11
43	13	IIR	1.20	1.16	1.13	1.31	1.20	1.18	1.27	1.57	1.24	1.21	1.09	1.11	1.22
44	28	IIR	2.41	2.31	2.45	2.46	2.25	2.56	2.50	2.59	2.46	2.42	2.51	2.50	2.46
45	21	IIR	1.85	1.35	1.30	1.36	1.11	1.16	1.13	1.22	1.13	1.09	1.02	1.07	1.21
46	11	IIR	1.26	1.37	1.63	1.31	1.38	1.54	1.33	1.50	1.38	1.81	1.83	1.83	1.53
47	22	IIR	1.96	2.02	2.04	1.79	1.85	1.75	1.84	1.76	2.11	1.95	1.89	1.75	1.89
48	7	IIR-M	1.20	1.13	1.20	1.14	1.17	1.10	1.15	1.06	1.24	1.29	1.23	1.22	1.18
50	5	IIR-M	0.95	0.93	1.04	0.99	0.96	0.98	1.03	1.04	0.98	0.99	0.96	0.97	0.99
51	20	IIR	0.95	0.96	1.01	1.14	0.96	1.06	1.03	1.08	0.98	0.99	0.99	1.01	1.01
52	31	IIR-M	1.23	1.31	1.18	1.43	1.29	1.26	1.32	1.21	1.43	1.36	1.30	1.43	1.31
53	17	IIR-M	1.67	1.60	2.03	1.46	1.65	1.60	1.54	1.36	1.55	1.31	1.78	1.71	1.61
54	18	IIR	0.98	0.99	0.98	1.00	1.02	0.96	0.94	1.30	1.90	1.33	1.42	1.61	1.19
55	15	IIR-M	0.99	0.95	0.95	0.97	0.96	1.03	0.98	0.97	0.98	0.99	0.99	1.03	0.98
56	16	IIR	1.00	0.96	0.97	1.01	0.93	0.93	0.95	0.95	0.94	0.95	0.98	0.96	0.96
57	29	IIR-M	1.18	1.48	1.69	1.48	1.50	1.37	1.31	1.52	1.55	1.40	1.45	1.41	1.43
58	12	IIR-M	1.11	1.18	0.93	0.97	0.95	1.04	1.04	1.05	1.00	1.03	1.01	0.98	1.02
59	19	IIR	1.01	1.07	1.08	1.03	0.98	1.00	0.98	1.04	0.97	1.00	0.97	0.98	1.01
60	23	IIR	0.96	1.01	1.00	0.97	0.96	1.01	0.98	0.95	0.95	0.92	0.95	0.99	0.97
61	2	IIR	1.02	1.11	1.00	0.97	1.04	1.11	1.07	1.03	0.98	1.00	0.98	1.00	1.02
62	25	IIF	0.94	0.95	1.02	1.07	0.99	1.00	1.03	1.06	1.13	0.99	0.99	0.98	1.02
63	1	IIF	0.97	1.00	0.97	0.92	0.90	0.95	0.97	0.99	1.00	0.99	0.94	0.94	0.96
64	30	IIF	1.14	1.01	0.95	1.27	1.02	1.09	1.13	1.24	0.99	0.99	1.00	1.07	1.06
65	24	IIF	2.45	2.45	2.34	2.39	2.62	2.28	2.40	2.36	2.11	2.27	2.38	2.56	2.40
66	27	IIF	1.00	0.96	0.91	0.93	0.95	1.00	1.01	0.97	0.96	0.97	0.99	0.99	0.97
67	6	IIF	1.00	1.03	0.94	0.90	0.89	0.93	0.99	1.05	0.96	0.97	0.92	0.96	0.97
68	9	IIF	0.99	0.94	0.96	1.02	1.08	1.03	0.97	0.93	1.23	1.00	1.01	0.99	1.01
69	3	IIF	1.07	1.34	1.64	1.41	1.05	0.89	0.93	1.02	1.03	1.11	1.10	0.97	1.16
71	26	IIF				2.03	1.50	1.11	1.11	1.08	1.15	1.03	1.02	0.99	1.16
72	8	IIF								2.07	2.02	2.03	1.95	2.25	2.07
73	10	IIF												1.24	1.24
Block IIA			2.02	2.07	2.10	2.24	2.37	2.22	1.97	1.69	1.75	1.55	1.48	1.40	2.02
Block IIR/IIR-M			1.30	1.29	1.36	1.32	1.28	1.29	1.29	1.29	1.38	1.33	1.34	1.35	1.32
Block IIF			1.24	1.33	1.34	1.47	1.34	1.20	1.20	1.41	1.36	1.40	1.44	1.49	1.36
All SVs			1.41	1.43	1.47	1.52	1.44	1.40	1.35	1.36	1.42	1.38	1.38	1.40	1.41

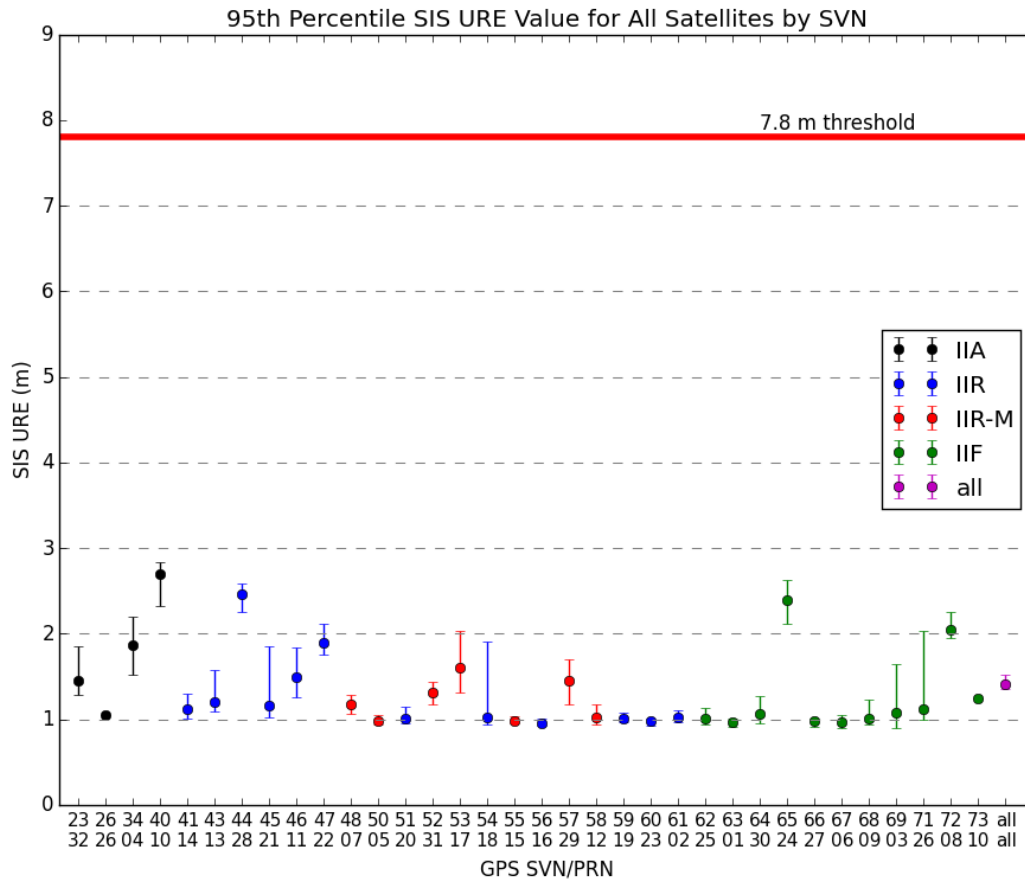


**Figure 3.2:** Range of the Monthly 95<sup>th</sup> Percentile Values for all SVs (via Alternate Method)

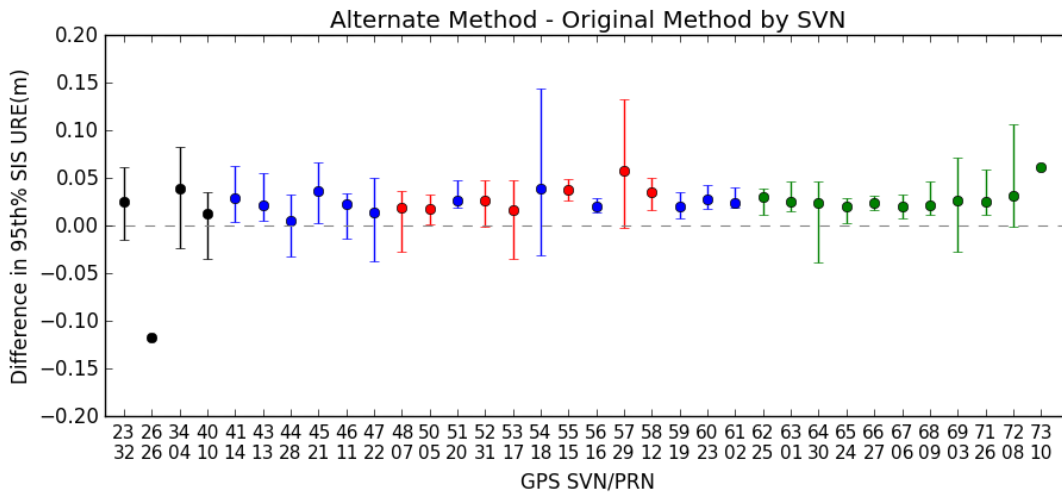


**Figure 3.3:** Range of Differences in Monthly Values for all SVs



phrase “at any AOD” is interpreted to mean that at any AOD where sufficient data can be collected to constitute a reasonable statistical set, the value of the required statistic should be  $\leq 12.8$  m. See Section 4.2 for a discussion of how the AOD is computed.

To examine this requirement, the same set of 30 s Instantaneous RMS SIS URE values used in Section 3.1.1 was analyzed using a bin approach. The details are covered in Appendix A. In summary, the RMS SIS URE values were divided into bins based on 15 minute intervals of AOD. The 95<sup>th</sup> percentile values for each bin were selected and the results were plotted as a function of the AOD.<sup>1</sup>

Figures 3.4 through Figure 3.9 show two curves: shown in blue is the 95<sup>th</sup> Percentile URE vs. AOD (in hours), and shown in green the count of points in each bin as a function of AOD. For satellites that are operating on the normal pattern (roughly one upload per day), the count of points in each bin is roughly equal from the time the upload becomes available until about 24 hours AOD. In fact, the nominal number of points can be calculated by multiplying the number of expected 30 s estimates in a 15 minute bin (30) by the number of days in the year (365). The result is 10950, or a little less than 11000. This corresponds well to the plateau area of the green curve for the well-performing satellites (e.g. Figures 3.7, 3.8, and 3.9). For satellites that are uploaded more frequently, the green curve will show a left-hand peak higher than the nominal count declining to the right. This is a result of the fact that there will be fewer points at higher AOD due to the more frequent uploads. The vertical scales on Figure 3.4 through 3.9 and the figures in Appendix A have been constrained to a constant value to aid in comparisons between the charts. Satellites that were only operational for part of the year (e.g. SVN 26, 34, 40, 71, 72, 73) will have a lower number of points per bin than the nominal.

The first three plots show the worst performing (i.e. highest URE values) Block IIA, Block IIR/IIR-M, and Block IIF SVs. These are SVN 40, SVN 44, and SVN 65 respectively. Note that the distribution of AOD samples for SVN 40 is concentrated at shorter values of AOD, which indicates that frequent uploads are occurring. SVN 44 shows similar behavior, but at a much larger AOD, indicating less frequent additional uploads.

The best performers for Block IIA, Block IIR/IIR-M, and Block IIF are shown in Figures 3.7 through 3.9. These figures show a very flat distribution of AODs, and the UREs appear to degrade roughly linearly with time, at least out to the point that the distribution (represented by the green curve) shows a marked reduction in the number of points.

The plots for all satellites are contained in Appendix A. (SVN 26 and SVN 73 are omitted from Appendix A as they broadcast for less than a month in 2015.) A review of the full set leads to the conclusion that the behaviors described in the previous two paragraphs are not block-specific but are rather characteristic of age or the type of

---

<sup>1</sup>*Bins with a small number of points are suppressed from the plots. Such bins tend to occur at the right-most end of the plots, and the results are sometimes dominated by outliers. To avoid such misleading distractions, we determine the bin with the maximum number of points, then plot bins from left-to-right until a bin is reached with  $\leq 10\%$  of the number of points in the bin with the maximum number of points.*

frequency standard. For example, two of the three Block IIA satellites exhibit evidence of more frequent uploads as indicated by an uneven distribution of observation across the time bins. Among the Block IIF SVs, the rate of URE growth is noticeably higher for the two satellites that use a Cesium frequency standard. While there are noticeable differences between individual satellites, all the results are well within the assertion for this metric.

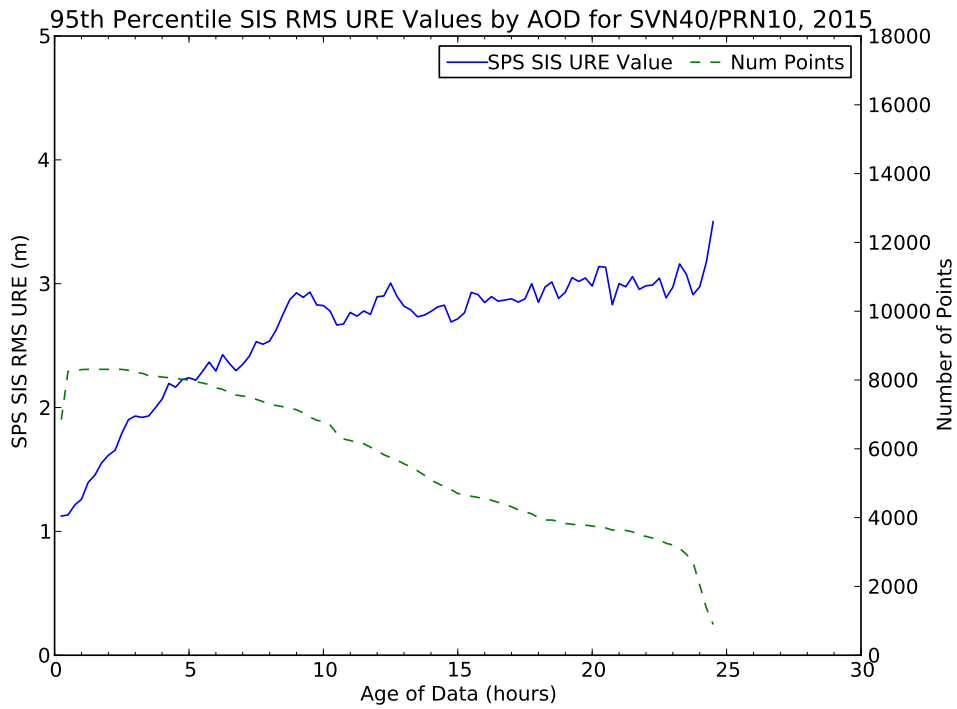


**Figure 3.4:** Worst Performing Block IIA SV in Terms of Any AOD (SVN 40/PRN 10)

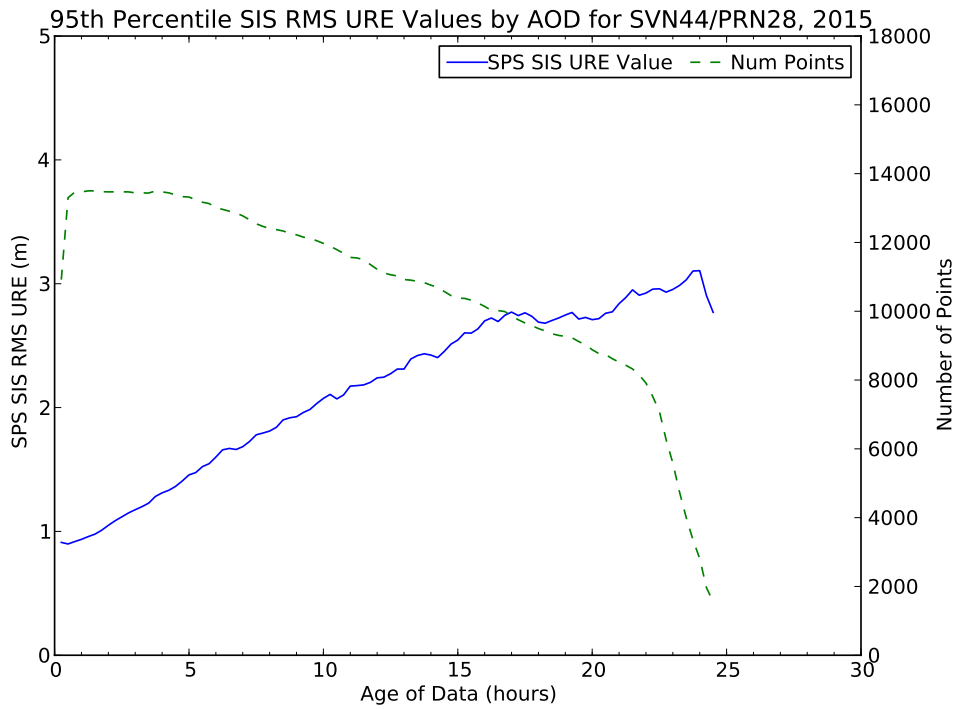


**Figure 3.5:** Worst Performing Block IIR/IIR-M SV in Terms of Any AOD (SVN 44/PRN 28)

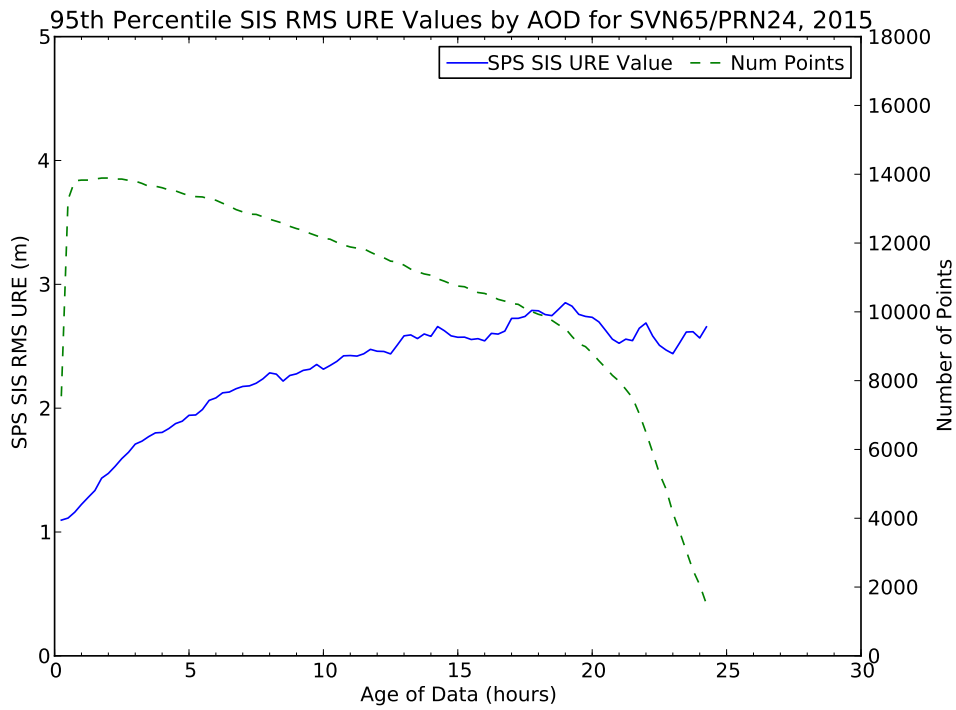


**Figure 3.6:** Worst Performing Block IIF SV in Terms of Any AOD (SVN 65/PRN 24)

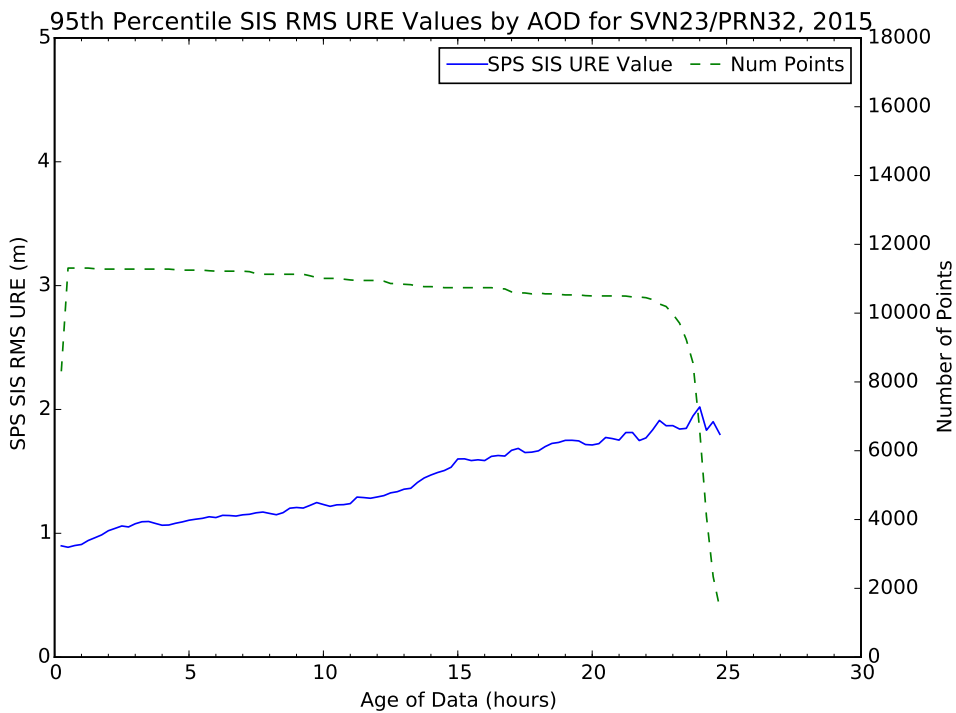


**Figure 3.7:** Best Performing Block IIA SV in Terms of Any AOD (SVN 23/PRN 32)

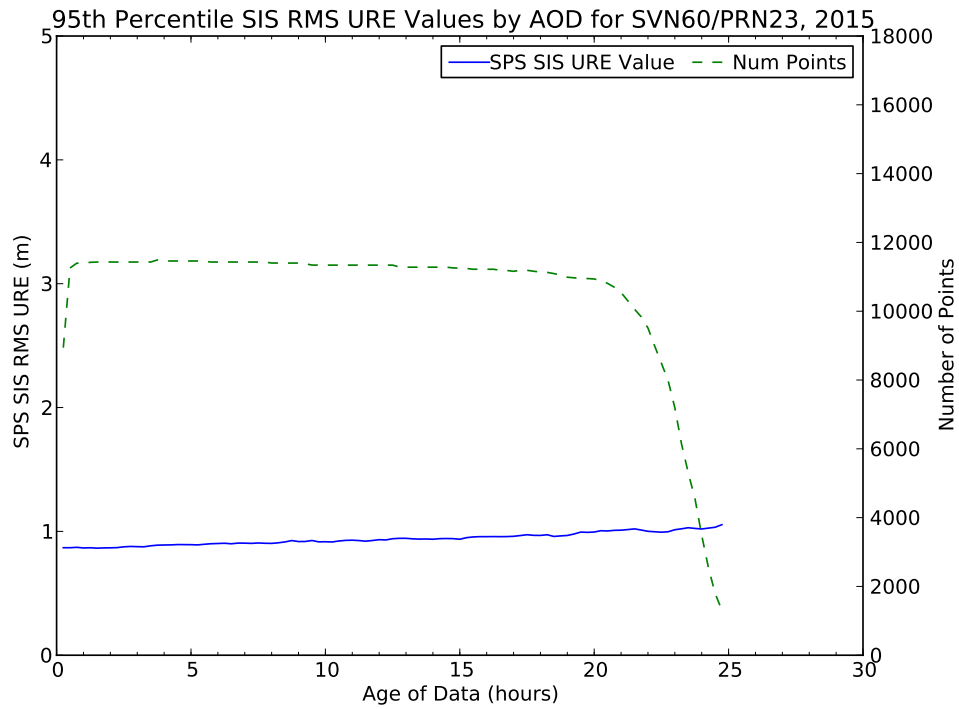


**Figure 3.8:** Best Performing Block IIR/IIR-M SV in Terms of Any AOD (SVN 60/PRN 23)

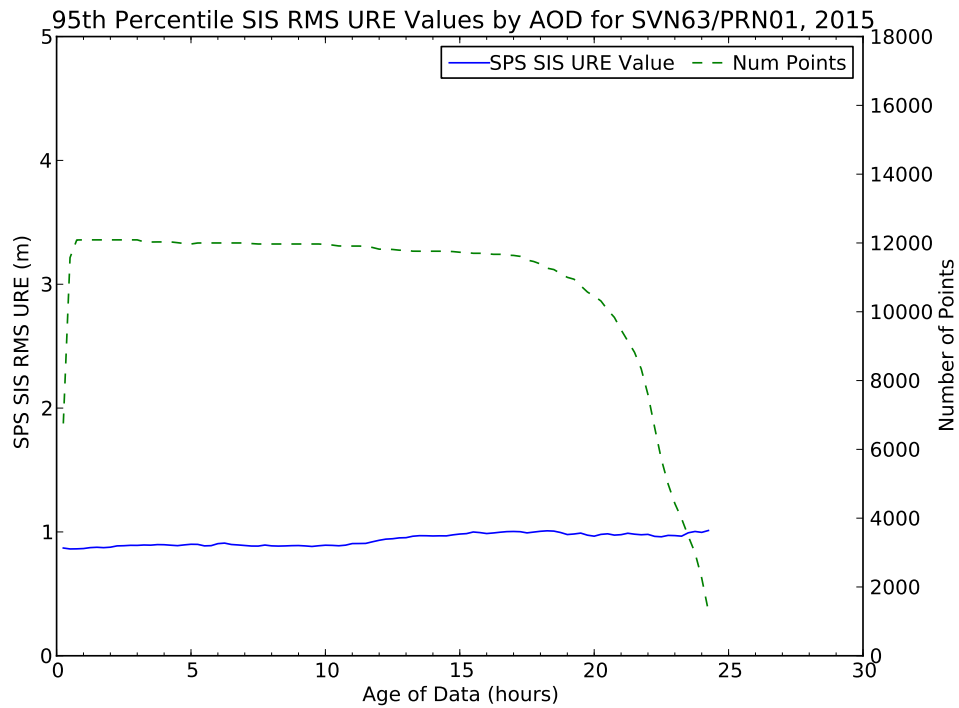


**Figure 3.9:** Best Performing Block IIF SV in Terms of Any AOD (SVN 63/PRN 01)

### 3.1.3 URE at Zero AOD

Another URE metric considered is the calculation of URE at Zero Age of Data (ZAOD). This is associated with the SPSPS08 Section 3-4 metric:

- “ $\leq 6.0$  m 95% Global Average URE during Normal Operations at Zero AOD”

This metric may be decomposed in a manner similar to the previous two metrics. The key difference is the term “at Zero AOD” and the change in the threshold values.

The broadcast ephemeris is never available to user equipment at ZAOD simply due to the delays inherent in preparing the broadcast ephemeris and uploading it to the SV. However, we can still make a case that this assertion is met by examining the 95<sup>th</sup> percentile SIS RMS URE value at 15 minutes AOD. These values are represented by the left-most data point on the red lines shown in Figure 3.4 through Figure 3.9. The ZAOD values should be slightly better than the 15 minute AOD values, or at worst roughly comparable. Inspection of the 15 minute AOD values shows that the values for all SVs are well within the 6.0 m value associated with the assertion. Therefore the assertion is fulfilled.

### 3.1.4 URE Bounding

The SPSPS08 asserts the following requirements for single-frequency C/A code:

- “ $\leq 30$  m 99.94% Global Average URE during Normal Operations”
- “ $\leq 30$  m 99.79% Worst Case Single Point Average URE during Normal Operations”

As noted earlier the 30 s instantaneous SIS RMS URE values were used to evaluate these requirements. However, there are limitations to our technique of estimating UREs that are worth noting such as fits across orbit/clock discontinuities, thrust events, and clock run-offs. These are discussed in Appendix B.5. As a result of these limitations, the UREs were used only as a screening tool to identify possible violations of this requirement. Possible candidate events were then screened further by examining the observed range deviations (ORDs) to determine actual values during the event.

The ORDs are formed using the observation data collected to support the position accuracy analysis described in Section 3.5.4. In the case of ORDs, the observed range is differenced from the range predicted by subtracting the known station position from the SV location derived from the broadcast ephemeris. The selected stations are geographically distributed such that at least two sets of observations are available for each SV at all times. As a result, any actual SV problems that would lead to a violation of this assertion will produce large ORDs from multiple stations.

The 30 s instantaneous SIS RMS URE values and the 30 s ORD values throughout 2015 were examined to determine if any values exceeded 30 m. No such values were found. As a result, these assertions are considered satisfied.

### 3.1.5 UTC Offset Error Accuracy

The SPS PS provides the following assertion regarding SPS PS UTC offset error (UTC OE) Accuracy:

- “ $\leq 40$  nsec 95% Global Average UTC OE during Normal Operations at Any AOD”

The conditions and constraints state that this assertion should be true for any healthy SPS SIS.

This assertion was evaluated by calculating the global average UTC OE at each 15 minute interval. The GPS-UTC offset available to the user was calculated based on the GPS broadcast navigation message data available from the SV at that time. The GPS-UTC offset truth information was provided by the USNO daily GPS-UTC offset values. A multi-day spline was fit to the daily truth values and the USNO value for GPS-UTC at each evaluation epoch was derived from this fit.

The selection and averaging algorithms are a key part of this process. The global average at each 15 minute epoch is determined by evaluating the UTC OE at each point on a 111 km  $\times$  111 km grid across the entire surface of the earth. (This grid spacing corresponds to roughly one degree at the Equator.) At each grid point, the algorithm determines the set of SVs visible at-or-above the 5° minimum elevation angle that are broadcasting a healthy indication in the navigation message. For each of these SVs, the UTC offset information in page 18, subframe 4 are compared in order to determine the data set that has an epoch time ( $t_{ot}$ ) that is the latest of those that fall in the range (*current time*)  $\leq t_{ot} \leq$  (*current time* + 72 hours). These data are used to form the UTC offset and UTC OE for that time-grid point.

The global averages at each evaluation epoch are assembled into monthly data sets. The 95<sup>th</sup> percentile values are then selected from these sets.

Table 3.4 provides the results for each month of 2015. None of these values exceed the assertion of 40 nsec. Therefore the assertion is verified for 2015.

## 3.2 SIS Integrity

### 3.2.1 URE Integrity

Under the heading of SIS Integrity, the SPSPS08 makes the following assertion in Section 3.5.1, Table 3.5-1:

- “ $\leq 1 \times 10^{-5}$  Probability Over Any Hour of the SPS SIS Instantaneous URE Exceeding the NTE Tolerance Without a Timely Alert During Normal Operations”

The associated conditions and constraints include a limitation to healthy SIS, a Not to Exceed (NTE) tolerance  $\pm 4.42$  times the upper bound on the user range accuracy (URA) currently broadcast, and a worst case for a delayed alert of 6 hours.

**Table 3.4:** 95<sup>th</sup> Percentile Global Average UTCOE for 2015

Month	95 <sup>th</sup> Percentile Global Avg. UTCOE (nsec)
Jan.	1.026
Feb.	1.645
Mar.	1.461
Apr.	2.252
May	1.437
Jun.	1.679
Jul.	1.358
Aug.	2.444
Sep.	2.023
Oct.	2.571
Nov.	1.460
Dec.	1.096

The reference to “a Timely Alert” in the assertion refers to any of a number of ways to issue an alert. See SPSPS08 Section A.5.5 for a complete description.

To estimate the worst-case probability of users experiencing misleading signal information (MSI), note that immediately below SPSPS08 Table 3.5-1 is an explanation that for a 32 SV constellation (full broadcast almanac) the corresponding average annual number of SPS SIS instantaneous URE integrity losses is 3. Assuming each of the 3 losses lasts no more than 6 hours over one year, the fraction of time in which MSI will occur is 0.002.

This assertion was verified using two methods:

- The Instantaneous SIS URE values at the worst case location in view of each SV at each 30 s interval were examined to determine the number of values that exceed  $\pm 4.42$  times the URA.
- ORDs from a network of tracking stations were examined to determine the number of values that exceed  $\pm 4.42$  times the URA.

Two methods were used due to the fact that each method may result in false positives in rare cases. For example, the URE values may be incorrect near discontinuities in the URE (as described in Appendix B.5). Similarly, the ORD values may be incorrect due to receiver or reception issues. Therefore, all reported violations are examined manually to determine whether a violation actually occurred, and if so, the extent of the violation.

Screening the 30 s instantaneous SIS URE values and the ORD data did not reveal any events for which this threshold was exceeded. Therefore the assertion is verified for 2015.



### 3.2.2 UTCOE Integrity

The SPS PS provides the following assertion regarding SPS PS UTCOE Integrity in Section 3.5.4:

- *“ $\leq 1 \times 10^{-5}$  Probability Over Any Hour of the SPS SIS Instantaneous UTCOE Exceeding the NTE Tolerance Without A Timely Alert during Normal Operations”*

The associated conditions and constraints include a limitation to healthy SIS, a NTE tolerance of  $\pm 120$  nsec, and the note that this holds true for any healthy SPS SIS. The reference to “a Timely Alert” in the assertion refers to any of a number of ways to issue an alert. See SPSPS08 Section A.5.5 for a complete description.

This assertion was evaluated by calculating the UTC offset for the page 18, subframe 4 data broadcast by each SV transmitting a healthy indication in the navigation message at each 15 minute interval. That offset was used to compute the corresponding UTCOE from truth data obtained from the USNO. Any UTCOE values that exceed the NTE threshold of  $\pm 120$  nsec were investigated to determine if they represent actual violations of the NTE threshold or were artifacts of data processing.

No values exceeding the NTE threshold were found in 2015. The value farthest from zero for the year was -4.5 nsec (during August). Therefore the assertion is verified for 2015.

## 3.3 SIS Continuity

### 3.3.1 Unscheduled Failure Interruptions

The metric is stated in SPSPS08 Table 3.6-1 as follows:

- *“ $\geq 0.9998$  Probability Over Any Hour of Not Losing the SPS SIS Availability from a Slot Due to Unscheduled Interruption”*

The conditions and constraints note the following:

- The empirical estimate of the probability is calculated as an average over all slots in the 24-slot constellation, normalized annually.
- The SPS SIS is available from the slot at the start of the hour.

The notion of SIS continuity is slightly more complex for an expandable slot, because multiple SVs are involved. Following SPSPS08 Section A.6.5, a loss of continuity is considered to occur when,

*“The expandable slot is in the expanded configuration, and either one of the pair of satellites occupying the orbital locations defined in Table 3.2-2 for the slot loses continuity.”*

Hence, the continuity of signal of the expanded slot will be determined by whether either SV loses continuity.

Another point is that there is some ambiguity in this metric, which is stated in terms of “a slot” while the associated Conditions and Constraints note that this is an average over all slots. Therefore both the per-slot and 24-slot constellation averages have been computed. As discussed below, while the per-slot values are interesting, the constellation average is the correct value to compare to the SPS PS metric.

Three factors must be considered in looking at this metric:

1. We must establish which SVs were assigned to which slots during the period of the evaluation.
2. We must determine when SVs were not transmitting (or not transmitting a PRN available to users).
3. We must determine which interruptions were scheduled vs. unscheduled.

The derivation of the SV/Slot assignments is described in Appendix E.

For purposes of this report, interruptions were considered to have occurred if one or more of the SV(s) assigned to the given slot is (are) unhealthy in the sense of SPSPS08 Section 2.3.2. The following specific indications were considered:

- If the health bits in navigation message subframe 1 are set to anything other than all zeros.
- If an appropriately distributed worldwide network of stations failed to collect any pseudorange data sets for a given measurement interval.

The latter case (failure to collect any data) indicates that the satellite signal was removed from service (e.g. non-standard code or some other means). The NGA MSN provides at least two-station visibility (and at least 90% three-station visibility) with redundant receivers at each station, both continuously monitoring up to 12 SVs in view. Therefore, if no data for a satellite are received for a specific time, it is highly likely that the satellite was not transmitting on the assigned PRN at that time. The 30 s Receiver Independent Exchange format (RINEX) [6] observation files from this network were examined for each measurement interval (i.e. every 30 s) for each SV. If at least one receiver collected a pseudorange data set on L1 C/A, L1 P(Y), and L2 P(Y) with a signal-to-noise level of at least 25 dB-Hz on all frequencies and no loss-of-lock flags, the SV is considered trackable at that moment. In addition, the 30 s IGS data collected to support the position accuracy estimates (Section 3.5.4) were

examined in a similar fashion to guard against any MSN control center outages that could have led to missing data across multiple stations simultaneously. This allows us to define an epoch-by-epoch availability for each satellite. Then, for each slot, each hour in year was examined, and if any SV occupying the slot was not available at the start of the hour, the hour was not considered as part of the evaluation of the metric. If the slot was determined to be available, then the remaining data was examined to determine if an outage occurred during the hour.

The preceding criteria were applied to determine the times and durations of interruptions. After this was done, the Notice Advisories to Navstar Users (NANUs) effective in 2015 were reviewed to determine which of these interruptions could be considered scheduled interruptions as defined in SPSPS08 Section 3.6. The scheduled interruptions were removed from consideration for purposes of assessing continuity of service. When a slot was available at the start of an hour but a scheduled interruption occurred during the hour, the hour was assessed based on whether data were available prior to the scheduled outage.

Unscheduled interruptions are not always documented with a NANU. A small number of short-duration outages not covered by NANUs were observed. When such outages occurred on satellites that are assigned to one of 24 slots, the outage was counted in evaluating this assertion.

Scheduled interruptions as defined in the ICD-GPS-240 [7] have a nominal notification time of 96 hours prior to the outage. Following the SPSPS08 Section 2.3.5, scheduled interruptions announced 48 hours in advance are not to be considered as contributing to the loss of continuity. So to contribute to a loss of continuity, the notification time for a scheduled interruption must occur less than 48 hours in advance of the interruption. In the case of an interruption not announced in a timely manner, the time from the start of the interruption to the moment 48 hours after notification time can be considered as a potential unscheduled interruption (for continuity purposes). However, a healthy SIS must exist at the start of any hour for an interruption to be considered to occur.

The following NANU types are considered to represent (or modify) scheduled interruptions (assuming the 48-hour advance notice is met):

- FCSTDV - Forecast Delta-V
- FCSTMX - Forecast Maintenance
- FCSTEXTD - Forecast Extension
- FCSTRESCD - Forecast Rescheduled
- FCSTUUFN - Forecast Unusable Until Further Notice

The FCSTSUMM (Forecast Summary) NANU that occurs after the outage is referenced to confirm the actual beginning and ending time of the outage.

For scheduled interruptions that extend beyond the period covered by a FCSTDV or FCSTMX NANU, the uncovered portion will be considered an unscheduled

interruption. However, if a FCSTEXTD NANU extending the length of a scheduled interruption is published 48 hours in advance of the effective time of extension, the interruption will remain categorized as scheduled. It is worth reiterating that, for the computation of the metric, only those hours for which a valid SIS is available from the slot at the start of the hour are actually considered in the computation of the values.

Table 3.5 is a summary of the results of the assessment of SIS continuity. Interpreting the metric as being averaged over the constellation, the constellation exceeded the goal of 0.9998 probability of not losing the SPS SIS availability due to a unscheduled interruption.

**Table 3.5:** Probability Over Any Hour of Not Losing Availability Due to Unscheduled Interruption

Plane-Slot	# of Hours with the SPS SIS available at the start of the hour <sup>b</sup>	# of Hours with Unscheduled Interruption <sup>c</sup>	Fraction of Hours in Which Availability was Not Lost
A1	8760	0	1.00000
A2	8760	1	0.99989
A3	8760	0	1.00000
A4	8760	0	1.00000
B1 <sup>a</sup>	6122	0	1.00000
B2	8760	0	1.00000
B3	8760	0	1.00000
B4	8760	0	1.00000
C1	8760	0	1.00000
C2	8760	1	0.99989
C3	8760	0	1.00000
C4	8760	0	1.00000
D1	8760	0	1.00000
D2 <sup>a</sup>	8726	2	0.99977
D3	8760	0	1.00000
D4	8760	0	1.00000
E1	8760	0	1.00000
E2	8760	0	1.00000
E3	8760	0	1.00000
E4	8760	0	1.00000
F1	8760	0	1.00000
F2 <sup>a</sup>	8760	1	0.99989
F3	8760	0	1.00000
F4	8740	1	0.99989
All Slots	207548	6	0.99997

<sup>a</sup>When B1, D2, and F2 are configured as expandable slots, both slot locations must be occupied by an available satellite for the slot to be counted as available.

<sup>b</sup>There are 8760 hours in 2015.

<sup>c</sup>Number of hours in which SPS SIS was available at the start of the hour and during the hour either (1.) an SV transmitted navigation message with subframe 1 health bits set to other than all zeroes without a scheduled outage, (2.) signal lost without a scheduled outage, or (3.) the URE NTE tolerance was violated.

To put this in perspective, there were 8760 hours in 2015. The required probability of not losing SPS SIS availability implies that there be less than  $8760 \times (1 - 0.9998) = 1.75$  hours that experience unscheduled interruptions in a year. If this were a per-slot metric, this would mean no slot may experience more than one unscheduled interruption in a year. The maximum number of unscheduled interruptions over the 24 slot constellation is given by  $8760 \times 24 \times (1 - 0.9998) = 42$  unscheduled hours that experience interruptions. This is less than two unscheduled interruptions per SV per year but allows for the possibility that some SVs may have no unscheduled interruptions while others may have more than one.

Slot B1 is considered empty at the beginning of 2015. The slot has been configured as an expanded slot for some time. (See Appendix E for more on sources of plane-slot information.) However, on 28 March 2013 the satellite occupying the B1F half of slot B1 experienced an unscheduled interruption (SVN 35/PRN 30, see NANU 2013022). It was later decommissioned (NANU 2013027). B1F remained empty until 20 April 2015 when SVN 70/PRN 26 was set initially usable (NANU 2015028). As a result, for purposes of this analysis, slot B1 is considered empty for several weeks at the beginning of 2015. In Table 3.5, the row associated with B1 shows a lower number of hours of availability than all other rows. While there are multiple unscheduled interruptions in slot B1 during 2015, the unavailable period at the beginning of the year is not counted as it was counted at the beginning of the interruption in 2013. This outage is also addressed in Section 3.4 in terms of the impact on availability.

Returning to Table 3.5, across the constellation slots the total number of hours lost was 6. This is smaller than the maximum number of hours of unscheduled interruptions (42) available to meet the metric (see the previous paragraph) and leads to empirical value for the fraction of hours in which SIS continuity was maintained of 0.99997. Therefore, this assertion is considered fulfilled in 2015.

### 3.3.2 Status and Problem Reporting Standards

#### 3.3.2.1 Scheduled Events

The SPSPS08 makes the following assertion in Section 3.6.3 regarding notification of scheduled events affecting service:

- *“Appropriate NANU issued to Coast Guard and the FAA at least 48 hours prior to the event”*

While beyond the assertion in the performance standards, ICD-GPS-240 [7] states a nominal notification time of 96 hours prior to outage start and an objective of 7 days prior to outage start.

This metric was evaluated by examining the NANUs provided throughout the year and comparing the NANU periods to outages observed in the data. In general, scheduled events are described in a pair of NANUs. The first NANU is a forecast of when the

outage will occur. The second NANU is provided after the outage and summarizes the actual start and end times of the outage. (This is described in ICD-GPS-240 Section 10.1.1.)

Table 3.6 summarizes the pairs found for 2015. The two leftmost columns provide the SVN/PRN of the subject SV. The next three columns specify the NANU #, type, and date/time of the NANU for the forecast NANU. These are followed by three columns that specify the NANU #, the date/time of the NANU for the FCSTSUMM NANU provided after the outage, and the date/time of the beginning of the outage. The final column is the time difference between the time the forecast NANU was released and the beginning of the actual outage (in hours). This represents the length of time between the release of the forecast and the actual start of the outage.

**Table 3.6:** Scheduled Events Covered in NANUs for 2015

SVN	PRN	Prediction NANU			Summary NANU (FCSTSUMM)			Notice (hrs)
		NANU #	TYPE	Release Time	NANU #	Release Time	Start Of Outage	
43	13	2015001	FCSTDV	02 Jan 1648Z	2015006	09 Jan 1340Z	09 Jan 0544Z	156.93
64	30	2015008	FCSTDV	30 Jan 2008Z	2015009	06 Feb 0558Z	06 Feb 0112Z	149.07
41	14	2015013	FCSTDV	27 Feb 1807Z	2015014	05 Mar 2128Z	05 Mar 1512Z	141.08
57	29	2015015	FCSTDV	07 Mar 0000Z	2015016	12 Mar 1054Z	12 Mar 0431Z	124.52
23	32	2015017	FCSTDV	13 Mar 1854Z	2015018	20 Mar 1530Z	20 Mar 0906Z	158.20
23	32	2015020	FCSTMX	26 Mar 2110Z	2015023	31 Mar 2335Z	30 Mar 0005Z	74.92
56	16	2015024	FCSTDV	09 Apr 2231Z	2015025	15 Apr 2134Z	15 Apr 1608Z	137.62
50	05	2015026	FCSTDV	17 Apr 1618Z	2015029	22 Apr 0352Z	21 Apr 2129Z	101.18
54	18	2015031	FCSTDV	24 Apr 1901Z	2015033	01 May 0552Z	01 May 0031Z	149.50
61	02	2015034	FCSTDV	05 May 2207Z	2015035	13 May 0150Z	12 May 1809Z	164.03
68	09	2015038	FCSTDV	19 May 2042Z	2015040	28 May 1922Z	28 May 1400Z	209.30
45	21	2015041	FCSTDV	29 May 1507Z	2015045	05 Jun 0902Z	05 Jun 0327Z	156.33
52	31	2015044	FCSTDV	04 Jun 2050Z	2015047	11 Jun 1505Z	11 Jun 0952Z	157.03
62	25	2015043	FCSTMX	04 Jun 1954Z	2015048	11 Jun 1814Z	11 Jun 1452Z	162.97
66	27	2015046	FCSTMX	10 Jun 1515Z	2015051	15 Jun 1657Z	15 Jun 1332Z	118.28
65	24	2015049	FCSTMX	12 Jun 1531Z	2015055	17 Jun 1451Z	17 Jun 1129Z	115.97
71	26	2015050	FCSTMX	12 Jun 1550Z	2015056	19 Jun 0351Z	19 Jun 0047Z	152.95
67	06	2015052	FCSTMX	16 Jun 1545Z	2015058	24 Jun 0121Z	23 Jun 2054Z	173.15
64	30	2015053	FCSTMX	16 Jun 1551Z	2015061	25 Jun 2043Z	25 Jun 1658Z	217.12
51	20	2015054	FCSTDV	16 Jun 1556Z	2015062	26 Jun 0846Z	26 Jun 0240Z	226.73
69	03	2015059	FCSTMX	24 Jun 1929Z	2015063	30 Jun 2237Z	30 Jun 1812Z	142.72
68	09	2015060	FCSTMX	24 Jun 2012Z	2015064	01 Jul 2232Z	01 Jul 1951Z	167.65
34	04	2015065	FCSTMX	02 Jul 1435Z	2015067	09 Jul 0621Z	09 Jul 0317Z	156.70
53	17	2015070	FCSTDV	21 Jul 1929Z	2015071	28 Jul 2144Z	28 Jul 1624Z	164.92
59	19	2015072	FCSTDV	07 Aug 1617Z	2015074	13 Aug 1057Z	13 Aug 0319Z	131.03
46	11	2015075	FCSTDV	19 Aug 1724Z	2015076	25 Aug 1942Z	25 Aug 1256Z	139.53
67	06	2015077	FCSTDV	26 Aug 1915Z	2015078	02 Sep 0058Z	01 Sep 1859Z	143.73
60	23	2015079	FCSTDV	03 Sep 2006Z	2015081	11 Sep 1003Z	11 Sep 0330Z	175.40
47	22	2015092	FCSTDV	03 Dec 1724Z	2015097	11 Dec 0025Z	10 Dec 1636Z	167.20
47	22	2015096	FCSTMX	10 Dec 2104Z	2015099	17 Dec 2041Z	15 Dec 2347Z	122.72
69	03	2015098	FCSTDV	11 Dec 1655Z	2015100	18 Dec 0135Z	17 Dec 2025Z	147.5
Average Notice Period								151.81

To meet the assertion in the performance standard, the number of hours in the rightmost column of Table 3.6 should always be greater than 48.0. The average notice was over 151 hours. The shortest notice was 75 hours. Therefore, the assertion has been met.

Satellites were decommissioned three times in 2015. These were handled as special cases of scheduled outages. A FCSTUUFN (Forecast unusable until further notice) NANU was provided specifying when the satellite would be set unusable. Following this, a DECOM (decommission) NANU was provided following the actual event. The details on the notice provided by these four pairs are provided in Table 3.7. Each of the pairs meets the assertion of the SPS PS and the nominal time of the ICD-GPS-240 for scheduled events.

**Table 3.7:** Decommissioning Events Covered in NANUs for 2015

SVN	PRN	FCSTUUFN NANU		DECOM NANU			Notice (hrs)
		NANU #	Release Time	NANU #	Release Time	End of Unusable Period	
26	26	2015002	02 Jan 1659Z	2015005	06 Jan 2219Z	05 Jan 1750Z	72.85
40	10	2015066	07 Jul 1852Z	2015069	16 Jul 2217Z	16 Jul 1624Z	213.53
34	04	2015089	28 Oct 2019Z	2015091	03 Nov 2216Z	02 Nov 2222Z	122.05
Average Notice Period							136.03

### 3.3.2.2 Unscheduled Outages

The SPS PS provides the following assertion in Section 3.6.3 regarding notification of unscheduled outages or problems affecting service:

- *“Appropriate NANU issued to Coast Guard and the FAA as soon as possible after the event”*

The ICD-GPS-240 states that the nominal notification times is less than 1 hour after the start of the outage with an objective of 15 minutes.

This metric was evaluated by examining the NANUs provided throughout the year and comparing the NANU periods to outages observed in the data. Unscheduled events may be covered by either a single NANU or a pair of NANUs. In the case of a brief outage, a NANU with type UNUNOREF (unusable with no reference) is provided to detail the period of the outage. In the case of longer outages, a UNUSUFN (unusable until further notice) is provided to inform users of an ongoing outage or problem. This is followed by a NANU with type UNUSABLE after the outage is resolved. (This is described in detail in ICD-GPS-240 Section 10.1.2.)

Table 3.8 provides a list of the unscheduled outages found in the NANU information for 2015. The two leftmost columns provide the SVN/PRN of the subject SV. The next two columns provide the NANU #, and date/time of the UNUSUFN NANU. These are followed by three columns that specify the NANU #, the date/time of the NANU for the UNUSABLE NANU provided after the outage, and the date/time of the beginning of the outage. The final column is the time difference between the time the outage began and the time the UNUSUFN NANU was released (in minutes). For the UNUNOREF NANUs, only the last four columns are used.

**Table 3.8:** Unscheduled Events Covered in NANUs for 2015

SVN	PRN	UNUSUFN NANU		UNUSABLE/UNUNOREF NANU			Lag Time (minutes)
		NANU #	Release Time	NANU #	Release Time	Start Of Event	
46	11	2015011	19 Feb 0631Z	2015012	20 Feb 1444Z	19 Feb 0450Z	101.00
34	04	2015036	19 May 1241Z	2015037	19 May 1454Z	19 May 1246Z	-5.00
41	14	2015082	08 Oct 1510Z	2015083	08 Oct 1523Z	08 Oct 1500Z	10.00
60	23	2015085	19 Oct 1853Z	2015086	20 Oct 1437Z	19 Oct 1800Z	53.00
63	01	2015094	09 Dec 1125Z	2015095	09 Dec 1305Z	09 Dec 1003Z	82.00
66	27			2015042	03 Jun 1510Z	03 Jun 0603Z	547.00
52	31			2015057	22 Jun 1936Z	22 Jun 1919Z	17.00
Average Lag Time							115.00

Because the performance standard states only “as soon as possible after the event”, there is no evaluation to be performed. However, the data are provided for information. With respect to the nominal notification times provided in ICD-GPS-240, it appears that the nominal times are typically met (five of seven cases in 2015), but there are exceptions.

### 3.3.2.3 Suspect NANUs

We noticed three suspect NANUs in 2015.

NANU 2015021: This is a NANU of type GENERAL that announced the decommissioning of SVN 38. It is suspect in two ways.

- A decommissioning event should be announced in a DECOM NANU and not in a GENERAL NANU.
- SVN 38 was already decommissioned on 30 Oct 2014. The announcement was provided in NANU 2014083. Both NANUs agree that SVN 38 was unusable as of 30 Oct 2014. However, NANU 2014083 states SVN 38 was removed from the constellation on 30 Oct 2014 while NANU 2015021 states SVN 38 was removed on 26 Mar 2015. It is worth noting that SVN 38 was transmitting for a period in early 2015 (see NANU 2015003) but remained unusable throughout (as in a typical test of a spare SV). Because SVN 38 was not usable in 2015, we regard NANU 2014083 as correct and NANU 2015021 as being provided in error.

NANU 2015022: This NANU is of type UNUSABLE and references the previous NANU 2015020 which is of type FCSTMX. NANU 2015020 is later appropriately closed by NANU 2015023 which is of the expected type of FCSTSUMM. We assume NANU 2015022 was released in error and have ignored it.

NANU 2015082: This NANU is an UNUSUFN but contains no information regarding the start time of the event. NANU 2015083 was issued 13 minutes after NANU 2015082, and contains identical start and end times. NANU 2015084 is a GENERAL NANU that explains NANU 2015082 was sent in error with NANU 2015083 following to close out NANU 2015082.



## 3.4 SIS Availability

### 3.4.1 Per-slot Availability

The SPSPS08 Section 3.7.1 makes two linked statements in this area:

- “ $\geq 0.957$  Probability that a Slot in the Baseline Configuration will be Occupied by a Healthy Navstar Satellite Broadcasting a Useable SPS SIS”
- “ $\geq 0.957$  Probability that a Slot in the Expanded Configuration will be Occupied by a pair of Healthy Navstar Satellites Each Broadcasting a Useable SPS SIS”

The constraints include the note that this is to be calculated as an average over all slots in the 24-slot constellation, normalized annually.

The derivation of the SV/Slot assignments is described in Appendix E.

This metric was verified by examining the status of each SV in the Baseline 24- Slot configuration (or pair of SVs in an Expandable Slot) at every 30 s interval throughout the year. The health status was determined from the subframe 1 health bits of the ephemeris being broadcast at the time of interest. In addition, data from monitor station networks were examined to verify that the SV was broadcasting a trackable signal at the time. The results are summarized in Table 3.9.

Slot B1 presented an unusual situation in 2015. Slot B1 has been configured as an expanded slot for some time. (See Appendix E for more on sources of plane-slot information.) However, the B1F half of slot B1 was unoccupied from the beginning of 2015 through April 20, 2015 (the events that led to this are described in Section 3.3). Therefore, B1 is considered empty for this period as only B1A was occupied.

It is unlikely that this unoccupied slot was noticed by users. As will be shown in Section 3.5, the Dilution of Precision (DOP) values were excellent throughout 2015. Therefore, 2 SOPS was managing the constellation, including the excess satellites above the slot definitions, in such a manner as to assure good geometric coverage.

The average availability for the constellation was 0.9867, meeting the threshold of 0.957. The availability values for all slots except B1 were better than the threshold. Therefore the assertions being tested in this section were met.

### 3.4.2 Constellation Availability

The SPSPS08 makes two linked statements in this area:

- “ $\geq 0.98$  Probability that at least 21 Slots out of the 24 Slots will be Occupied Either by a Satellite Broadcasting a Healthy SPS SIS in the Baseline 24-Slot Configuration or by a Pair of Satellites Each Broadcasting a Healthy SPS SIS in the Expanded Slot Configuration”

- “ $\geq 0.99999$  Probability that at least 20 Slots out of the 24 Slots will be Occupied Either by a Satellite Broadcasting a Healthy SPS SIS in the Baseline 24-Slot Configuration or by a Pair of Satellites Each Broadcasting a Healthy SPS SIS in the Expanded Slot Configuration”

**Table 3.9:** Per-Slot Availability in 2015 for Baseline 24 Slots

Plane-Slot	# Missing Epochs	Available
A1	391	0.999628
A2	622	0.999408
A3	1009	0.999040
A4	0	1.000000
B1 <sup>a</sup>	316960	0.698478
B2	397	0.999622
B3	0	1.000000
B4	0	1.000000
C1	751	0.999286
C2	403	0.999617
C3	0	1.000000
C4	614	0.999416
D1	912	0.999132
D2 <sup>a</sup>	4250	0.995957
D3	658	0.999374
D4	1220	0.998839
E1	1123	0.998932
E2	0	1.000000
E3	758	0.999279
E4	601	0.999428
F1	752	0.999285
F2 <sup>a</sup>	930	0.999115
F3	943	0.999103
F4	3141	0.997012
All Slots	336435	0.986665

*Notes: For each slot there were 1051200 total 30 s epochs.*

<sup>a</sup>When B1, D2, and F2 are configured as expandable slots, both slot locations must be occupied by an available satellite for the slot to be counted as available.

To evaluate this metric the subframe 1 health condition and the availability of signal was evaluated for each SV every 30 s for all of 2015. Following a literal reading of the requirement, the number of SVs broadcasting a healthy SIS was examined for each measurement interval and assigned to the correct slot. For non-expanded baseline slots, if an SV qualified as being in the slot and was transmitting a healthy signal, the slot was counted as occupied. For expanded slots, the slot was counted as occupied if two healthy SVs were found: one in each of the two portions of the expanded slot. If the count of occupied slots was greater than 20, the measurement interval was counted as a 1; otherwise the measurement interval was assigned a zero. The sum of the 1 values was

then divided by the total number of measurement intervals. The value for 2015 is 1.00. Thus, both requirements are satisfied.

While this satisfies the metric, it does not provide much information on exactly how many SVs are typically healthy. To address this, at each 30 s interval the number of SVs broadcasting a healthy SIS was counted. This was both for count of occupied slots and for the number of SVs. The daily averages as a function of time are shown in Figure 3.10. As is clear, the number of occupied slots always exceeds 21.

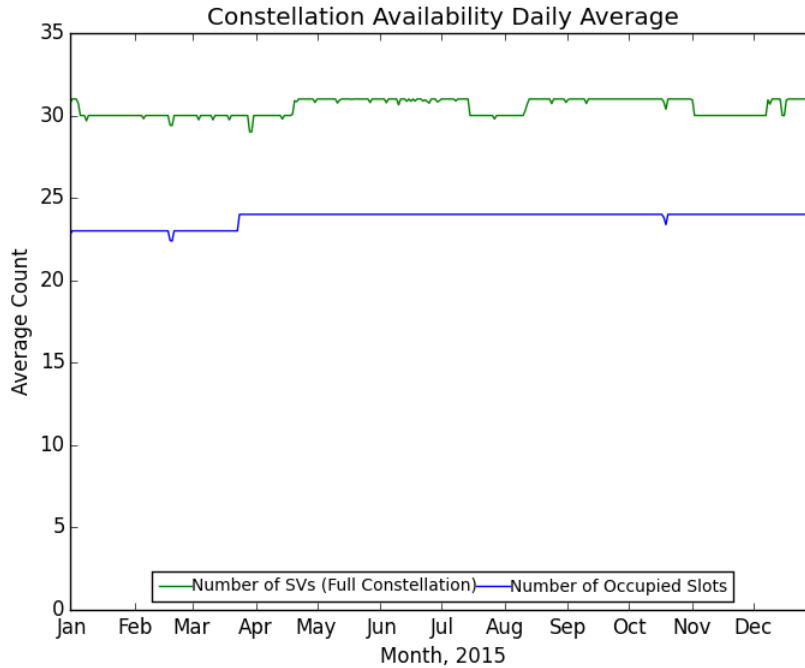


**Figure 3.10:** Daily Average Number of Occupied Slots

### 3.4.3 Operational Satellite Counts

In Table 3.7-3, the SPSPS08 states:

- “ $\geq 0.95$  Probability that the Constellation will Have at least 24 Operational Satellites Regardless of Whether Those Operational Satellites are Located in Slots or Not”

Under “Conditions and Constraints” the term Operational is defined as

*“any satellite which appears in the transmitted navigation message almanac... regardless of whether that satellite is currently broadcasting a healthy SPS SIS or not or whether the broadcast SPS SIS also satisfies the other performance standards in this SPS PS or not.”*

Given the information presented in sections 3.4.1 and 3.4.2, we conclude that 24 SVs were operational 100% of the time for 2015. However, the navigation message was examined for consistency. The process selected an almanac for each day in 2015. IS-GPS-200 Section 20.3.3.5.1.3 [2] assigns a special meaning to the SV health bits in the almanac's subframe 4 Page 25 and subframe 5 Page 25 (Data ID 51 and 63). When these bits are set to all ones it indicates "the SV which has that ID is not available, and there might be no data regarding that SV in that page of subframes 4 and 5...". Given this definition, the process examines the subframe 4 and 5 health bits for the individual SVs and counts the number of SVs for which the health bits are other than all ones. The results are shown in Figure 3.11. This plot is very similar to the full constellation healthy satellite count shown in Figure 3.10. The almanac health data are not updated as frequently as those in Subframe 1. As a result, the plot in Figure 3.11 contains only integer values. Therefore, on days when it appears the operational SV count is lower than the number of healthy SVs in the constellation, these reflect cases where an SV was set unhealthy for a small portion of the day. In Figure 3.10, such effects are averaged over the day, yielding a higher availability.

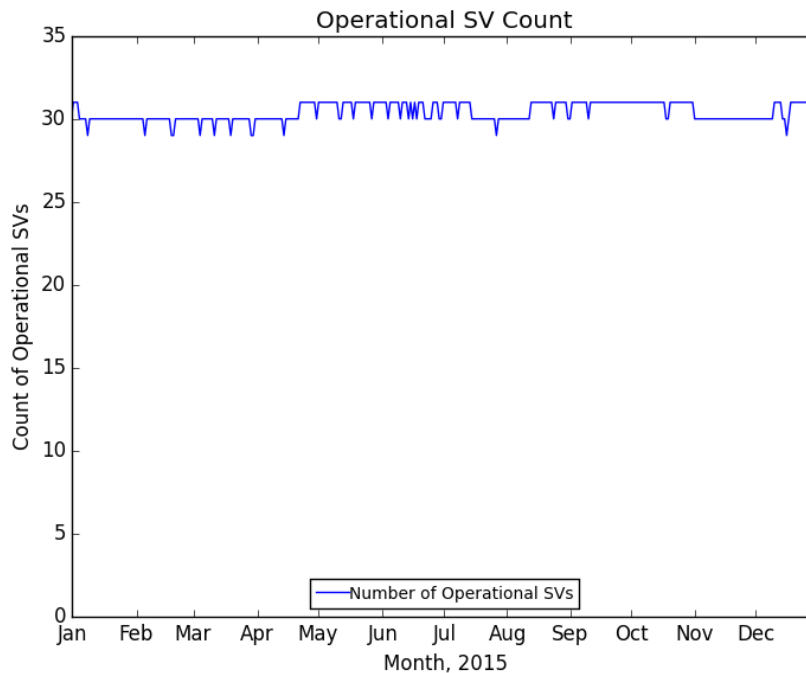


**Figure 3.11:** Count of Operational SVs by Day

## 3.5 Position/Time Domain Standards

### 3.5.1 PDOP Availability

Given representative user conditions and considering any 24 hour interval the SPSPS08 calls for:

- “ $\geq 98\%$  global PDOP of 6 or less”
- “ $\geq 88\%$  worst site PDOP of 6 or less”

Based on the definition of a representative receiver contained in SPS PS Section 3.8, a  $5^\circ$  minimum elevation angle is used for this evaluation.

These assertions were verified empirically throughout 2015 using a regularly-spaced grid, containing  $N_{grid}$  points, to represent the terrestrial service volume at zero altitude and an archive of the broadcast ephemerides transmitted by the SVs throughout the year. All healthy, transmitting SVs were considered. The grid was  $111 \text{ km} \times 111 \text{ km}$  (roughly  $1^\circ \times 1^\circ$  at the Equator). The time started at 0000Z each day and stepped through the entire day at one minute intervals (1440 points/day, or more generically,  $N_t$ ). The overall process followed is similar to that defined in Section 5.4.6 of the GPS Civil Monitoring Performance Specification (CMPS) [8].

The Position Dilution of Precision (PDOP) values were formed using the traditional PDOP algorithm, without regard for the impact of terrain. The coordinates of the grid locations provided the ground positions at which the PDOP was computed. The position of each SV was computed from the broadcast ephemeris available to a receiver at the time of interest. The only filtering performed was to identify and exclude from the calculations any unhealthy SVs (those with subframe 1 health bits set to other than all 0's). The results of each calculation were tested with respect to the threshold of  $PDOP \leq 6$ . If the condition was violated, a bad PDOP counter associated with the particular grid point,  $b_i$  for  $1 \leq i \leq N_{grid}$ , was incremented.

At least four SVs must be in view for a valid PDOP computation. This condition was fulfilled for all grid points at all times in 2015.

Once the PDOPs had been computed across all grid points, for each of the 1440 time increments during the day, the percentage of time the PDOP was  $\leq 6$  for the day was computed using the formula:

$$(\%PDOP \leq 6) = 100 \left( 1 - \frac{\sum_{i=1}^{N_{grid}} b_i}{N_{grid} N_t} \right)$$

The worst site for a given day was identified from the same set of counters by finding the site with the maximum bad count:  $b_{max} = \max_i b_i$ . The ratio of  $b_{max}$  to  $N_t$  is an estimate of the fraction of time the worst site PDOP exceeds the threshold. This value was averaged over the year, and the percentage of time the PDOP is  $\leq 6$  was computed.

Table 3.10 summarizes the results of this analysis for the configurations of all SVs available. The first column (“Average daily % over 2015”) duplicates the values shown in Section 2. The additional column is provided to verify that no single-day value actually dropped below the goal. From this table we conclude that the PDOP availability metrics are met for 2015.

**Table 3.10:** Summary of PDOP Availability

Metric	Average daily % over 2015	Minimum daily % over 2015
$\geq 98\%$ Global Average PDOP $\leq 6$	$\geq 99.999$	99.958
$\geq 88\%$ Worst site PDOP $\leq 6$	99.655	98.194

In addition to verifying the standard, several additional analyses go beyond the direct question and speak to the matter of how well the system is performing on a more granular basis. The remainder of this Chapter describes those analyses and results.

### 3.5.2 Additional DOP Analysis

There are several ways to look at Dilution of Precision (DOP) values when various averaging techniques are taken into account. Assuming a set of DOP values, each identified by latitude ( $\lambda$ ), longitude ( $\theta$ ), and time ( $t$ ), then each individual value is represented by  $DOP_{\lambda,\theta,t}$ .

The global average DOP for a day,  $\langle DOP \rangle(\text{day})$ , is defined to be

$$\langle DOP \rangle(\text{day}) = \frac{\sum_t \sum_\theta \sum_\lambda DOP_{\lambda,\theta,t}}{N_{grid} \times N_t}$$

Another measure of performance is the average DOP over the day at the worst site,  $\langle DOP \rangle_{worst\ site}$ . In this case the average over a day is computed for each unique latitude/longitude combination and the worst average of the day is taken as the result.

$$\langle DOP \rangle_{worst\ site}(\text{day}) = \max_{\lambda,\theta} \left( \frac{\sum_t DOP_{\lambda,\theta,t}}{N_t} \right)$$

This statistic is the most closely related to the description of worst site used in Section 3.5.1.

The average of worst site DOP,  $\langle DOP_{worst\ site} \rangle$ , is calculated by obtaining the worst DOP in the latitude/longitude grid at each time, then averaging these values over the day.

$$\langle DOP_{worst\ site} \rangle(\text{day}) = \frac{\sum_t \max_{\lambda,\theta} (DOP_{\lambda,\theta,t})}{N_t}$$

This represents a measure of the worst DOP performance. It is not particularly useful from the user’s point of view because the location of the worst site varies throughout the day.

Finally, the absolute worst time-point in a day is given by taking the maximum of the individual DOP values for all locations and all times.

$$DOP_{abs. \text{ worst}}(day) = \max_{\lambda, \theta, t}(DOP_{\lambda, \theta, t})$$

Given that the  $\langle DOP \rangle_{worst \ site}(day)$  is most closely related to the worse site definition used in Section 3.5.1, this is the statistic that will be used for “worst site” in the remainder of this section. For 2015, both  $\langle DOP \rangle_{worst \ site}(day)$  and  $\langle DOP_{worst \ site} \rangle(day)$  satisfy the SPS PS assertions.

It is worth noting the following mathematical relationship between these quantities:

$$\langle DOP \rangle \leq \langle DOP \rangle_{worst \ site} \leq \langle DOP_{worst \ site} \rangle \leq DOP_{abs. \text{ worst}}$$

This serves as a sanity check on the DOP results in general and establishes that these metrics are increasingly sensitive to outliers.

In calculating the percentage of the time that the  $\langle DOP \rangle$  and  $\langle DOP \rangle_{worst \ site}$  are within bounds, several other statistics were calculated which provide insight into the availability of the GPS constellation throughout the world. Included in these statistics are the annual means of the daily globally average DOP and the  $\langle DOP \rangle_{worst \ site}$  values. These values are presented in Table 3.11, with values for 2012 through 2014 provided for comparison. The average number of satellites and the fewest satellites visible across the grid are calculated as part of the DOP calculations. Also shown in Table 3.11 are the annual means of the global average number of satellites visible to grid cells on a 111 km  $\times$  111 km (latitude by longitude) global grid and the annual means of the number of satellites in the worst-site grid cell (defined as seeing the fewest number of satellites). It should be noted that the worst site for each of these values was not only determined independently from day-to-day, it was also determined independently for each metric. That is to say, it is not guaranteed that the worst site with respect to Horizontal DOP (HDOP) is the same as the worst site with respect to PDOP. For all quantities shown in Table 3.11 the values are very similar across all four years.

There are a few other statistics that can add insight regarding the GPS system availability. The primary availability metric requires that the globally averaged PDOP be in-bounds at least 98% of the time. There are two related values: the number of days for which the PDOP is in bounds and the 98<sup>th</sup> percentile of the daily globally averaged PDOP values. Similarly, calculations can be done for  $\langle DOP \rangle_{worst \ site}$  criteria of having the PDOP  $\leq 6$  greater than 88% of the time. Table 3.12 presents these values.

Table 3.12 shows that the average DOP values for 2015 are nearly identical to previous years.

**Table 3.11:** Additional DOP Annually-Averaged Visibility Statistics for 2012 through 2015

	$\langle DOP \rangle$				$\langle DOP \rangle_{worst\ site}$			
	2015	2014	2013	2012	2015	2014	2013	2012
Horizontal DOP	0.85	0.86	0.83	0.84	0.97	0.99	0.96	0.96
Vertical DOP	1.37	1.39	1.35	1.36	1.71	1.73	1.69	1.69
Time DOP	0.70	0.81	0.78	0.79	0.92	0.94	0.91	0.91
Position DOP	1.62	1.64	1.59	1.60	1.88	1.89	1.85	1.85
Geometry DOP	1.81	1.83	1.77	1.79	2.08	2.10	2.05	2.05
Number of visible SVs	10.33	10.30	10.71	10.44	5.16	4.97	5.65	5.94

**Table 3.12:** Additional PDOP Statistics

	2015	2014	2013	2012
Percentage of Days with the $\langle PDOP \rangle \leq 6$	100	100	100	100
Percentage of Days with the $\langle PDOP \rangle$ at Worst Site $\leq 6$	100	100	100	100
98 <sup>th</sup> Percentile of $\langle PDOP \rangle$	1.65	1.67	1.63	1.65
88 <sup>th</sup> Percentile of $\langle PDOP \rangle_{worst\ site}$	1.91	1.91	1.88	1.87

Behind the statistics are the day-to-day variations. Figure 3.12 provides a time history of the four PDOP metrics considering all satellites for 2015. Four metrics are plotted:

- Daily Global Average PDOP,  $\langle PDOP \rangle$
- Average Worst Site PDOP,  $\langle PDOP \rangle_{worst\ site}$
- Average PDOP at Worst Site,  $\langle PDOP_{worst\ site} \rangle$
- Absolute Worst PDOP,  $PDOP_{abs.\ worst}$

$PDOP_{abs.\ worst}$  is most sensitive to outliers and has features that are idiosyncratic to the particular events in a year, such as SV outages. This is because  $PDOP_{abs.\ worst}$  is the only quantity that does not include averaging.



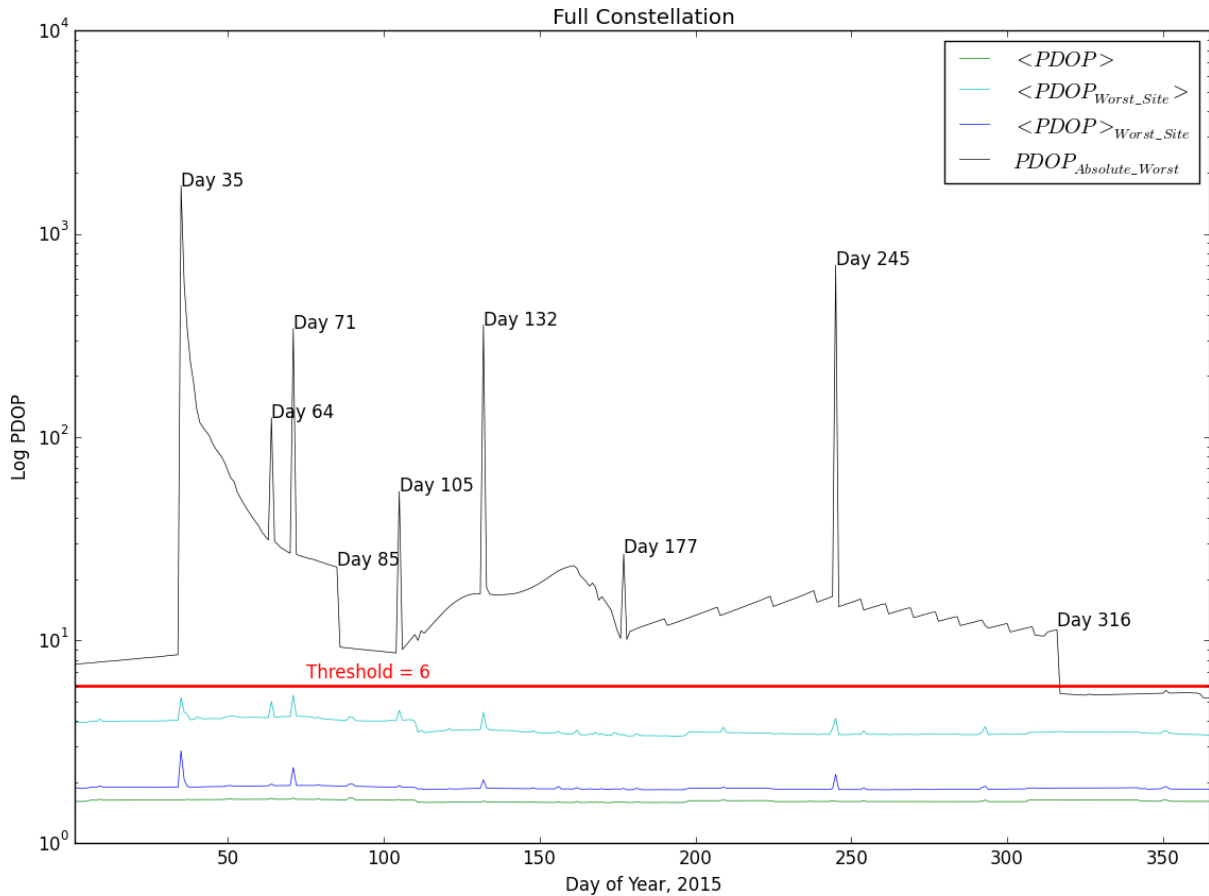


**Figure 3.12:** Daily PDOP Metrics Using all SVs, 2015

The  $PDOP_{abs.worst}$  trace for 2015 shown in Figure 3.12 has several features that were examined in further detail.

The large values on days 064, 071, 105, 132, 177, and 245 are each the result of single SVs being set unhealthy. The SVs and NANUs are listed in Table 3.13. Generally, these spikes are of limited duration and effect only a small area at a given moment.

The elevated worst DOP time-history trace between Day 035 and Day 316 in Figure 3.12 is not typical. (Figures for the previous two years are provided in Figure 3.13 and Figure 3.14 for comparison.) Despite the appearance of high worst-point PDOP values, it is unlikely that this presented a problem to users. These high worst-point PDOP values were very short duration spikes (generally less than a minute) that were visible in very small areas.

As an example, we'll describe the situation surrounding the worst point value on Day 035. The daily analysis indicates a maximum value located at 63.00 N, 36.44 E at time 01:11. Table 3.14 summarizes a DOP analysis for this location at one second intervals. The left side of Table 3.14 shows the situation on Day 034, when there was no large value observed. The right side of Table 3.14 shows the situation on Day 035, when the large values occurred. The two tables are aligned such that each row corresponds to the

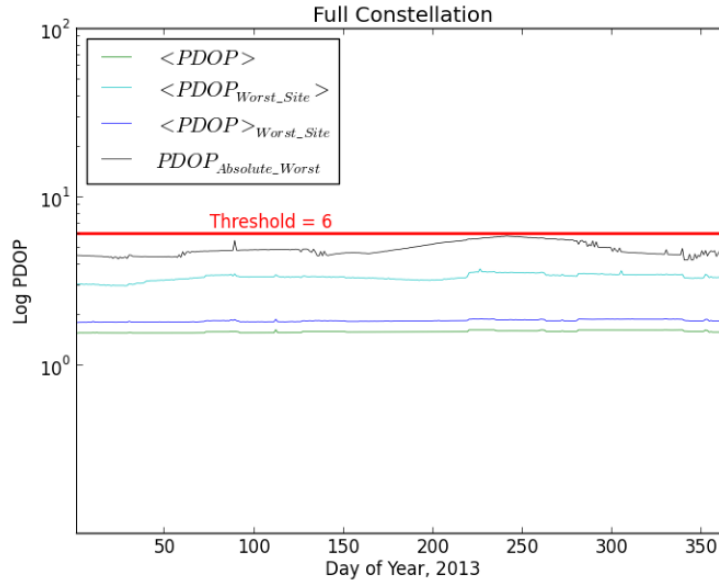


Figure 3.13: Daily PDOP Metrics Using All SVs, 2013

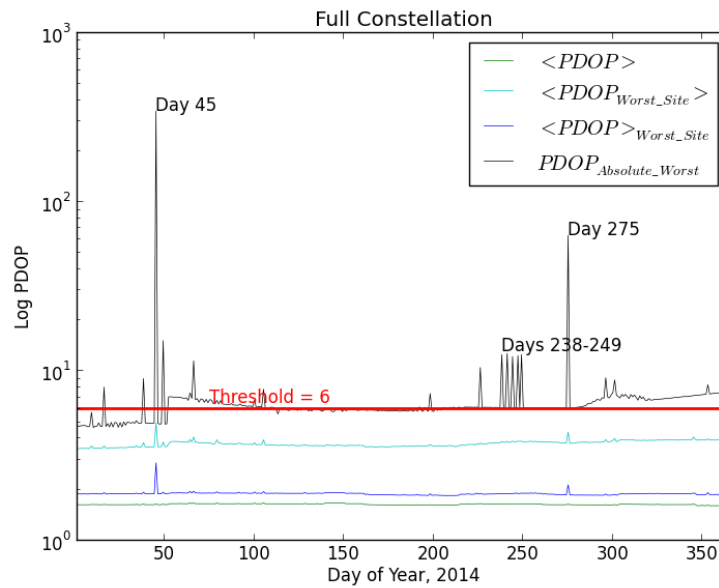


Figure 3.14: Daily PDOP Metrics Using All SVs, 2014

**Table 3.13:** Satellite and NANUs Associated with Single-Day Large DOP Values

Day of Year	Unhealthy SV		NANU
	SVN	PRN	
064	41	14	2015014
071	57	29	2015016
105	56	16	2015025
132	61	02	2015035
177	51	20	2015062

same sidereal time. That is to say the nominal ground tracks should be the same for each row.

The location of the SVs relative to the point of interest at the time of the large value on Day 035 is illustrated in Figure 3.15. This plot shows a polar projection looking down at the earth over the time-location at which the  $PDOP_{abs. worst}$  occurred. The satellite locations at the time of the  $PDOP_{abs. worst}$  are shown as circles labeled with PRN number. The thick green lines illustrate the path of the SV for the preceding 15 minutes. The thin blue lines are the projection of the SV path for the next 15 minutes. Note that SVN 38/PRN 8 highlighted in red was already decommissioned at this time. It was broadcasting an unhealthy signal throughout the period, so it was not included in the analysis.

Considering this plot in association with the data in Table 3.14, it can be seen that on Day 035, SVN 68/PRN 09 left the field of view of the location at 1:10:58 and SVN 48/PRN 07 did not come into view until 1:11:05. During that six second interval, only four SVs were in view. All of these SVs were located above  $30^\circ$  in elevation with respect to the location of interest, leaving no lines of sight to any low-elevation SVs (needed to help reduce uncertainty in the horizontal plane). The satellites drifted between Day 034 and Day 035 in a manner in which the hole did not exist on Day 034 and was evident on Day 035.

The preceding analysis shows that the duration of the period of large values was very short. To determine the area over which the effect was observed, a different type of analysis is needed. The program that produces the grid data creates a log of all the times and grid points for which the PDOP exceeds a value of 10. Recall that the grid size is 111 km. The daily log files show that only a SINGLE grid point observes an absolute worst point PDOP value greater than 10. Therefore, this large value is not only limited in duration but also very limited in the area it effects.

This summary describes the worst PDOP values found by this particular analysis, but it should be noted that this analysis may not reflect actual user experience. The analysis also assumes that the broadcast orbit is immediately available and ignores the 18 s-30 s required to collect the necessary subframe 1, 2, 3 data. In addition, this analysis is based on a firm  $5^\circ$  elevation angle cutoff, consistent with the constraints in the performance standard. However, some user equipment continues to track SVs as

**Table 3.14:** DOP Results for 63N, 36.44E on Day 34/35

Day 034				Day 035			
HH:MM:SS	PDOP	#SVs	List of SVs	HH:MM:SS	PDOP	#SVs	List of SVs
01:14:35	1.8	6	5 9 16 21 25 29	01:10:39	1.8	6	5 9 16 21 25 29
01:14:36	1.8	6		01:10:40	1.8	6	
01:14:37	1.8	6		01:10:41	1.8	6	
01:14:38	1.8	6		01:10:42	4.6	5	5 9 16 21 29
01:14:39	1.8	6		01:10:43	4.6	5	
01:14:40	1.8	6		01:10:44	4.6	5	
01:14:41	1.8	6		01:10:45	4.6	5	
01:14:42	1.8	6		01:10:46	4.6	5	
01:14:43	1.8	6		01:10:47	4.6	5	
01:14:44	1.8	6		01:10:48	4.6	5	
01:14:45	4.6	5	5 9 16 21 29	01:10:49	4.6	5	
01:14:46	4.6	5		01:10:50	4.6	5	
01:14:47	4.6	5		01:10:51	4.6	5	
01:14:48	4.6	5		01:10:52	4.6	5	
01:14:49	4.6	5		01:10:53	4.6	5	
01:14:50	4.6	5		01:10:54	4.6	5	
01:14:51	4.6	5		01:10:55	4.6	5	
01:14:52	4.6	5		01:10:56	4.6	5	
01:14:53	4.6	5		01:10:57	4.6	5	
01:14:54	4.6	5		01:10:58	4.6	5	
01:14:55	4.6	5		01:10:59	1997.9	4	5 16 21 29
01:14:56	4.6	5		01:11:00	1719.7	4	
01:14:57	4.6	5		01:11:01	1509.5	4	
01:14:58	4.6	5		01:11:02	1345.1	4	
01:14:59	4.6	5		01:11:03	1213.0	4	
01:15:00	4.6	5		01:11:04	1104.5	4	
01:15:01	4.6	5		01:11:05	4.8	5	5 7 16 21 29
01:15:02	4.6	5		01:11:06	4.8	5	
01:15:03	4.6	5		01:11:07	4.8	5	
01:15:04	4.6	5		01:11:08	4.8	5	
01:15:05	4.6	5		01:11:09	4.8	5	
01:15:06	4.8	5	5 7 16 21 29 <sup>a</sup>	01:11:10	4.8	5	
01:15:07	4.8	5		01:11:11	4.8	5	
01:15:08	4.8	5		01:11:12	4.8	5	
01:15:09	4.8	5		01:11:13	4.8	5	
<sup>b</sup>	-	-		-	-	-	
01:15:21	4.8	5		01:11:25	4.8	5	
01:15:22	4.8	5		01:11:26	4.8	5	
01:15:23	4.8	5		01:11:27	4.8	5	
01:15:24	4.8	5		01:11:28	4.8	5	
01:15:25	4.8	5		01:11:29	1.8	6	5 7 16 18 21 29
01:15:26	4.8	5		01:11:30	1.8	6	
01:15:27	4.8	5		01:11:31	1.8	6	
01:15:28	4.8	5		01:11:32	1.8	6	
01:15:29	4.8	5		01:11:33	1.8	6	
01:15:30	4.8	5		01:11:34	1.8	6	
01:15:31	1.8	6	5 7 16 18 21 29	01:11:35	1.8	6	
01:15:32	1.8	6		01:11:36	1.8	6	
01:15:33	1.8	6		01:11:37	1.8	6	
01:15:34	1.8	6		01:11:38	1.8	6	

<sup>a</sup>Note that one SV was dropped (PRN 9) and one added (PRN 7) within a one-second interval.

<sup>b</sup>12 seconds of repeated data omitted.

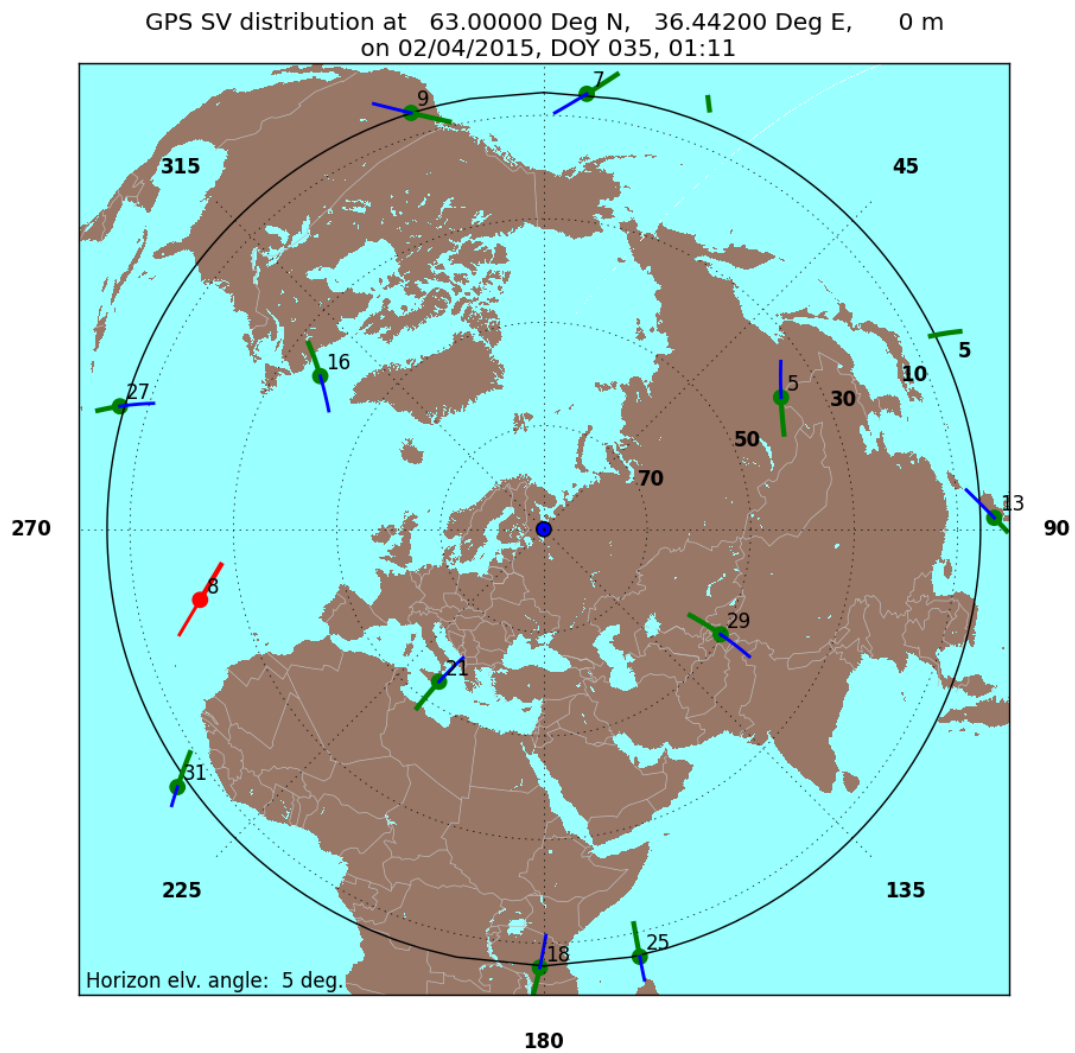


Figure 3.15: GPS Visibility on Day 035 at 01:11 Relative to 63N, 36.44E

low as possible until the signal is lost. Such a receiver may not have experienced these large values as other SVs came into view providing alternate means of achieving good PDOP values prior to losing the SV dropping below  $5^\circ$ . In addition, given the very short durations of these worst points, implementations that differed on how to round the elevation angle value could achieve different results.

As a result, we conclude that in 2015 there existed a larger-than-normal probability that high PDOP values might be observed over small areas for very short periods of time. However, the user impact was almost certainly negligible. In addition, these short events do not result in a violation of any of the assertions in the performance standards.

### 3.5.3 Position Service Availability

The positioning and timing availability standards are stated in Table 3.8-2 of SPSPS08 as follows:

- “ $\geq 99\%$  Horizontal Service Availability, average location”
- “ $\geq 99\%$  Vertical Service Availability, average location”
- “ $\geq 90\%$  Horizontal Service Availability, worst-case location”
- “ $\geq 90\%$  Vertical Service Availability, worst-case location”

The conditions and constraints associated with the standards include the specification of a 17 m horizontal 95<sup>th</sup> percentile threshold and a 37 m vertical 95<sup>th</sup> percentile threshold.

These are derived values as described in the sentence preceding SPSPS08 Table 3.8-2:

*“The commitments for maintaining PDOP (Table 3.8-1) and SPS SIS URE accuracy (Table 3.4-1) result in support for position service availability standards as presented in Table 3.8-2.”*

Because the commitments for PDOP and constellation SPS SIS URE have not only been met, but exceeded, this assertion in the SPSPS08 implies that the position and timing availability standards have also been fulfilled. A direct assessment of these metrics was not undertaken.

### 3.5.4 Position Accuracy

The positioning accuracy standards are stated in Table 3.8-3 of SPSPS08 as follows:

- “ $\leq 9$  m 95% Horizontal Error Global Average Position Domain Accuracy”

- “ $\leq 15$  m 95% Vertical Error Global Average Position Domain Accuracy”
- “ $\leq 17$  m 95% Horizontal Error Worst Site Position Domain Accuracy”
- “ $\leq 37$  m 95% Vertical Error Worst Site Position Domain Accuracy”

These are derived values as described in the sentence preceding SPSPS08 Table 3.8-3:

*“The commitments for maintaining PDOP (Table 3.8-1) and SPS SIS URE accuracy (Table 3.4-1) result in support for position service availability standards as presented in Table 3.8-3.”*

Because the commitments for PDOP and constellation SPS SIS URE have been met and exceeded, then the position and timing accuracy standards have also been fulfilled.

While this answer is technically correct, it is not very helpful. Position accuracy is the primary reason that GPS exists. At the same time, position accuracy is a particularly difficult metric to evaluate due to the fact that GPS provides the SIS, but the user is responsible for appropriately processing the SIS to derive a position.

Section 2.4.5 of SPSPS08 provides usage assumptions for the SPS PS and some of the notes in Section 2.4.5 are relevant to the question of position determination. The following is quoted from section 2.4.5:

*“The performance standards in Section 3 of this SPS PS do not take into consideration any error source that is not under direct control of the Space Segment or Control Segment. Specifically excluded errors include those due to the effects of:*

- *Signal distortions caused by ionospheric and/or tropospheric scintillation*
- *Residual receiver ionospheric delay compensation errors*
- *Residual receiver tropospheric delay compensation errors*
- *Receiver noise (including received signal power and interference power) and resolution*
- *Multipath and receiver multipath mitigation*
- *User antenna effects*
- *Operator (user) error”*

In addition, at the beginning of Section 3.8, the SPSPS08 explains that in addition to the error exclusions listed in 2.4.5, the following assumptions are made regarding the SPS receiver:

*“The use of a representative SPS receiver that:*

- *is designed in accordance with IS-GPS-200*
- *is tracking the SPS SIS from all satellites in view above a 5° mask angle... It is assumed the receiver is operating in a nominal noise environment...*
- *accomplishes satellite position and geometric range computations in the most current realization of the WGS 84 Earth-Centered, Earth-Fixed (ECEF) coordinate system.*
- *generates a position and time solution from data broadcast by all satellites in view*
- *compensates for dynamic Doppler shift effects on nominal SPS ranging signal carrier phase and C/A code measurements.*
- *processes the health-related information in the SIS and excludes marginal and unhealthy SIS from the position solution.*
- *ensures the use of up-to-date and internally consistent ephemeris and clock data for all satellites it is using in its position solution.*
- *loses track in the event a GPS satellite stops transmitting a trackable SIS.*
- *is operating at a surveyed location (for a time transfer receiver)."*

ARL:UT adopted the following approach for computing a set of accuracy statistics:

1. 30 s GPS observations were collected from the NGA GPS monitor station network and a similar set of 18 IGS stations. This decision addressed the following concerns:
  - (a) All stations selected collect dual-frequency observations. Therefore the first-order ionospheric effects can be eliminated from the results.
  - (b) All stations selected collect weather observations. The program that generates the positions (PRSOLVE) uses the weather data to eliminate first order tropospheric effects.
  - (c) The receiver thermal noise will not be eliminated, but both the NGA and IGS stations are generally using the best available equipment, so effects will be limited.
  - (d) Similarly, multipath cannot be eliminated, but both networks use antennas designed for multipath reduction, and station sites are chosen to avoid the introduction of extraneous multipath.
  - (e) Antenna phase center locations for such stations are very well known. Therefore, position truth is readily available.
2. Process the data using a comprehensive set of broadcast ephemerides that have been checked for consistency. The set of ephemerides used in the URE studies



- described in Section 3.1 of this report had already been extensively tested and examined. They constitute a complete (or very nearly complete) set of the broadcast ephemeris available for 2015.
3. Process the collected observations using the PRSOLVE program of the ARL:UT-hosted open source GPS Toolkit (GPSTk)[9]. Note:
    - (a) PRSOLVE meets the relevant requirements listed above. For example, SV positions are derived in accordance with IS-GPS-200, the elevation mask is configurable, weather data is used to estimate tropospheric effects, and WGS 84 [10] conventions are used. Data from unhealthy SVs were removed from PRSOLVE using an option to exclude specific satellites.
    - (b) PRSOLVE is highly configurable. Several of the items in the preceding list of assumptions are configuration parameters to PRSOLVE.
    - (c) Any other organization that wishes to reproduce the results should be able to do so. (Both the algorithm and the IGS data are available.)
  4. Process the collected 30 s observations in two ways:
    - (a) Use all SVs in view without data editing in an autonomous pseudorange solution to generate 30 s position residuals at all sites.
    - (b) Use a receiver autonomous integrity monitoring (RAIM) algorithm (another PRSOLVE option) to remove outlier pseudorange measurements from which a “clean” set of 30 s position residuals is generated at all sites. The RAIM algorithm used by PRSOLVE is dependent on several parameters, the two most important of which are the RMS limit on the post-fit residuals (default: 3.0 m) and the number of SVs that can be eliminated in the RAIM process (default: unlimited). This analysis was conducted using the default values.
  5. Compute statistics on each set of data independently.

In contrast to previous years, we conducted the elevation angle processing with a 5° minimum elevation angle for greater agreement with the standard. (Previous years were processed with a 10° minimum elevation angle.)

This process yields four sets of results organized as detailed in Table 3.15.

**Table 3.15:** Organization of Positioning Results

Case	Constellation Considered	Data Editing Option	Data Source
1	All in View	RAIM	IGS Data
2			NGA Data
3		None	IGS Data
4			NGA Data

Once the solutions are computed, two sets of statistics are developed. The first set is a set of daily average values across all stations. In the second set, the worst site is determined on a day-to-day basis and the worst site 95<sup>th</sup> percentile values are computed. These are empirical results and should not be construed to represent a proof that the metrics presented in the standard have been met. Instead, they are presented as a means of corroboration that the standards have been met through the fulfillment of the more basic commitments of PDOP and SPS SIS URE.

#### 3.5.4.1 Results for Daily Average

Using the approach outlined above, position solutions were computed at each 30 s interval for data from both the NGA and IGS stations. In the nominal case in which all stations are operating for a complete day, this yields 2880 solutions per station per day. Truth positions for the IGS stations were taken from the weekly Station Independent Exchange format (SINEX) files. Truth locations for the NGA stations were taken from station locations defined as part of the latest WGS84 adjustment with corrections for station velocities applied.

Residuals between estimated locations and the truth locations were computed (using PRSOLVE options) in the form of North, East and Up components in meters. The horizontal residual was computed from the North and East components, and the vertical residual was computed from the absolute value of the Up component. As a result, the residuals will have non-zero mean values. The statistics on the residuals were compiled across all stations in a set for a given day. Figure 3.16 through Figure 3.19 show the daily average for the horizontal and vertical residuals corresponding to the options shown in Table 3.15.

The statistics associated with the processing are provided in Table 3.16 through Table 3.19. There is one table each for the mean, median, maximum, and standard deviation of the daily values across 2015. The results are organized in this fashion to facilitate comparison of the same quantity across the various processing options. The results are expressed to the centimeter level. This choice of precision is based on the fact that the truth station positions are known only at the few-centimeter level.

The following general observations may be drawn from the charts and the supporting statistics:

- Outliers - Figure 3.17 shows a number of large outliers for the IGS averages computed with a simple pseudorange solution and no data editing. The outliers are distributed among several stations. These outliers are missing from Figure 3.16. This indicates the importance of conducting at least some level of data editing in the positioning process.
- Mean & Median values - The means and medians of the position residuals given in Table 3.16 and Table 3.17 are nearly identical for the NGA data sets, suggesting that if there are any 30 s position residual outliers, they are few in

**Table 3.16:** Mean of Daily Average Position Errors for 2015

Quantity	Data Source	Position Residual Mean (m)	
		RAIM	No Editing
Horizontal	IGS Data	1.37	8.09
	NGA Data	1.08	1.10
Vertical	IGS Data	2.10	10.56
	NGA Data	1.46	1.49

**Table 3.17:** Median of Daily Average Position Errors for 2015

Quantity	Data Source	Position Residual Median (m)	
		RAIM	No Editing
Horizontal	IGS Data	1.38	1.42
	NGA Data	1.08	1.09
Vertical	IGS Data	2.10	2.18
	NGA Data	1.45	1.48

**Table 3.18:** Maximum of Daily Average Position Errors for 2015

Quantity	Data Source	Position Residual Maximum (m)	
		RAIM	No Editing
Horizontal	IGS Data	1.57	262.05
	NGA Data	1.17	1.25
Vertical	IGS Data	2.44	176.48
	NGA Data	1.61	1.77

**Table 3.19:** Standard Deviation of Daily Average Position Errors for 2015

Quantity	Data Source	Position Residual Std. Dev. (m)	
		RAIM	No Editing
Horizontal	IGS Data	0.05	22.22
	NGA Data	0.03	0.04
Vertical	IGS Data	0.09	22.91
	NGA Data	0.04	0.06

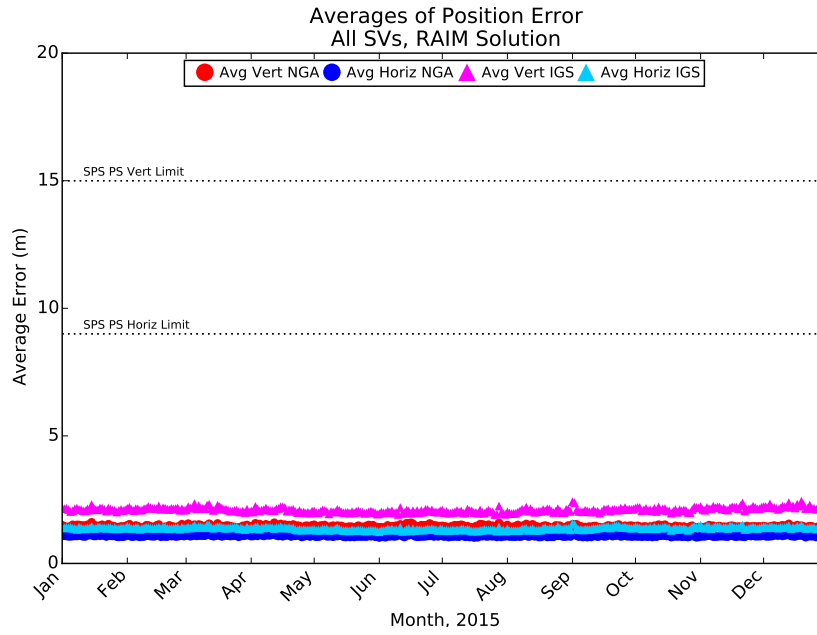


Figure 3.16: Daily Averaged Position Residuals Computed Using a RAIM Solution

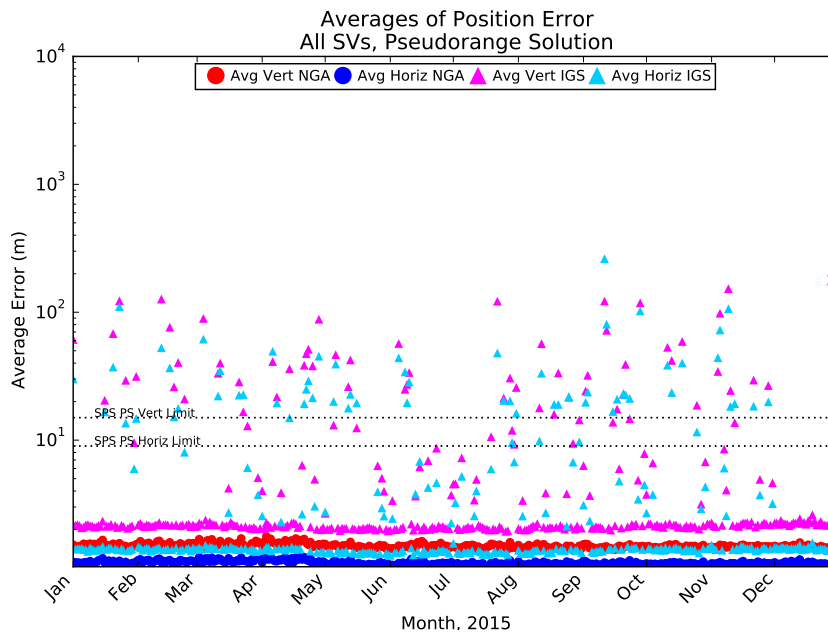
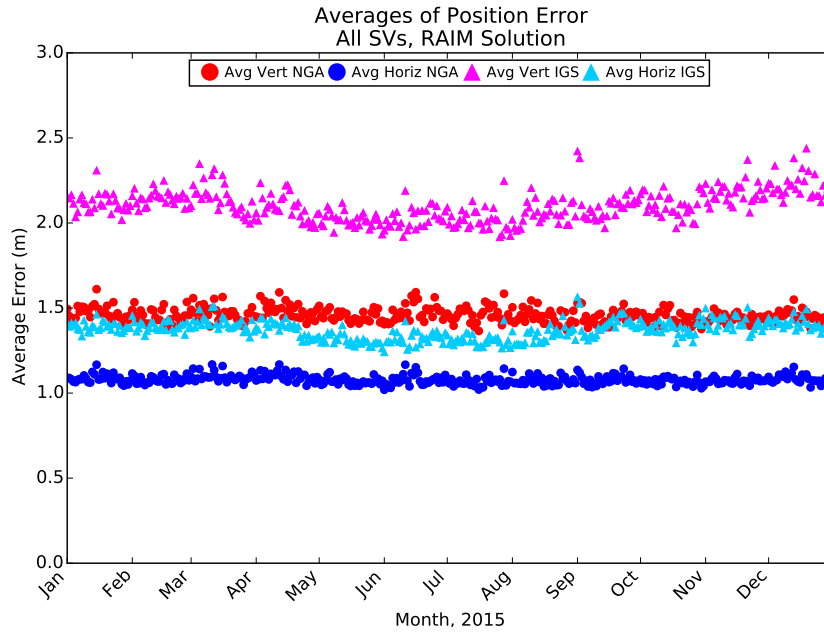
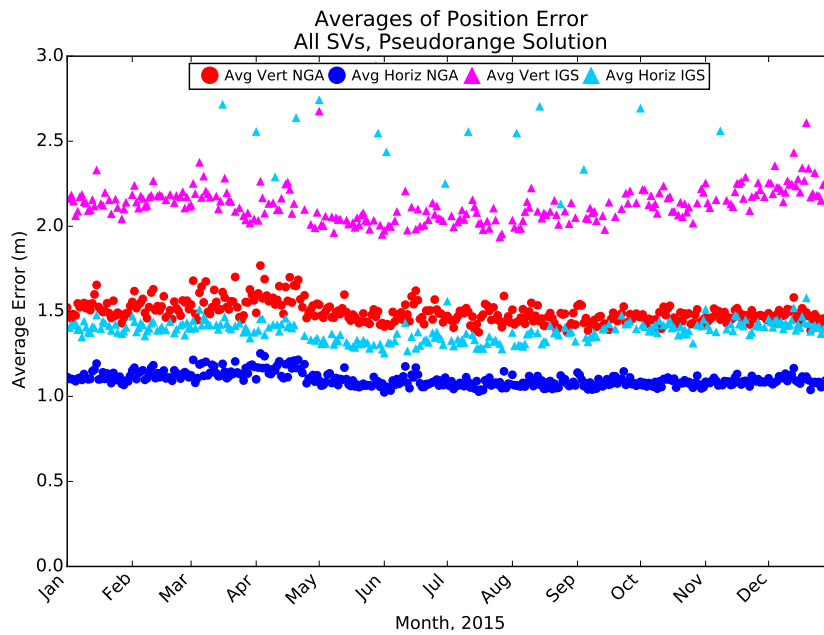


Figure 3.17: Daily Averaged Position Residuals Computed Using No Data Editing



**Figure 3.18:** Daily Averaged Position Residuals Computed Using a RAIM Solution (enlarged)



**Figure 3.19:** Daily Averaged Autonomous Position Residuals Computed Using No Data Editing (enlarged)

number and not too large. This also holds true for the RAIM solutions from the IGS data sets. However, the means and medians for the IGS data set solutions with no data editing are very different. This is consistent with the outliers observed in Figure 3.17 and with the maximum and standard deviation values for the IGS data set solutions. This suggest that there are some large 30 s position residuals in the epoch-by-epoch results for these data sets.

- Differences between NGA and IGS results - The average magnitude of the position residual as reported in Table 3.16 is slightly smaller for the NGA stations than for the IGS stations. There are a number of differences between the two station sets. The NGA station set is more homogeneous in that the same receiver model is used throughout the data processed for this analysis, the data are derived from full-code tracking, and a single organization prepared all the data sets using a single set of algorithms. By contrast, the IGS data sets come from a variety of receivers and were prepared and submitted by a variety of organizations. These differences likely account for the greater variability in the results derived from the IGS data sets.

#### 3.5.4.2 Results for Worst Site 95<sup>th</sup> Percentile

The edited, and the non-edited, 30 s position residuals were then processed (independently) to determine the worst site 95<sup>th</sup> percentile values. In this case, the 95<sup>th</sup> percentile was determined for each station in a given set, and the worst of these was used as the final 95<sup>th</sup> percentile value for that day. Figure 3.20 and Figure 3.21 show these values for the various processing options described in the previous section. The plots are followed by tables of the statistics for the average, median, maximum, and standard deviation of the daily worst site 95<sup>th</sup> percentile values. Some general observations on the results are included following the tables.

The statistics associated with the worst site 95<sup>th</sup> percentile values are provided in Table 3.20 through Table 3.23. There is one table each for the average, median, maximum, and standard deviation of the daily values across 2015. As before, the results are organized in this fashion to facilitate comparison of the same quantity across the various processing options. Precisions are chosen to be at the centimeter level, a choice based on:

- The magnitude of the standard deviation.
- The fact that the station positions are known only at the few-centimeter level.

Most of the observations from the daily averages hold true in the case of the results for the worst site 95<sup>th</sup> percentile case. However, there are a few additional observations:

- Comparison to threshold - The values for both mean and median of the worst 95<sup>th</sup> percentile for both horizontal and vertical errors are well within the standard

for both solutions. Compared to the thresholds of 17 m 95<sup>th</sup> percentile horizontal and 37 m 95<sup>th</sup> percentile vertical these results are outstanding.

- Comparison between processing options - The statistics for the RAIM solutions are slightly better than the statistics for the pseudorange solutions with respect to mean and median. However, the worst values (Table 3.22) for the IGS data with no editing exceed the 95<sup>th</sup> percentile error worst site assertion. This illustrates the importance of some form of data editing.

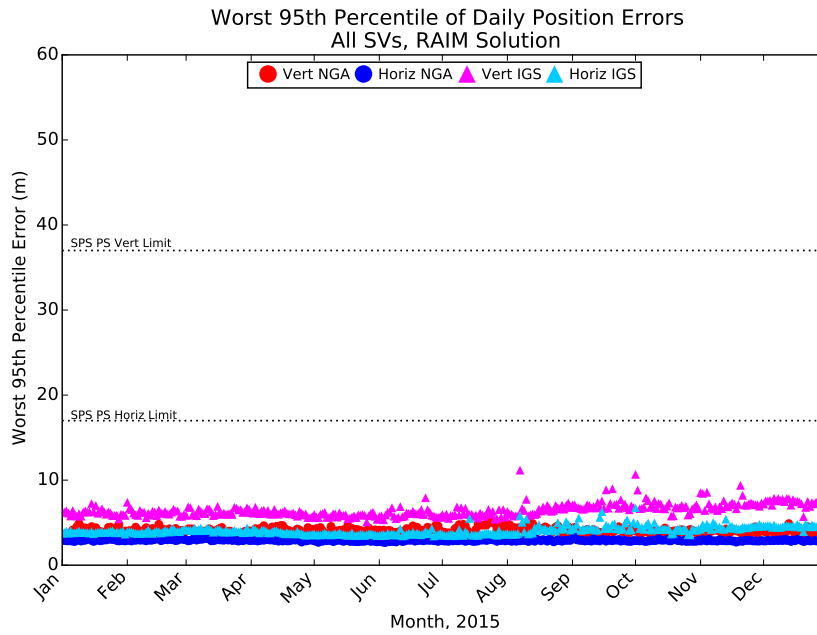


**Figure 3.20:** Worst Site 95<sup>th</sup> Daily Averaged Position Residuals Computed Using a RAIM Solution

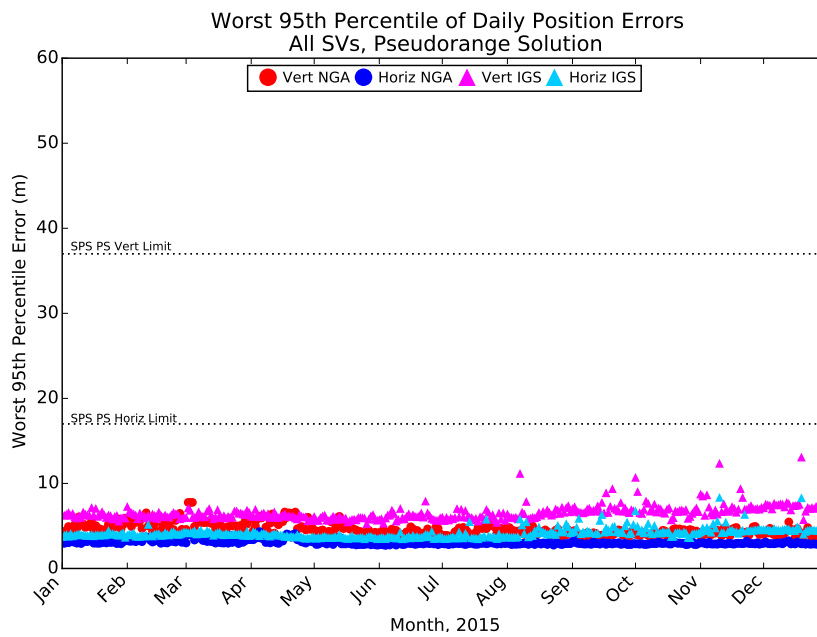


**Figure 3.21:** Worst Site 95<sup>th</sup> Daily Averaged Position Residuals Computed Using No Data Editing



**Table 3.20:** Mean of Daily Worst Site 95<sup>th</sup> Percentile Position Errors for 2015

Quantity	Data Source	Position Residual Mean (m)	
		RAIM	No Editing
Horizontal	IGS Data	4.08	323.17
	NGA Data	2.91	3.05
Vertical	IGS Data	6.49	65.35
	NGA Data	4.08	4.60

**Table 3.21:** Median of Daily Worst Site 95<sup>th</sup> Percentile Position Errors for 2015

Quantity	Data Source	Position Residual Median (m)	
		RAIM	No Editing
Horizontal	IGS Data	3.97	4.07
	NGA Data	2.90	2.97
Vertical	IGS Data	6.33	6.38
	NGA Data	4.02	4.46

**Table 3.22:** Maximum of Daily Worst Site 95<sup>th</sup> Percentile Position Errors for 2015

Quantity	Data Source	Position Residual Maximum (m)	
		RAIM	No Editing
Horizontal	IGS Data	6.76	68159.75
	NGA Data	3.44	4.33
Vertical	IGS Data	11.18	21833.25
	NGA Data	5.31	7.77

**Table 3.23:** Standard Deviation of Daily Worst Site 95<sup>th</sup> Percentile Position Errors for 2015

Quantity	Data Source	Position Residual Std. Dev. (m)	
		RAIM	No Editing
Horizontal	IGS Data	0.47	4360.32
	NGA Data	0.10	0.25
Vertical	IGS Data	0.75	1140.90
	NGA Data	0.32	0.70

# Chapter 4

## Additional Results of Interest

### 4.1 Frequency of Different SV Health States

Several of the assertions require examination of the health information transmitted by each SV. We have found it useful to examine the rate of occurrence for all possible combinations of the six health bits transmitted in subframe 1.

Table 4.1 presents a summary of health bit usage in the ephemerides broadcast during 2015. Each row in the table presents a summary for a specific SV. The summary across all SVs are shown at the bottom. The table contains the count of number of times each unique health code was seen, the raw count of unique sets of subframe 1, 2, 3 collected during the year, and the percentage of sets of subframe 1, 2, 3 data that contained specific health codes.

Only two unique health settings were observed throughout 2015: binary  $000000_2$  (0x00) and binary  $111111_2$  (0x3F).

### 4.2 Age of Data

The Age of Data (AOD) represents the elapsed time between the observations that were used to create the broadcast navigation message and the time when the contents of subframes 1, 2, 3 are available to the user to estimate the position of a SV. The accuracy of GPS (at least for users that depend on the broadcast ephemeris) is indirectly tied to the AOD because the prediction accuracy degrades over time (see Section 3.1.2). This is especially true for the clock prediction. It has been recognized that reducing the AOD improves position, velocity, or time (PVT) solutions for autonomous users; however, there is an impact in terms of increased operations tempo at 2<sup>nd</sup> Space Operations Squadron (2 SOPS).

Note that there is no need for a GPS receiver to refer to AOD in any PVT computation other than the optional application of the navigation message correction table (NMCT).

**Table 4.1:** Frequency of Health Codes

SVN	PRN	Count by Health Code		Total # SF 1, 2, 3 Collected	Percent of Time by Health Code		Operational Days for 2015	Avg # SF 1, 2, 3 per Operational Day
		0x3F	0x00		0x3F	0x00		
23	32	29	4729	4758	0.6	99.4	365	13.0
26	26	3	62	65	4.6	95.4	5	13.0
34	04	5	4008	4013	0.1	99.9	306	13.1
40	10	0	2628	2628	0.0	100.0	197	13.3
41	14	4	4762	4766	0.1	99.9	365	13.1
43	13	5	4757	4762	0.1	99.9	365	13.0
44	28	0	4823	4823	0.0	100.0	365	13.2
45	21	4	4764	4768	0.1	99.9	365	13.1
46	11	16	4744	4760	0.3	99.7	365	13.0
47	22	31	4768	4799	0.6	99.4	365	13.1
48	07	0	4760	4760	0.0	100.0	365	13.0
50	05	4	4756	4760	0.1	99.9	365	13.0
51	20	4	4757	4761	0.1	99.9	365	13.0
52	31	4	4760	4764	0.1	99.9	365	13.1
53	17	3	4783	4786	0.1	99.9	365	13.1
54	18	3	4759	4762	0.1	99.9	365	13.0
55	15	0	4762	4762	0.0	100.0	365	13.0
56	16	3	4756	4759	0.1	99.9	365	13.0
57	29	4	4768	4772	0.1	99.9	365	13.1
58	12	0	4763	4763	0.0	100.0	365	13.0
59	19	5	4753	4758	0.1	99.9	365	13.0
60	23	17	4741	4758	0.4	99.6	365	13.0
61	02	4	4758	4762	0.1	99.9	365	13.0
62	25	3	4773	4776	0.1	99.9	365	13.1
63	01	0	4777	4777	0.0	100.0	365	13.1
64	30	6	4774	4780	0.1	99.9	365	13.1
65	24	3	4838	4841	0.1	99.9	365	13.3
66	27	3	4781	4784	0.1	99.9	365	13.1
67	06	7	4770	4777	0.1	99.9	365	13.1
68	09	7	4783	4790	0.1	99.9	365	13.1
69	03	6	4775	4781	0.1	99.9	365	13.1
71	26	2	3340	3342	0.1	99.9	256	13.1
72	08	9	1860	1869	0.5	99.5	142	13.2
73	10	0	300	300	0.0	100.0	23	13.0
Total		194	145692	145886	0.1	99.9	365	399.7

(See IS-GPS-200 Section 20.3.3.5.1.9 for a description of the NMCT.) It is computed here to validate that the operators at 2 SOPS are not modifying the operational tempo in order to maintain the URE accuracy described in Section 3.1.

The average AOD throughout 2015 is shown in the following table, along with values for the previous five years. The 2015 values for Block IIR, IIR-M, and IIF SVs are nearly unchanged from 2012, while the average AOD for Block IIA SVs has recovered somewhat from a drop in 2012. The daily average AOD for the constellation and for each block is illustrated in the following figure. The AOD appears to be generally constant throughout 2015, which indicates that any variations in the URE results discussed earlier are not due to changes in operations tempo at 2 SOPS.

**Table 4.2:** Age of Data of the Navigation Message by SV Type

	Average Age of Data (hours)					
	2010	2011	2012	2013	2014	2015
Full Constellation	11.6	11.6	11.3	11.5	11.6	11.6
Block II/IIA	11.5	11.4	10.3	10.9	11.2	11.6
Block IIR/IIR-M	11.8	11.7	11.7	11.8	11.8	11.7
Block IIF	12.2	12.0	11.5	11.5	11.5	11.4

The AOD values (in both this section and in Section 3.1.1) were calculated by examination of the broadcast ephemeris and not by any information provided from the MCS. The method of calculation is described here to allow other organizations to independently repeat this analysis. As mentioned earlier, such an analysis is relevant only to a performance assessment such as this report.

The AOD may be calculated by finding the upload times based on the  $t_{oe}$  offsets as defined in IS-GPS-200 Section 20.3.4.5 and then examining the  $t_{nmct}$  under the following assumptions:

- A complete set of the subframe 1, 2, 3 data broadcast by all SVs of interest is available throughout the time period of interest.
- The term  $t_{nmct}$  defined in IS-GPS-200 Section 20.3.3.4.4 represents the time of the Kalman state used to derive the corresponding navigation message.

Given these assumptions, the AOD at any point in time can be determined by the following process:

- Working backward from the time of interest to finding the time when the most recent preceding upload was first broadcast
- Finding the AOD offset (AODO) of the associated subframe 2
- Subtracting the AODO from the  $t_{oe}$  (as described in IS-GPS-200 20.3.3.4.4) to determine the time of the Kalman state parameters

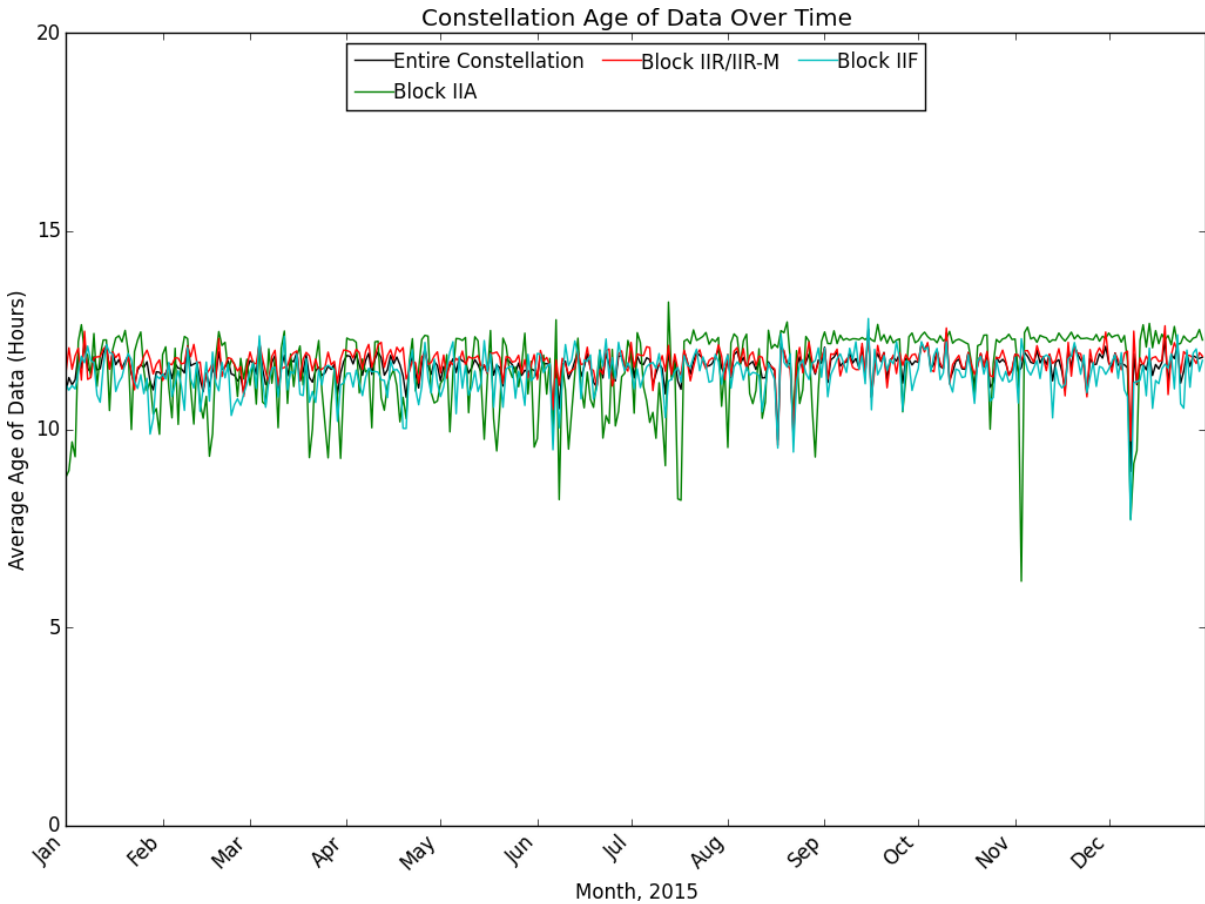


**Figure 4.1:** Constellation Age of Data for 2015

- Calculating the difference between the time of interest and the Kalman state parameter time

The search for the preceding upload is necessary because the AODO has a limited range and is not sufficiently large to maintain an accurate count for a complete upload cycle.

The results of this algorithm are generally consistent with the results provided by MCS analysis. The first assumption is fulfilled by the NGA MSN archive. The remaining assumptions were discussed with systems engineers supporting 2 SOPS and are believed to be valid.

### 4.3 User Range Accuracy Index Trends

Tables 4.3 on page 61 and 4.4 on page 62 present a summary of the analysis of the URA index values throughout 2015. The total number of navigation messages examined differs from the health summary in Section 4.1 because only URA index values corresponding to health settings of 0x00 are included in this analysis. Both the absolute count and the count as a percentage of the total are shown.

The vast majority of the values are 0, 1, or 2 (over 99.9%). Index values between 3 and 5 were very rare. No values over 5 were observed.

## 4.4 Extended Mode Operations

IS-GPS-200 defines Normal Operations as the period of time when subframe 1, 2, 3 data sets are transmitted by the SV for periods of two hours with a curve fit interval of four hours (IS-GPS-200 Section 20.3.4.4). This definition is taken to be the same as the definition of Normal Operations in SPSPS08 for the URE metrics. To determine if any SV operated in other than Normal Operations at any time in 2015, the broadcast ephemerides were examined to determine if any contained fit interval flags set to 1. (See IS-GPS-200 20.3.3.4.3.1 for definition of the fit interval flag.)

The analysis found a total of 48 examples of extended operations for satellites set healthy. The examples were distributed across 34 days. The average time of an occurrence was 50 minutes. The minimum duration was 150 seconds and the maximum duration was 5 hours 35 minutes. These results are summarized in Table 4.5 on page 63.

Given the relative rarity of occurrence, the URE values for the periods summarized in Table 4.5 are included in the statistics presented in Section 3.1.1, even though a strict interpretation of the SPSPS08 would suggest that they be removed. However, the SVs involved were still set healthy and (presumably) being used by user equipment, it is appropriate to include these results to reflect performance seen by the users.

Examination of the ephemerides from past years reveals that 2015 is not an anomaly. Such periods have been found in all years checked (back to 2005).

Past discussions with the operators have revealed several reasons for these occurrences. Some are associated with Alternate MCS (AMCS) testing. When operations are transitioned from the MCS to the AMCS (and reverse) it is possible that SVs nearing the end of their daily cycle may experience a longer-than-normal upload cycle. Other occurrences may be caused by delays due to ground antenna maintenance or due to operator concentration on higher-priority issues with the constellation at the time.

**Table 4.3:** Distribution of URA Index Values

SVN	PRN	URA Index						Total # SF 1, 2, 3 examined	Oper. Days for 2015	Avg # SF 1, 2, 3 per Oper. Day
		5	4	3	2	1	0			
23	32					236	4493	4729	365	13.0
26	26					10	52	62	5	12.4
34	04				1	180	3827	4008	306	13.1
40	10				85	797	1746	2628	197	13.3
41	14				25	829	3908	4762	365	13.0
43	13				3	331	4423	4757	365	13.0
44	28				3	910	3910	4823	365	13.2
45	21			11	485	1011	3257	4764	365	13.1
46	11				4	417	4323	4744	365	13.0
47	22			1	217	1291	3259	4768	364	13.1
48	07			23	224	397	4116	4760	365	13.0
50	05			2	5	179	4570	4756	365	13.0
51	20				2	100	4655	4757	365	13.0
52	31		2	1	5	226	4526	4760	365	13.0
53	17	2	5	1	8	584	4183	4783	365	13.1
54	18			1	6	185	4567	4759	365	13.0
55	15				1	301	4460	4762	365	13.0
56	16				3	293	4460	4756	365	13.0
57	29					584	4184	4768	365	13.1
58	12					228	4535	4763	365	13.0
59	19					267	4486	4753	365	13.0
60	23				2	286	4453	4741	365	13.0
61	02				4	51	4703	4758	365	13.0
62	25				1	232	4540	4773	365	13.1
63	01					62	4715	4777	365	13.1
64	30			1	8	239	4526	4774	365	13.1
65	24				3	1020	3815	4838	365	13.3
66	27					176	4605	4781	365	13.1
67	06				2	83	4685	4770	365	13.1
68	09				0	311	4472	4783	365	13.1
69	03	1	5	2	7	632	4128	4775	365	13.1
71	26					368	2972	3340	256	13.0
72	08				80	426	1354	1860	142	13.1
73	10				2	44	254	300	23	13.0
Total		3	12	43	1186	13286	131162	145692	365	399.2

**Table 4.4:** Distribution of URA Index Values As a Percentage of All Collected

SVN	PRN	URA Index					
		5	4	3	2	1	0
23	32					5.0	95.0
26	26					16.1	83.9
34	04					4.5	95.5
40	10				3.2	30.3	66.4
41	14				0.5	17.4	82.1
43	13				0.1	7.0	93.0
44	28				0.1	18.9	81.1
45	21			0.2	0.2	21.2	68.4
46	11				0.1	8.8	91.1
47	22				4.6	27.1	68.4
48	07			0.5	4.7	8.3	86.5
50	05				0.1	3.8	96.1
51	20					2.1	97.9
52	31				0.1	4.7	95.1
53	17		0.1		0.2	12.2	87.5
54	18				0.1	3.9	96.0
55	15					6.3	93.7
56	16				0.1	6.2	93.8
57	29					12.2	87.8
58	12					4.8	95.2
59	19					5.6	94.4
60	23					6.0	93.9
61	02				0.1	1.1	98.8
62	25					4.9	95.1
63	01					1.3	98.7
64	30				0.2	5.0	94.8
65	24				0.1	21.1	78.9
66	27					3.7	96.3
67	06					1.7	98.2
68	09					6.5	93.5
69	03		0.1		0.1	13.2	86.5
71	26					11.0	89.0
72	08				4.3	22.9	72.8
73	10				0.7	14.7	84.7
Constellation Average		0.0	0.0	0.0	0.8	9.1	90.0

*Notes: Values smaller than 0.1 are not shown. Constellation averages are weighted by the number of observations.*



**Table 4.5:** Summary of Occurrences of Extended Mode Operations

SVN	PRN	# of Occurrences		Duration (minutes)	
		Healthy	Unhealthy	Healthy	Unhealthy
34	04	1	0	240	0
43	13	1	0	104	0
44	28	3	0	120	0
45	21	2	0	73	0
46	11	1	0	78	0
47	22	1	0	85	0
48	07	2	0	59	0
50	05	1	0	25	0
51	20	1	0	31	0
52	31	1	0	45	0
53	17	4	0	114	0
55	15	1	0	33	0
56	16	2	0	59	0
57	29	1	0	64	0
58	12	1	0	3	0
59	19	4	0	240	0
60	23	2	0	449	0
61	02	3	0	50	0
62	25	2	0	106	0
63	01	1	0	49	0
64	30	2	0	15	0
65	24	1	0	27	0
66	27	2	0	45	0
67	06	1	0	13	0
68	09	1	0	34	0
69	03	4	0	230	0
71	26	1	0	2	0
72	08	1	0	18	0
Totals		48	0	2411	0

# Appendix A

## URE as a Function of AOD

This appendix contains supporting information for the results presented in Section 3.1.2. The SIS RMS URE vs. AOD charts are presented for each GPS SV. The charts are organized by SV Block and by ascending SVN within each block.

These charts are based on the same set of 30 s Instantaneous RMS SIS URE values used in Section 3.1.1. For each SV, a period of 48 hours was divided into a set of 192 bins, each 15 minutes in duration. An additional bin was added for any AOD that appeared beyond 48 hours. All of the 30 s URE values for the year for a given SV were grouped according to AOD bin. The values in each bin were sorted and the 95<sup>th</sup> percentile and the maximum were determined. Once the analysis was complete, it was clear that most bins beyond the 26 hour mark contained too few points to be considered statistically relevant. Therefore, when the number of points in a bin falls below 10% of the number of points in most populated bin, the bin is not used for plotting purposes. The problem with bins with low counts is that, in our experience, the results tend to be dominated by one or two very good or very bad observations and this can lead to erroneous conclusions about behavior.

The figures on the following pages each show two curves. The blue curve represents the 95<sup>th</sup> Percentile SIS RMS URE vs. AOD (in hours). The green curve represents the number of data points that were available to form each URE estimate.

Note that for most SVs, the green curve has a well-defined horizontal plateau that begins near zero AOD, continues for roughly 24 hours, and then drops quickly toward zero. The location of the right-hand drop of the green curve toward zero provides an estimate of the typical upload period for the SV. In cases where the SV is uploaded more frequently, the shape of the green curve will vary reflecting that difference.

Data for SVN 26/PRN 26 and SVN 73/PRN 10 are omitted from this appendix as these two SVs were operational for less than a month in 2015.

## A.1 Notes

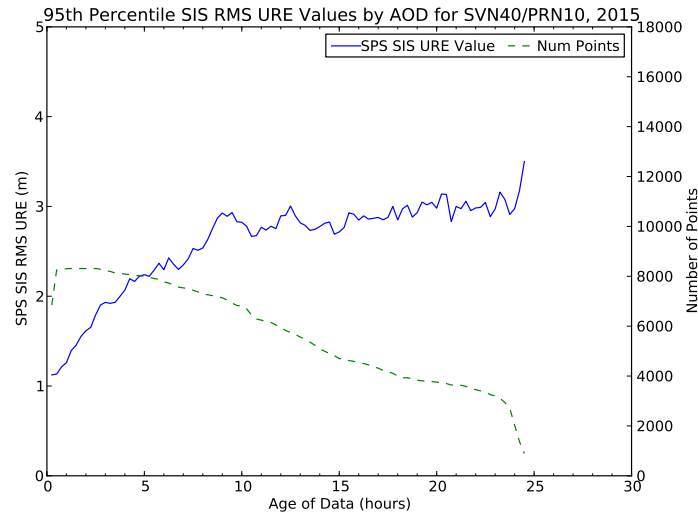
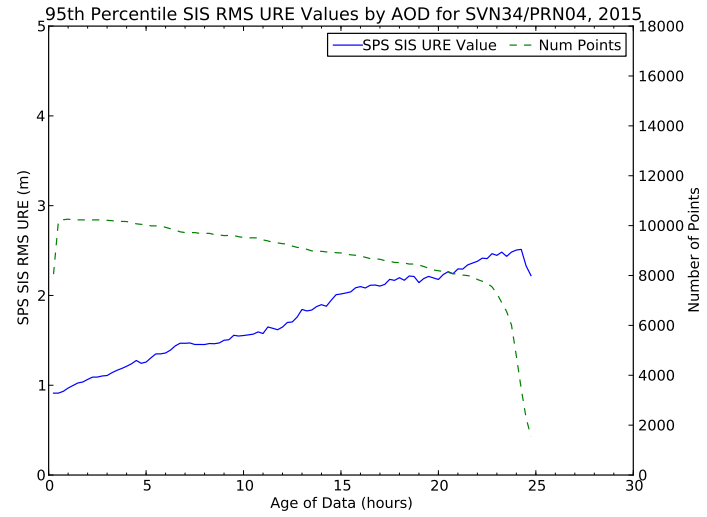
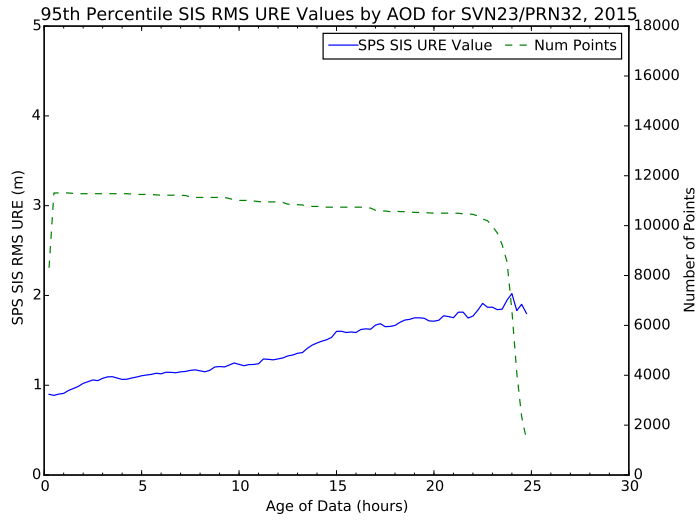
This section contains some notes on SV-specific behavior observed in the following charts.

SVN 23/PRN 32: This SV presents a minor problem for this analysis. This problem is limited to the type of performance analysis presented in this report. There is no similar concern for a GPS receiver. The AOD values are based on the AODO field in subframe 2. The definition of the AODO field is tied to how AODO is used to determine the age of the data in the NMCT. Because PRN 32 can never be represented in the NMCT, the AODO field for PRN 32 is never reset to zero at a new upload but remains at the “all ones” state. Therefore, the AOD for PRN 32 cannot be independently derived from the navigation message data. For the purposes of this plot, we looked at the AODO across the entire constellation and determined the annual average AODO was about 5153 seconds ( $\sim 1.4$  hours). For purposes of this report we examined all upload cutovers through 2015 for all SVs except SVN 23/PRN 32. For each upload cutover we computed the AOD at the time of the upload cutover. We then computed the mean of these samples to determine an average AOD at the time of the upload cutover. There were 12091 samples with an average AOD of 1126 sec (about 19 minutes). We assumed this average holds true for SVN 23/PRN 32 and conducted the analysis accordingly.

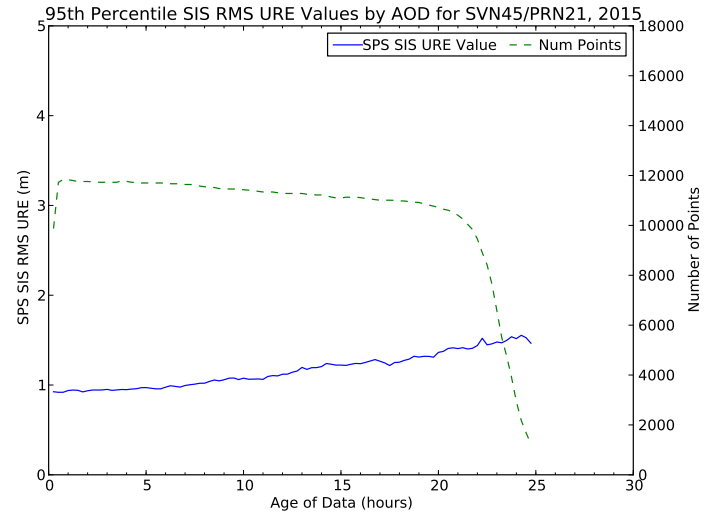
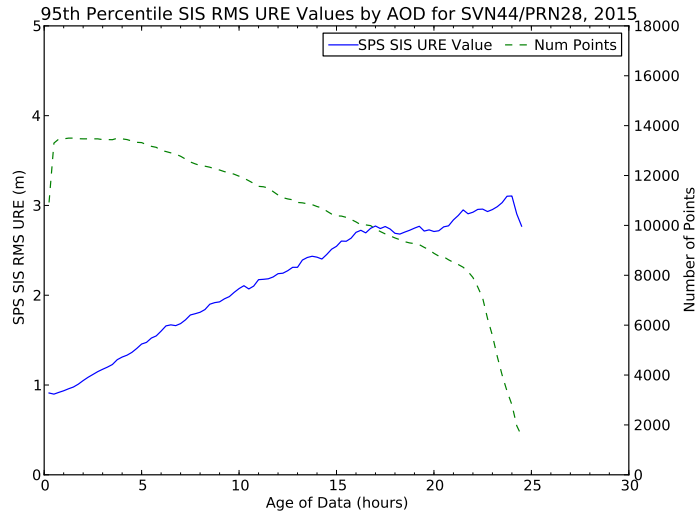
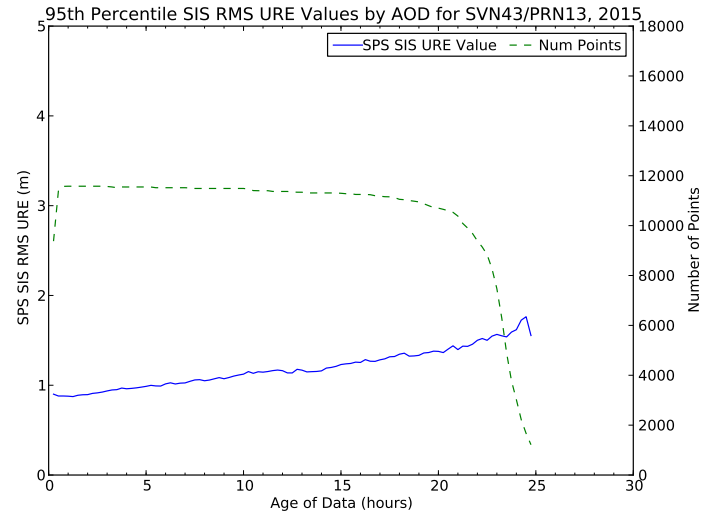
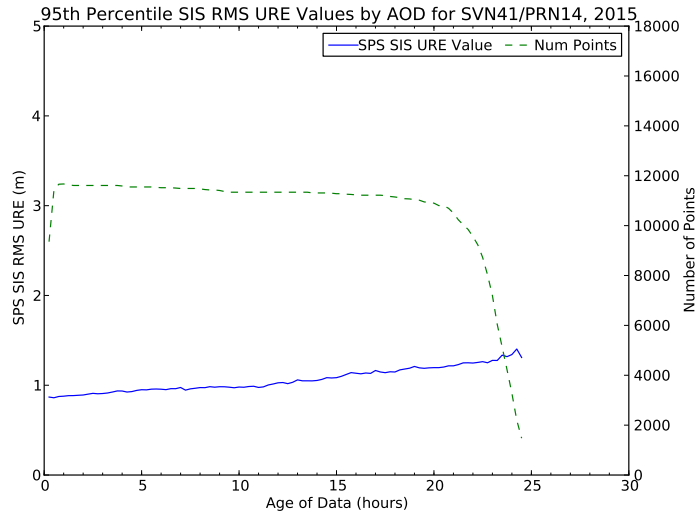
SVN 40/PRN 10: This is the most obvious example of a SV that is being uploaded more frequently than normal. The fact that it is being uploaded more frequently is based on the shape of the dashed green curve which indicates the number of points in each AOD bin. The scale for this curve is on the right-hand vertical axis. The green curve does not exhibit the plateau seen in most plots but instead has a fairly rapid, near-linear decrease in number of points with AOD after about 2.5 hours. If the SV were consistently being uploaded at a given interval, there would still be a plateau, only shorter than the typical plateau. For example, if an SV were being uploaded every 12 hours, one would expect a plateau from somewhere around an hour AOD out to 12 hours AOD. The near linear trend implies that the upload time for this SV is variable over a fairly large range.

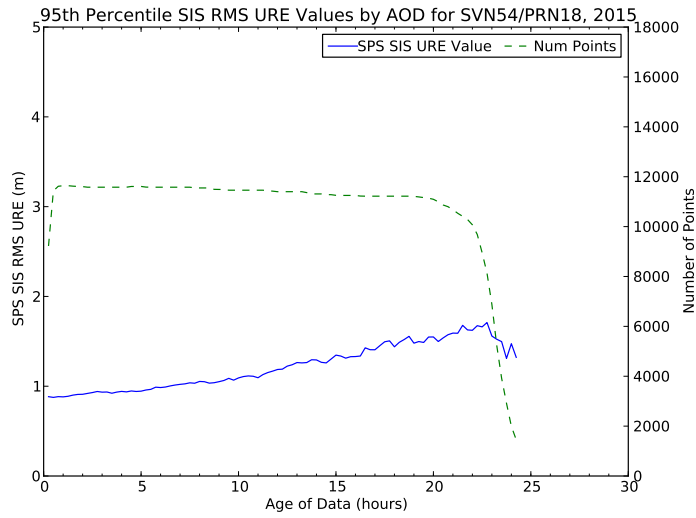
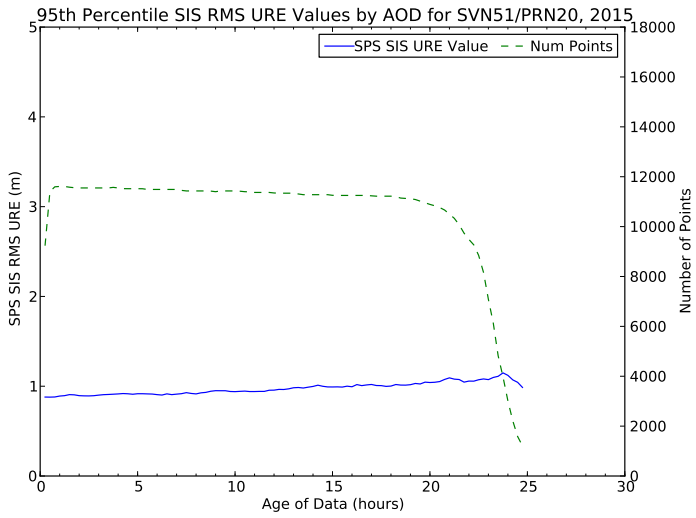
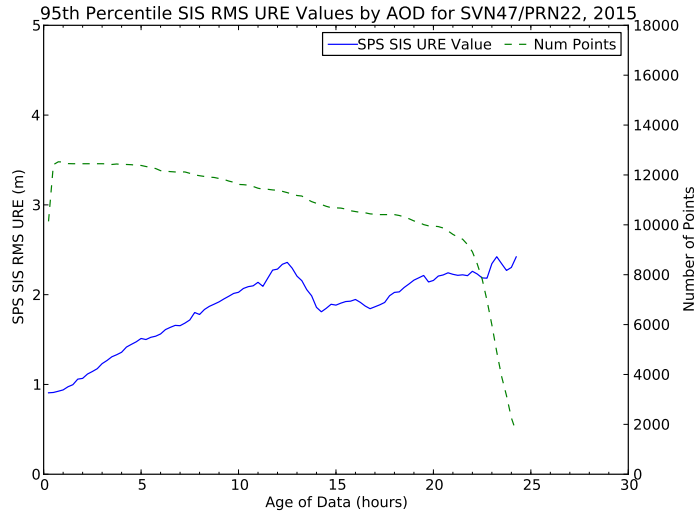
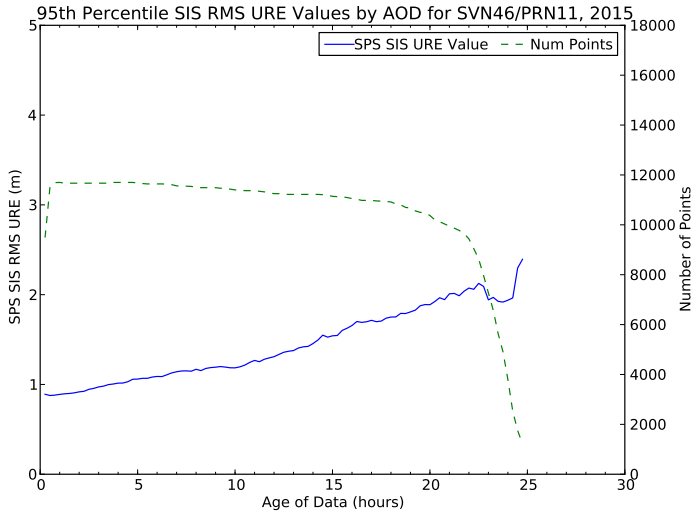
SVN 65/PRN 24: This Block IIF shows indications of occasional contingency uploads. This conclusion is based on the manner in which the SIS URE value line tends to flatten as it approaches the 3 m magnitude and the fact that the number of points starts to decline far earlier than the other Block IIF SVs. This is consistent with the higher 95<sup>th</sup> percentile URE shown in Table 3.1 and Figure 3.1. It is likely related to the fact that SVN 65/PRN 24 is using a Cesium frequency reference. SVN 72/PRN 8 (which also uses a Cesium frequency reference) shows similar characteristics but less pronounced as it was only available for five months of 2015.

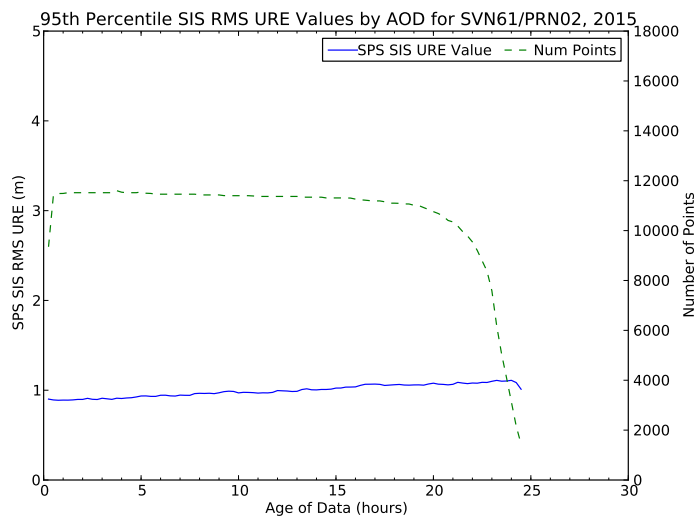
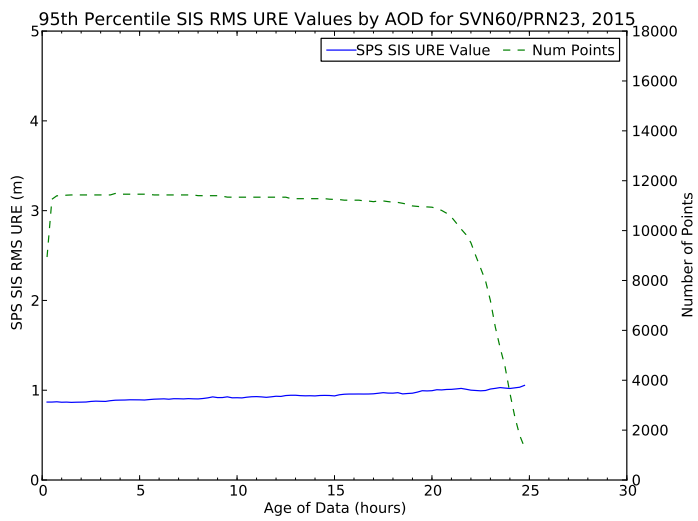
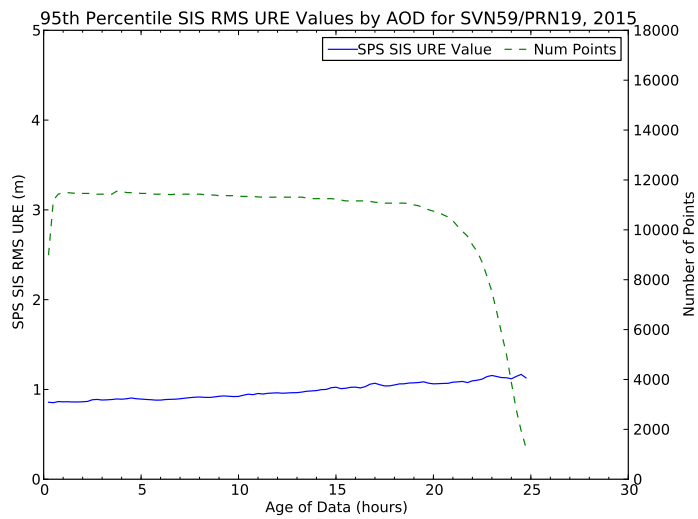
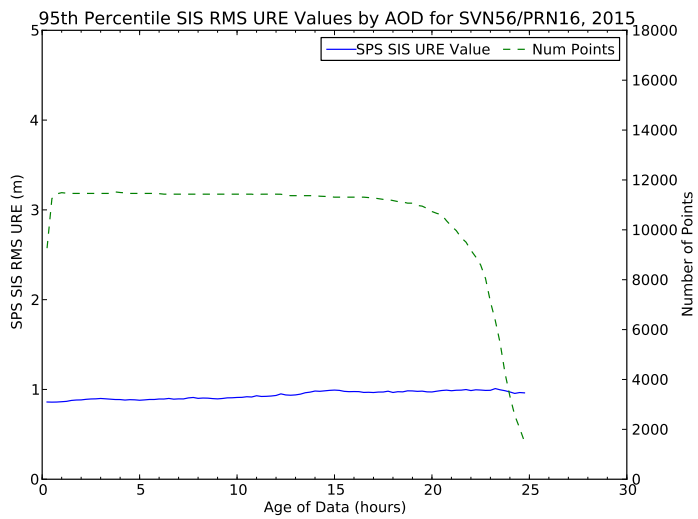
## A.2 Block IIA SVs



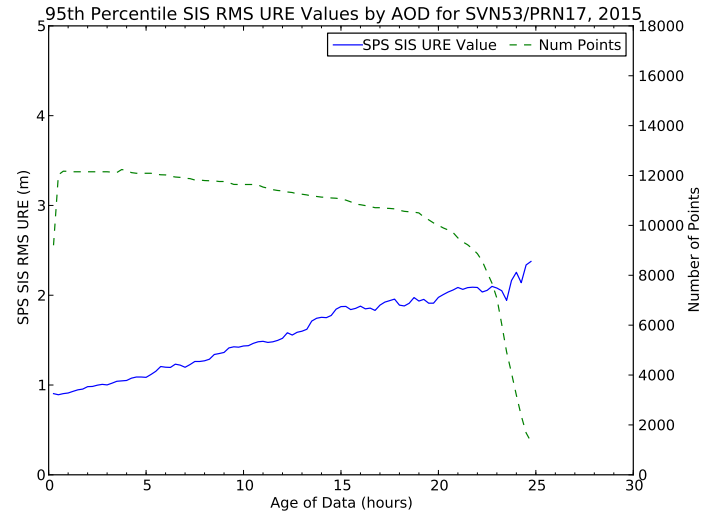
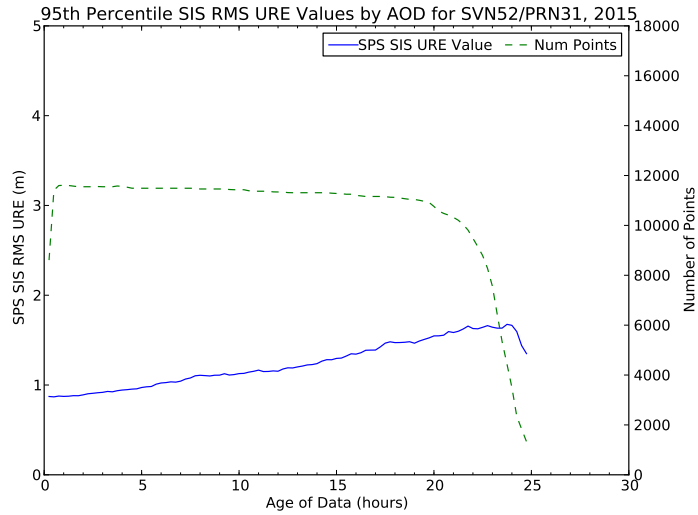
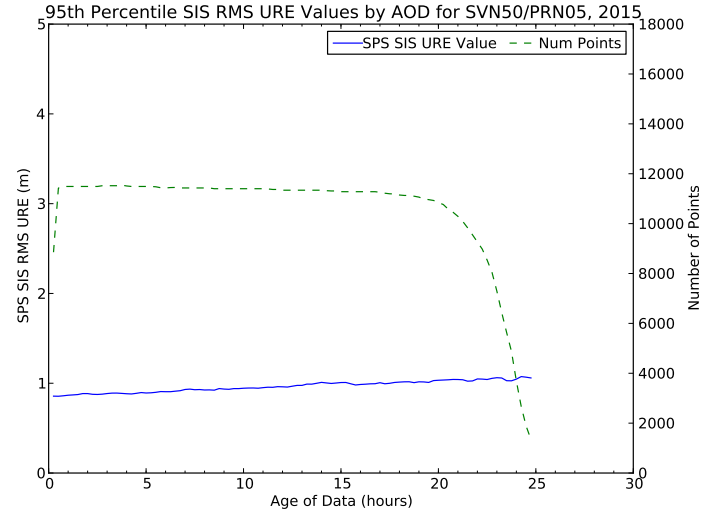
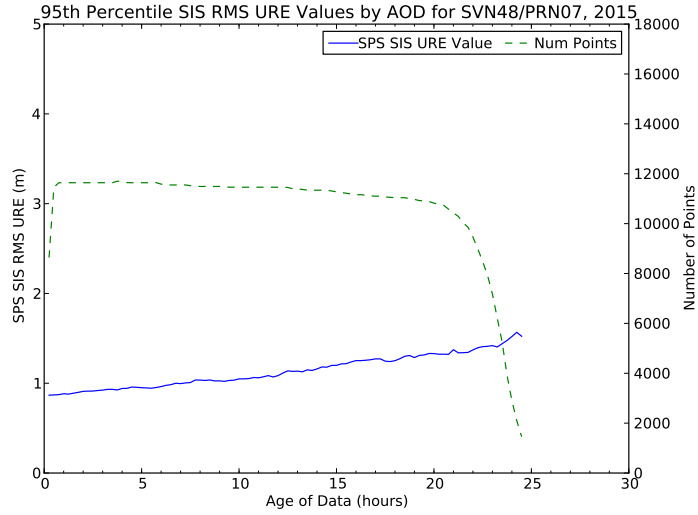
### A.3 Block IIR SVs



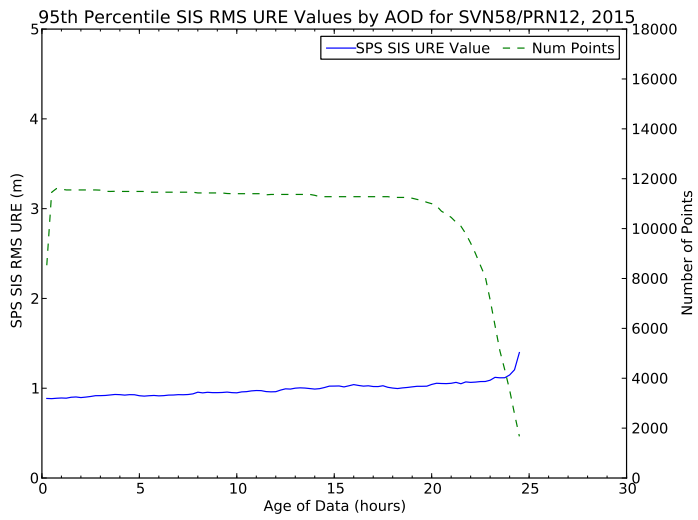
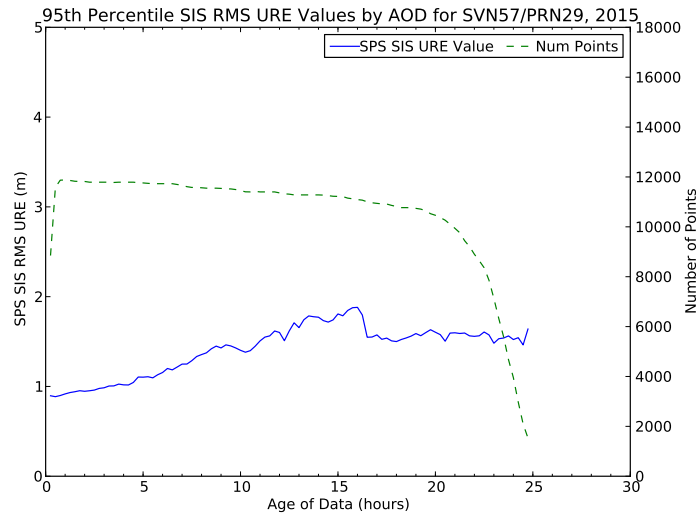
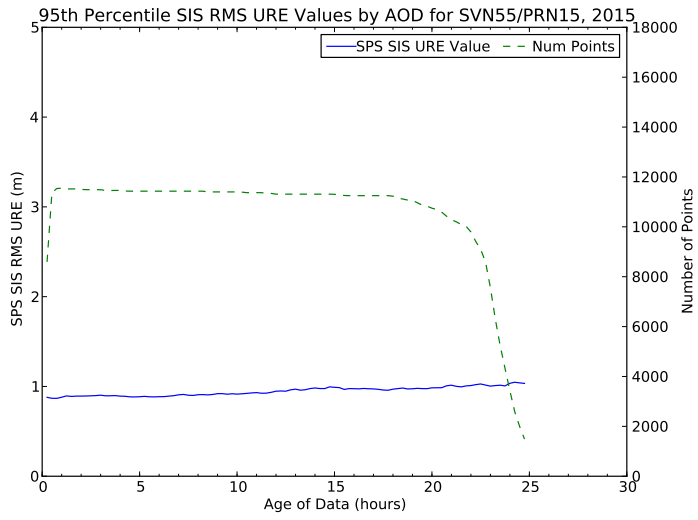




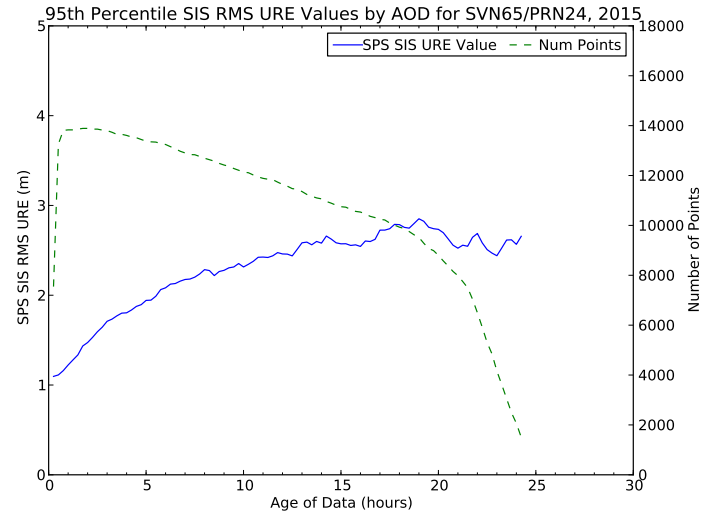
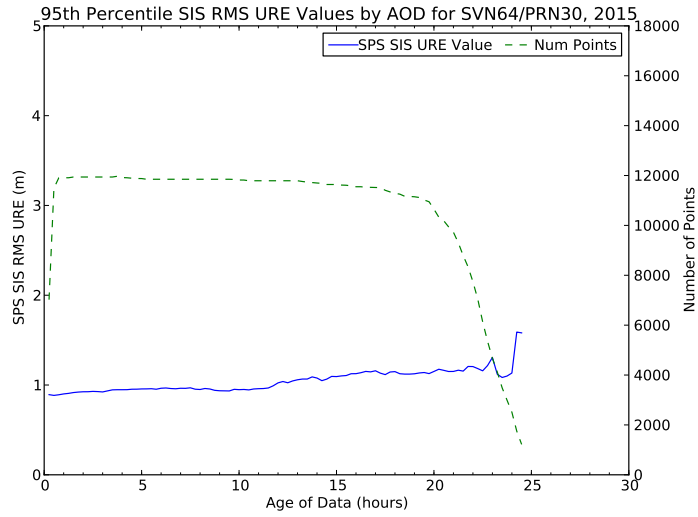
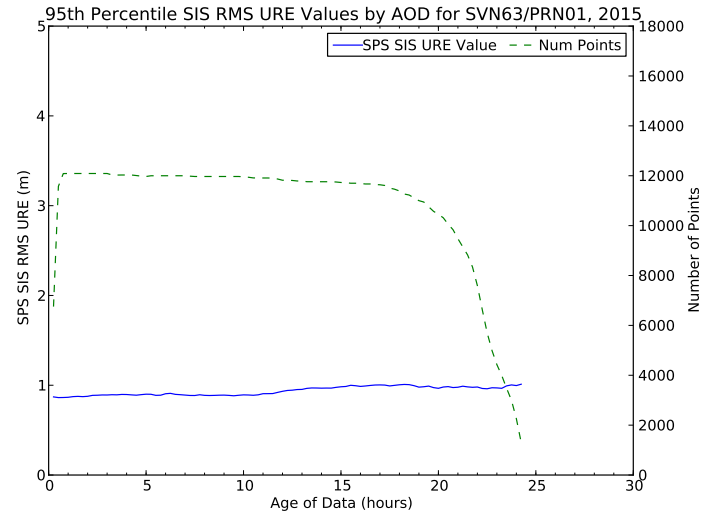
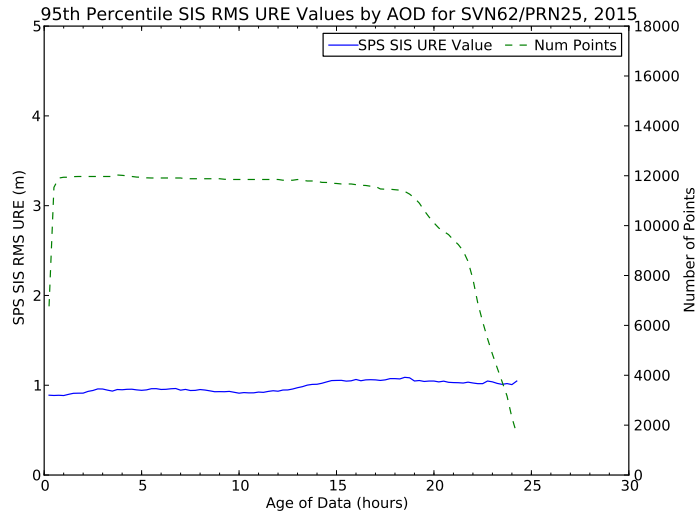
## A.4 Block IIR-M SVs

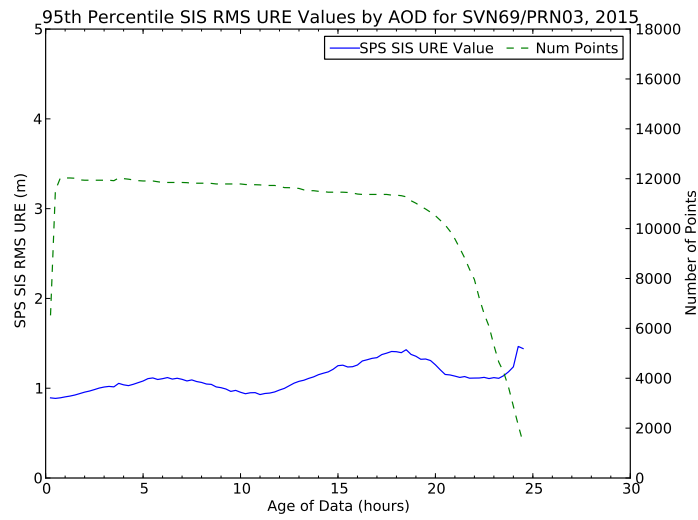
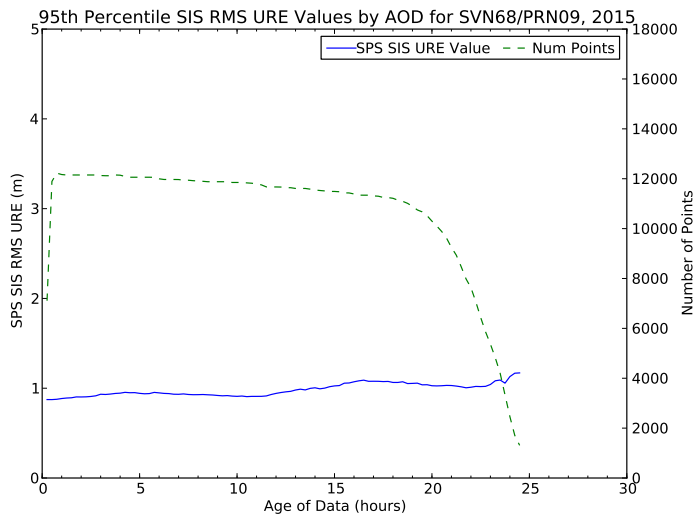
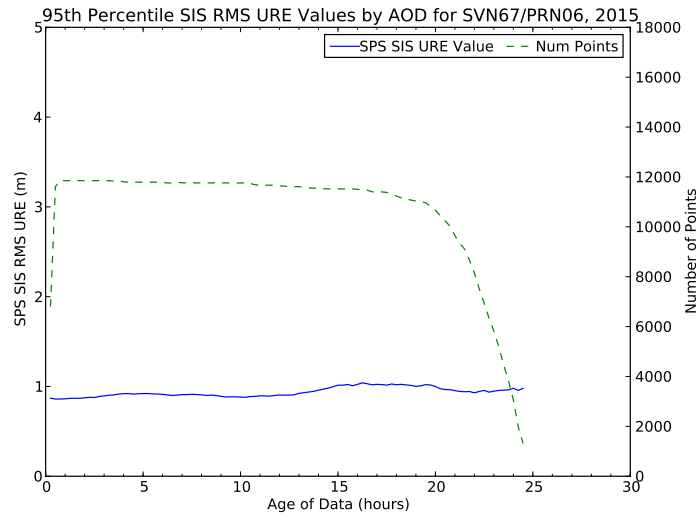
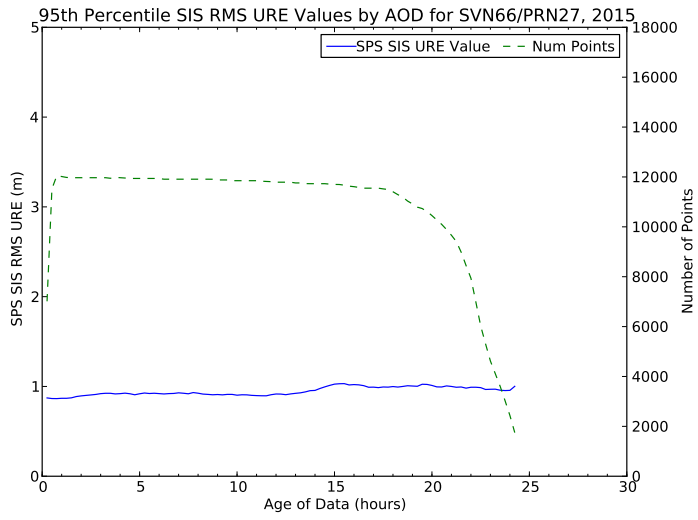


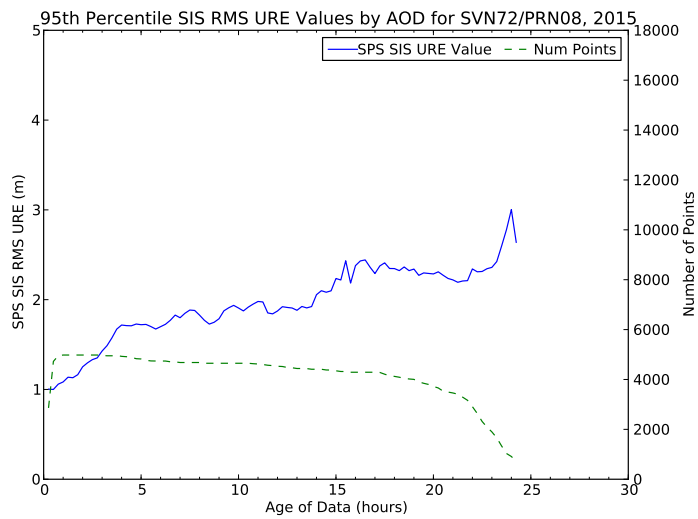
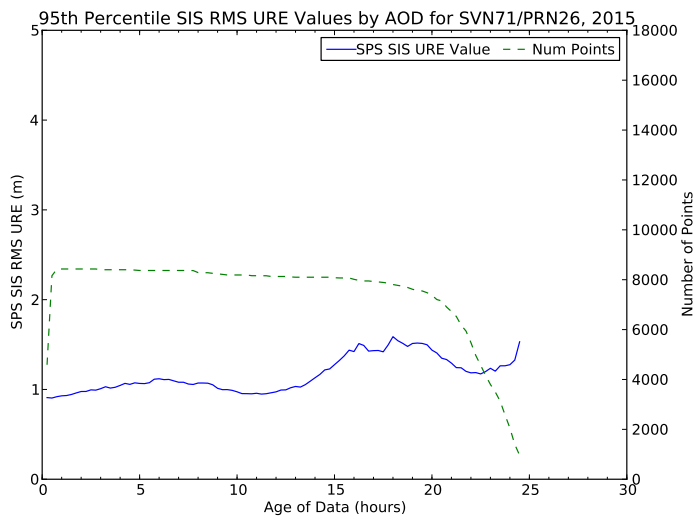




## A.5 Block IIF SVs







# Appendix B

## URE Analysis Implementation Details

### B.1 Introduction

The User Range Error (URE) accuracy represents the accuracy of the broadcast navigation message. There are a number of error sources that affect the URE, including errors in broadcast ephemeris and timing errors.

Two approaches to URE analysis are provided in this report. The first approach uses separate statistical processes over space and time to arrive at the result. The second approach derives the result by a single statistical process but is more computationally demanding.

### B.2 Clock and Position Values for Broadcast and Truth

The URE values in this report are derived by comparison of the space vehicle (SV) clock and position representations as computed from the broadcast Legacy Navigation (LNAV) message data (BCP) against the SV truth clock and position data (TCP) provided by a precise orbit calculated after the time of interest.

The broadcast LNAV message data used in the calculations were collected by the NGA MSN. These include the complete 300-bit subframes for nearly all unique sets of subframe 1, 2, 3 data and all the unique sets of subframe 4, 5 data. The broadcast LNAV messages provide a set of parameters for an equation which can be evaluated at any time for which the parameters are valid. Our process evaluates the parameters at either a 30 s or 5 min cadence (depending on the process).

The TCP values are computed from the archived National Geospatial-Intelligence Agency (NGA) products. The archived NGA products used in the calculations are the

antenna phase center (APC) precise ephemeris files available from the NGA public website [11]. The NGA products are provided in tabular SP3 format, with positions and clocks provided at a 5 min cadence. When TCP data are needed at a 5 min cadence, a simple table look-up is sufficient. When TCP data are needed at a 30 s cadence, a Lagrange interpolation scheme is used, in which the five points prior to and after the estimation time are used to estimate the SV position. Clock interpolation is handled via a linear interpolation since a multipoint Lagrange interpolation is not appropriate for clock dynamics.

## B.3 95<sup>th</sup> Percentile Global Average As Per the SPS PS

The SPSPS08 specifications for URE suggest averaging across the service volume visible to a GPS SV at any specified point in time. The process is illustrated in Figure B.1.

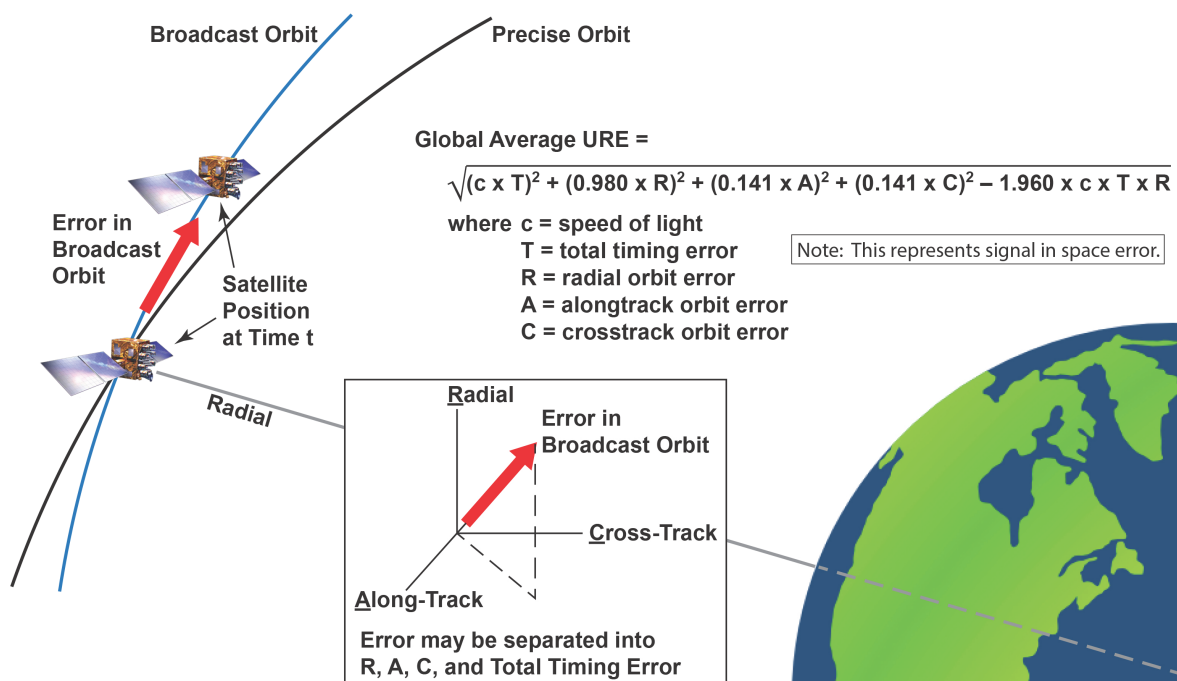


**Figure B.1:** Global Average URE as defined in SPS PS

The equation shown in Figure B.1 is equation A-1 of SPSPS08 Section A.4.11. This expression allows us to compute the URE accuracy from known errors.

For purposes of this report, the Instantaneous RMS SIS URE values were generated at 30 s intervals for all of 2015. The URE was formed by differencing the BCP and TCP to obtain the radial, along-track, cross-track, and time errors at each epoch. These errors were used as inputs to the SPSPS08 equation A-1.

After all the Instantaneous RMS SIS URE values were computed, values for periods when each SV was unhealthy or not broadcasting were discarded. The remaining values were then grouped by monthly period for each SV and sorted; the maximum and the 95<sup>th</sup> percentile values were identified for each SV, and this is the basis for Table 3.2. The monthly grouping corresponds closely to the 30 day period suggested in the SPSPS08 and PPSPS07 for URE Accuracy over all AODs while being more intuitive to the reader.

## B.4 An Alternate Approach

The previous approach computes an SIS Instantaneous RMS URE (an average over space) at each time point over a month, then selects a 95<sup>th</sup> percentile value from that set. An alternate approach is to compute the SIS Instantaneous URE for a large number of locations at each time point and store those results. For each SV, this is done for a series of time points at a selected cadence, and the collection of SIS Instantaneous URE values at each time point are stored. When all the time points for a month have been computed, the absolute values of SIS Instantaneous URE values for all time points are gathered together in one monthly set. The 95<sup>th</sup> percentile value is selected from that set.

For this particular implementation, we selected an approximation of an equidistant grid with a spacing of roughly 550 km (five degrees of latitude on the surface of the Earth). This yields a set of 577 SIS Instantaneous URE values for each SV for each evaluation time. Figure B.2 illustrates this set of grid points for a particular SV-time shown as a projection onto the surface of the Earth.

We did this at a cadence of 5 min for each SV for all of 2015 and stored all 577 values for all time points. We then extracted sets of values corresponding to each month (approximately 5 million values per SV-month), took the absolute value of each, and selected the 95<sup>th</sup> percentile value as the result for the SV-month. This is the basis for Table 3.3.

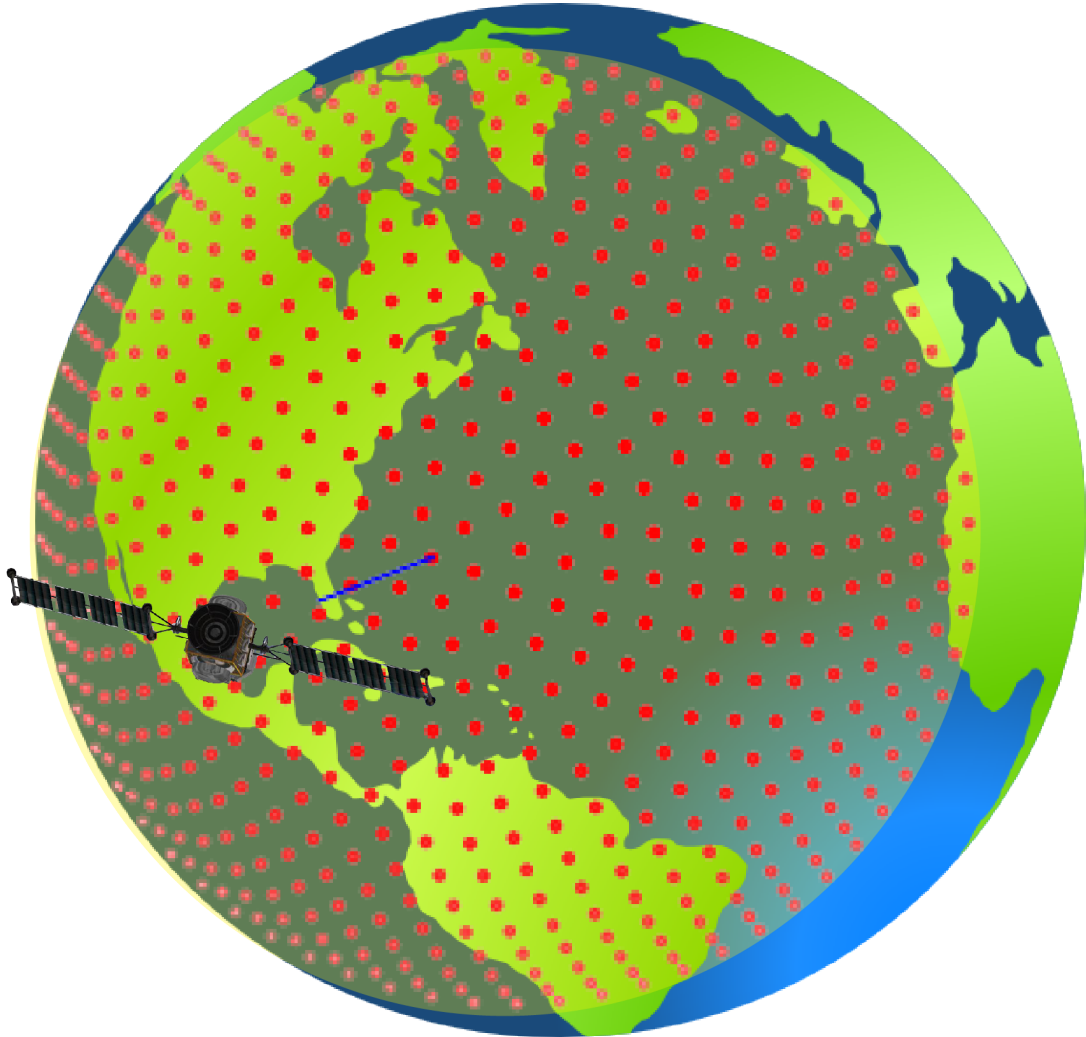


Figure B.2: Illustration of the 577 Point Grid



## B.5 Limitations of URE Analysis

There are a number of subtleties in this approach to computing URE accuracies, and the following paragraphs detail some of these.

Selective Availability (SA) would be an additional significant difference between PPS and SPS results; however, SA was set to zero throughout this period [12].

The approaches described in B.2 - B.4 work well when the estimated URE accuracy is under the required thresholds, as it verifies that the system is operating as expected. However, experience has shown that when an actual problem arises, the use of this procedure, without other cross-check mechanisms, can create some issues and may lead to incorrect results. Consider the following two cases.

- In cases where an SV is removed from service for reasons that invalidate the broadcast ephemeris (such as a clock run-off) we need to compare the time at which the removal from service occurred with the time at which any of the URE accuracy bounds were exceeded to assess whether or not a violation of the SPS PS metrics occurred. However, because we have relied on the interpolation process to generate 30 s values, we cannot obtain an accurate estimate of the time at which the URE bound was exceeded. As a general rule, the UREs computed in our process should be reviewed when they are contained between two SP3 epochs, one of which contains a clock event.
- When a SV is set unhealthy or cannot be tracked, the precise ephemeris may provide misleading results. The analyst preparing the precise ephemeris has several options for handling discontinuities that occur during outages. Therefore, the URE values generated near such events may be incorrect. As a result, it is necessary to avoid accepting UREs into the statistical process under conditions in which the SV could not be tracked or was set unhealthy. This has been done for all the results presented here.

In all cases, when an apparent violation of the URE limits is encountered, we choose to reconcile the analysis described above with the behavior of ORDs formed from the data collected at NGA and IGS sites. Because the observational data used is collected at a 30 s cadence, we obtain a much higher resolution insight into the details of the actual event than we do with the interpolated PE.

# Appendix C

## SVN to PRN Mapping for 2015

Throughout the report, SVs have been referred to by both SVN and PRN. Keeping track of this relationship has become more challenging over the past few years as the number of operational SVs is typically very close to the number of available PRNs. As a result, the relationships have been changing several times throughout a year. Therefore it is useful to have a summary of the PRN to SVN mapping as a function of time. Figure C.1 presents that mapping for 2015. SVNs on the right vertical axis appear in the order in which they were assigned the PRN values in 2015. Start and end times of relationships are indicated by the dates along the upper horizontal axis.

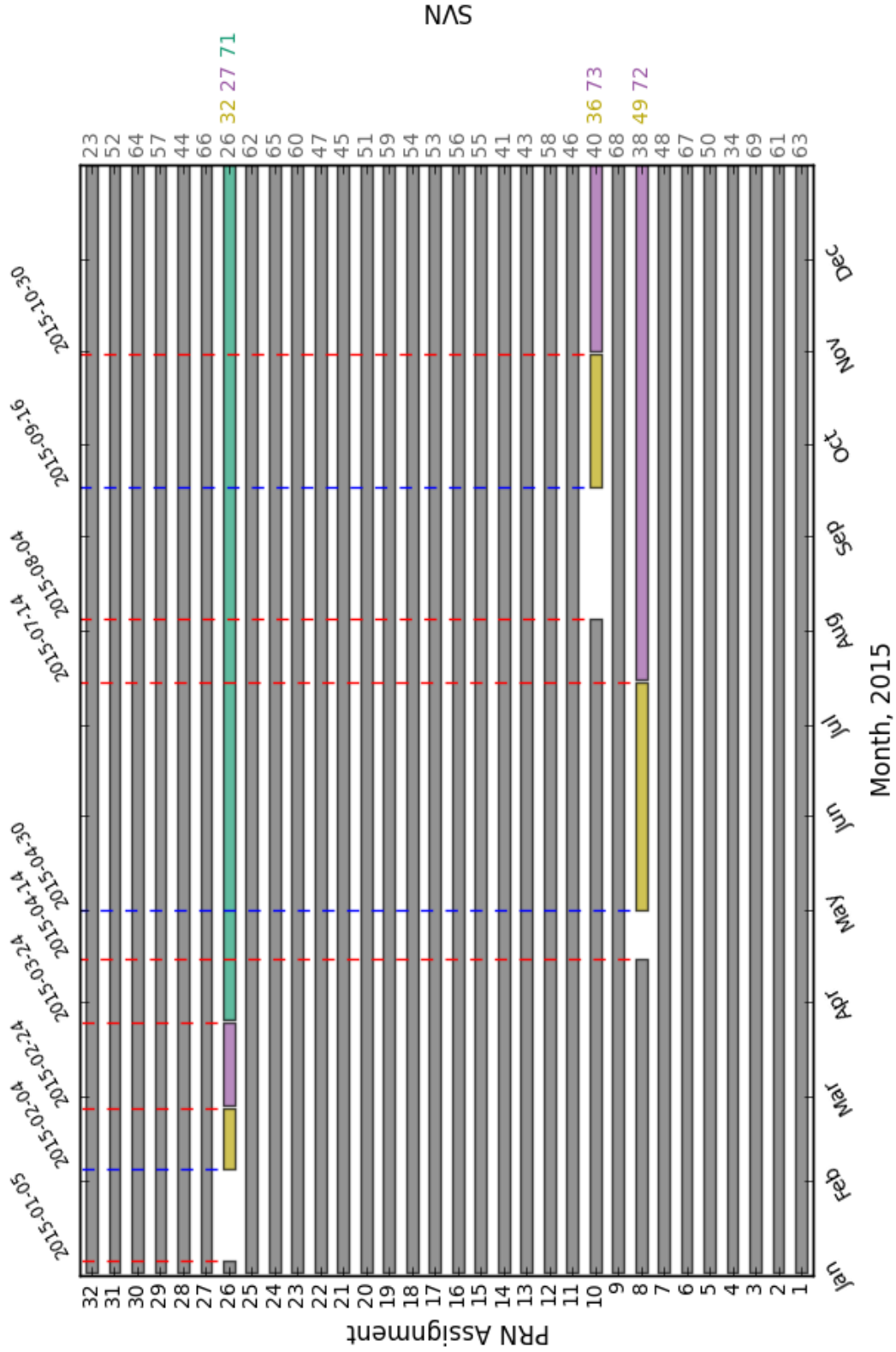


Figure C.1: PRN to SVN Mapping for 2015

# Appendix D

## NANU Activity in 2015

Several sections in the report make use of NANUs. It is useful to have a time history of the relevant NANUs sorted by SVN. This makes it convenient to determine which NANU(s) should be examined if an anomaly is observed for a particular satellite at a particular time.

Figure D.1 presents a plot of the NANU activity in 2015. Green bars are scheduled outages and red bars represent unscheduled outages. Gray bars represent SVs that have been decommissioned. NANU numbers are indicated next to each bar. In the event there is more than one NANU for an outage, the last NANU number is displayed.

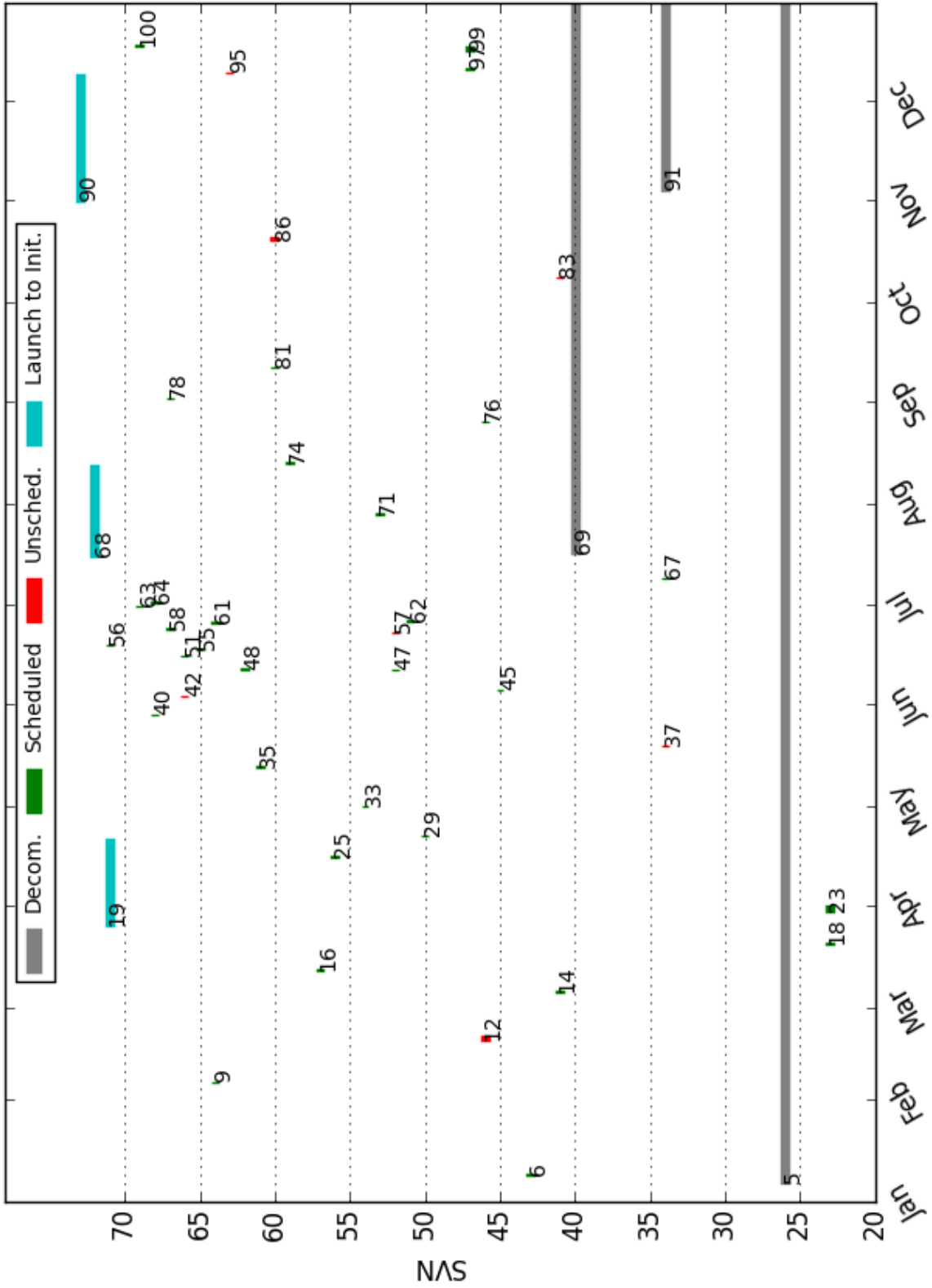


Figure D.1: Plot of NANU Activity for 2015

# Appendix E

## SVN to Plane-Slot Mapping for 2015

Several assertions in the PPS PS are related to the performance of the constellation as defined by the plane-slot arrangement specified in the performance standard. Evaluation of these assertions requires information on the plane-slot occupancy during the year.

The operational advisory (OA) provided by 2 SOPS to the United States Coast Guard (USCG) Navigation Center and defined in ICD-GPS-240 includes information on plane-slot assignments. This is a publicly available document and is one of few ways the public is informed of slot assignments. However, the format of the OA does not permit it to clearly convey the status of expanded slots. The format is limited to a letter representing the plane and a number representing the slot. There is no provision of the “fore/aft” designation. The OA designations are also cluttered by use of numbers greater than the number of defined slots. These are “slots of convenience” defined by the operators but have no fixed meaning in terms of position within the constellation. As a result, interpretation of the OA is challenging.

For the past several years, the plane-slot assignments have been provided to ARL:UT by Aerospace Corporation analysts supporting 2 SOPS. The assignments are provided as a set of daily plane-slot relationships for the year. This information source is not publicly available.

Both of these sources are limited in that only a single satellite may be designated as being present in a slot at a given moment. In fact, as satellites are moved within the constellation, there exists occasional periods when more than one SV may be present within the defined boundaries of a slot. From the user’s point of view, if a satellite transmitting a healthy signal is present within the slot boundaries, the slot should be counted as occupied.

ARL:UT has developed a process to independently assess the plane-slot relationships. In what follows, we present an initial independent verification of the plane-slot relationships.

Figure E.1 provides a graphical illustration of the plane-slot relationships throughout 2015. Table E.1 provides the plane-slot relationships in a tabular form. The contents of

Figure E.1 and Table E.1 are primarily drawn from the information provided by Aerospace, cross-checked against the Operational Advisories, and compared with the ARL:UT assessment. In the cases where an SV decommissioned or a new SV is launched, the appropriate NANUs were also checked to confirm dates. In some cases, multiple satellites fall within the slot definition for a period of time. The dates when satellites are judged to be present in a slot location are noted only when a change occurs in the plane-slot during the year. This allows the reader to determine when multiple satellites occupied a slot.

Figure E.1 and Table E.1 both indicate that the B1 slot was considered to be an expanded slot throughout 2015, but only one of the two expanded slot locations was occupied until April 2015. Slot B1F became vacant in March 2013 when SVN 35 was decommissioned and persisted until SVN 71 became available in April 2015. The ramifications for this are discussed further in Section 3.3 and Section 3.4.

**Table E.1:** Summary of SV-Slot Relationships for 2015

Plane-Slot	SVN	Start Date <sup>†</sup>	End Date <sup>†</sup>
A1	65		
A2	52		
A3	64		
A4	48		
B1A	56		
B1F	71	04/20/2015	
B2	62		
B3	44		
B4	58		
C1	57		
C2	66		
C3	59		08/16/2015
C3	72	08/12/2015	
C4	53		
D1	61		
D2A	63		
D2F	46		
D3	45		
D4	67		
E1	69		
E2	47		12/12/2015
E2	73	12/09/2015	
E3	50		
E4	54		
F1	41		
F2A	55		
F2F	26		01/04/2015
F2F	43		
F3	68		
F4	60		

---

<sup>†</sup>If unspecified, the SV was the sole occupant of the slot for the entire year.



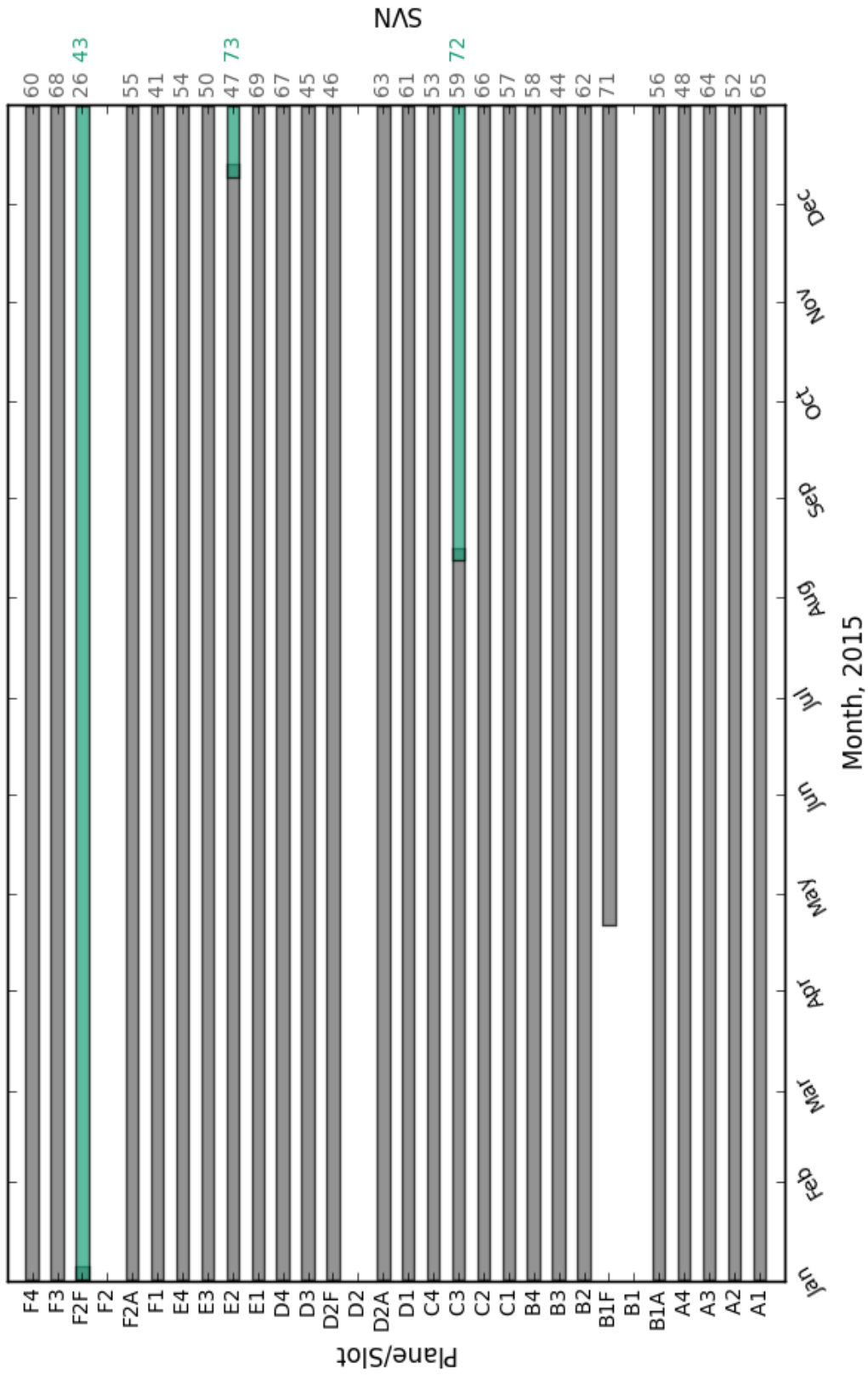


Figure E.1: Time History of Satellite Plane-Slots for 2015

# Appendix F

## Translation of URE Statistics Between Signals

The URE process described in Appendix B is based on the data broadcast in subframes 1, 2, 3 of the navigation message and the NGA PE. Both of these estimates of the satellite orbits and clock offsets are referenced to the dual-frequency P(Y)-code signal. Therefore, the URE results are directly related to the PPS dual-frequency performance. This appendix explains how these results have been interpreted to apply to the SPS assertions.

The PPS dual-frequency results may be mapped to SPS equivalent results by considering the effects of both the group delay differential and the intersignal bias (ISB) between the P(Y)-code and the C/A-Code on L1.

### F.1 Group Delay Differential

As described in IS-GPS-200 Section 3.3.1.7, the group delay through the satellite transmission hardware is accounted for in the satellite clock offset. However, there remains a group delay differential effect that comes about due to the fact that the signals passing through the different frequency chains experience slightly different delays. An estimate of the group delay differential is transmitted to the users in the navigation message using the  $T_{GD}$  term in Subframe 1. Note that  $T_{GD}$  is not the group delay differential but the group delay differential scaled to account for the difference between a dual-frequency observation and a single-frequency observation. This is described in IS-GPS-200 Section 20.3.3.3.2. This distinction will be relevant below when comparisons to other estimates are discussed.

IS-GPS-200 Section 3.3.1.7.2 states that the random plus non-random variations about the mean of the differential delay shall not exceed 3.0 nsec (95% probability). While this establishes an upper bound on the uncertainty, it does not represent actual performance. The quantization in the  $T_{GD}$  term is 0.5 nsec. Therefore, even with

perfect estimation, the floor on the uncertainty would be on the order of 0.25 nsec.

If one assumes that  $T_{GD}$  is correct and that the user equipment properly applies the correction, then the single-frequency results would be aligned with the dual-frequency results to within that quantization error. However, once the satellite is on orbit it is not possible to directly observe  $T_{GD}$ . Instead it must be estimated, and the estimates are subject to a variety of factors including receiver group delay differential effects and ionospheric dispersion. This uncertainty has the effect of inflating the PPS dual-frequency results when these results are interpreted in terms of the PPS single-frequency or SPS services. In fact, because the errors are not directly observable, the best that can be done is to examine the repeatability in the estimate or the agreement between independent estimates and consider these as proxies for the actual uncertainty.

Since 1999, the  $T_{GD}$  values have been estimated by Jet Propulsion Laboratory (JPL) and provided to 2 SOPS on a quarterly basis. Shortly before this process was instituted there was a study of the proposed estimation process and a comparison of the estimates to those independently developed by two other sources [13]. The day-to-day uncertainty in the JPL estimates appeared to be about 0.3 nsec and the RMS of the differences between the three processes (after removal of a bias) was between 0.2 nsec and 0.7 nsec.

The Center For Orbit Determination (CODE) at the University of Bern estimates the P1-P2 bias [14]. CODE provides a group delay differential estimate for each SV every month. CODE does not provide details on the estimation process, but it must include a constraint that the group differential delay averaged over the constellation is zero as all sets of monthly values exhibit a zero mean.

A comparison of the CODE estimates and the  $T_{GD}$  values (scaled by the group differential delay values) shows a  $\sim 5$  nsec bias between the estimates. This bias can be removed as we are comparing mean-removed vs non-mean removed values. After the bias across the constellation is removed, the level of agreement between the scaled  $T_{GD}$  values and the monthly CODE estimates is between 0.1 nsec and 0.8 nsec RMS. (Note: Results for SVN 49 appear to be out-of-family and have been excluded in this comparison)

Considering all these factors, for the purpose of this analysis the uncertainty in the  $T_{GD}$  is assumed to be 0.5 nsec RMS.

## F.2 Intersignal Bias

The ISB represents the difference between two signals on the same frequency. This bias is due to differences in the signal generation chain coupled with dispersive effects in the transmitter due to the differing bandwidths of the signals. It is not possible to observe these effects directly. When examining the signal structure at the nanosecond level the chip edges are not instantaneous transitions with perfectly vertical edges but exhibit rise times that vary by signal. Therefore, measuring the biases requires assumptions

about the levels at which one decides a transition is in progress. These assumptions will vary between receivers.

There is no estimate of the ISB provided in the GPS legacy navigation message. However, CODE estimates the bias between the L1 P(Y)-code and the L1 C/A-code [14]. An estimate is provided for each SV every month. When this adjustment process was developed, these estimates were examined for each month in 2013. The monthly mean across all SVs is zero, indicating the estimation process is artificially enforcing a constraint. The RMS of the monthly values across the constellation is 1.2 nsec for each month. Because there is no estimate of the ISB, this RMS value represents an estimate of the error C/A users experience due to the ISB.

### F.3 Adjusting PPS dual-frequency Results for SPS

The PPS dual-frequency and SPS cases are based on a different combination and a different code. Therefore, the uncertainties in both  $T_{GD}$  and ISB must be considered. The PPS dual-frequency URE results are all stated as 95<sup>th</sup> percentile (2-sigma) values. This means that the RMS errors estimated in F.1 and F.2 must be multiplied by 1.96 (effectively 2, given that the amount of uncertainty in the values).

If it is assumed that these errors are uncorrelated, the total error may be estimated as

$$\begin{aligned} \text{Total error} &= \sqrt{((2 * T_{GD} \text{ uncertainty})^2 + (2 * \text{ISB uncertainty})^2)} \\ &= \sqrt{((2 * 0.5 \text{ nsec})^2 + (2 * 1.2 \text{ nsec})^2)} \\ &= \sqrt{(1 \text{ nsec}^2 + 5.76 \text{ nsec}^2)} \\ &= 2.6 \text{ nsec} \end{aligned} \tag{F.3.1}$$

Converted to equivalent range at the speed of light and given only a single significant digit is justified, the total error is about 0.8 m. This adjustment may then be combined with the PPS dual-frequency result in a root-sum-square manner.

# Appendix G

## Acronyms and Abbreviations

**Table G.1:** List of Acronyms and Abbreviations

2 SOPS	-	2 <sup>nd</sup> Space Operations Squadron
AMCS	-	Alternate Master Control Station
AOD	-	Age of Data
AODO	-	Age of Data Offset
ARL:UT	-	Applied Research Laboratories, The University of Texas at Austin
BCP	-	Broadcast Clock and Position
CMPS	-	Civil Monitoring Performance Specification
CODE	-	Center For Orbit Determination
DECOM	-	Decommission
DOP	-	Dilution of Precision
ECEF	-	Earth-Centered, Earth-Fixed
FAA	-	Federal Aviation Administration
FCSTDV	-	Forecast Delta-V
FCSTEXTD	-	Forecast Extension
FCSTMX	-	Forecast Maintenance
FCSTRESCD	-	Forecast Rescheduled
FCSTUUFN	-	Forecast Unusable Until Further Notice

GNSS	-	Global Navigation Satellite System
GPS	-	Global Positioning System
GPSTK	-	GPS Toolkit
HDOP	-	Horizontal Dilution Of Precision
IGS	-	International GNSS Service
IODC	-	Issue of Data, Clock
IODE	-	Issue of Data, Ephemeris
ISB	-	Intersignal Bias
JPL	-	Jet Propulsion Laboratory
LSB	-	Least Significant Bit
MCS	-	Master Control Station
MSB	-	Most Significant Bit
MSI	-	Misleading Signal Information
MSN	-	Monitor Station Network
NANU	-	Notice Advisory to Navstar Users
NAV	-	Navigation Message
NGA	-	National Geospatial-Intelligence Agency
NMCT	-	Navigation Message Correction Table
NTE	-	Not to Exceed
OA	-	Operational Advisory
ORD	-	Observed Range Deviation
PDOP	-	Position Dilution of Precision
PE	-	Precise Ephemeris
PRN	-	Pseudo-Random Noise
PVT	-	Position, Velocity, and Time
RAIM	-	Receiver Autonomous Integrity Monitoring
RINEX	-	Receiver Independent Exchange Format
RMS	-	Root Mean Square

SA	-	Selective Availability
SINEX	-	Station Independent Exchange Format
SIS	-	Signal-in-Space
SMC/GP	-	Global Positioning Systems Directorate
SNR	-	Signal-to-Noise Ratio
SP3	-	Standard Product 3
SPS	-	Standard Positioning Service
SPS PS(SPSPS08)	-	2008 Standard Positioning Service Performance Standard
SV	-	Space Vehicle
SVN	-	Space Vehicle Number
TCP	-	Truth Clock and Position
T <sub>GD</sub>	-	Group Delay
UNUNOREF	-	Unusable with No Reference
UNUSUFN	-	Unusable Until Further Notice
URA	-	User Range Accuracy
URAE	-	User Range Acceleration Error
URE	-	User Range Error
URRE	-	User Range Rate Error
USCG	-	United States Coast Guard
USNO	-	U.S. Naval Observatory
UTC	-	Coordinated Universal Time
UTC OE	-	UTC Offset Error
WGS 84	-	World Geodetic System 1984
ZAOD	-	Zero Age of Data

# Bibliography

- [1] U.S. Department of Defense. Standard Positioning Service Performance Standard, 4th Edition, 2008.
- [2] U.S. Department of Defense. Navstar GPS Space Segment/Navigation User Interfaces, IS-GPS-200, Revision G, September 2012.
- [3] John M. Dow, R.E. Neilan, and C. Rizos. The International GNSS Service in a changing landscape of Global Navigation Satellite Systems. *Journal of Geodesy*, 2009.
- [4] B. Renfro, D. Munton, and R. Mach. Around the World for 26 Years - A Brief History of the NGA Monitor Station Network. In *Proceedings of the Institute of Navigation International Technical Meeting*, Newport Beach, CA, 2012.
- [5] U.S. Naval Observatory. Block II Satellite Information. <ftp://tycho.usno.navy.mil/pub/gps/gpstd.txt>.
- [6] W. Gurtner and L. Estey. RINEX: The Receiver Independent Exchange Format Version 2.11, 2006.
- [7] U.S. Department of Defense. Navstar GPS Control Segment to User Support Community Interfaces, ICD-GPS-240, Revision A, January 2010.
- [8] U.S. Department of Transportation. Global Positioning System (GPS) Civil Monitoring Performance Specification, DOT-VNTSC-FAA-09-08, April 2009.
- [9] B. Tolman et al. The GPS Toolkit - Open Source GPS Software. In *Proceedings of the 17th International Technical Meeting of the Satellite Division of the Institute of Navigation (ION GNSS 2004)*, Long Beach, CA, 2004.
- [10] NIMA Technical Report TR8350.2. Department of Defense World Geodetic System 1984, Its Definition and Relationships With Local Geodetic Systems, July 1997.
- [11] National Geospatial-Intelligence Agency. NGA Antenna Phase Center Precise Ephemeris products. <http://earth-info.nga.mil/GandG/sathtml/ephemeris.html>.
- [12] The White House, Office of the Press Secretary. Statement by the President Regarding the United States' Decision to Stop Degrading Global Positioning System Accuracy, May 2000.



- [13] Colleen H. Yinger, William A. Feess, Ray Di Esposti, The Aerospace Corporation, Andy Chasko, Barbara Cosentino, Dave Syse, Holloman Air Force Base, Brian Wilson, Jet Propulsion Laboratory, Maj. Barbara Wheaton, and SMC/CZUT. GPS Satellite Interfrequency Biases, June 1999.
- [14] GPS satellite bias estimates for 2013. <ftp://ftp.unibe.ch/aiub/CODE/2013>, 2013.